

NOISE AND DELAYS IN ADAPTIVE INTERACTING OSCILLATORY SYSTEMS

DOKTORARBEIT

ZUR ERLANGUNG DES DOKTORGRADES

DER FAKULTÄT FÜR PHYSIK

DER UNIVERSITÄT BIELEFELD

VORGELEGT VON

Dr. Julio RODRIGUEZ

... à Robert DESNOS ...

... pour que le cadran des rêves soit période de réalité ...

Summary

In this thesis, we explore the global behavior of complex systems composed of interacting local dynamical systems, each set on a vertex of a network which characterizes the mutual interactions. We consider heterogeneous arrangements, meaning that for each vertex the local dynamics can be different. To better match potential applications we allow mutual interactions to be time delayed and subject to noise sources affecting either the orbits of the local dynamics and/or the connectivity of the network. Within this very general dynamical context, we construct and focus on interactions enabling a certain level of adaptation between the local dynamical systems. By propagation of information via the coupling network, the local parameters are adaptively tuned and ultimately reach a set of consensual values. This is explicitly and analytically carried out for frequency- and radius-adapting HOPF oscillators. We then consider adapting the time scale and the shape of periodic signals. We also study how adaptive mechanisms can be implemented in heterogeneous networks formed by a couple of subnetworks, the first one with adaptive capability and the second one without. The first subnetwork defines interactions between phase oscillators with adaptive frequency capability, the other subnetwork connects damped vibrating systems without adaptation. Next, noise sources are introduced into the dynamics via stochastic switchings of the network connections. This extra time-dependence in the network opens the possibility for parametric resonance and destabilization of a consensual oscillatory state, found for purely static networks. Finally, we introduce external noise environments which corrupt the orbits of the local systems. For “All-to-All” network topology, we analytically derive the effects of Gaussian and non-Gaussian noise sources and unveil noise induced emergent oscillating patterns of the relevant order parameter that characterizes this dynamics. Although in this thesis the emphasis is made on deriving analytical results, we systematically supplement our findings with extensive numerical simulations. They not only corroborate and illustrate our theoretical assertions but provide additional insights where analytical results could not be found.

Keywords: coupled phase oscillators, damped vibrating systems, periodic signal generator and HOPF oscillators, time-dependent Laplacian matrices, heterogenous complex networks, ЛЯПУНОВ functions, super-diffusive stochastic processes, non-Gaussian noise, adaptive frequency and attractor-shaping mechanisms, order parameter, second-order DDE, second-order ODE with time-dependent parameters, KURAMOTO dynamics, adaptation, synchronization, stochastic parametric resonance, self-propelled agents, noise-induced global bifurcation diagram, time-oscillating order parameter,

Danksagung

Je remercie mes professeurs de thèse pour ce chemin que nous avons fait ensemble. Je vous remercie pour nos échanges et discussions - sur la science en général, sur les thèmes de société et de politique. C'est aussi dans le cadre de cette thèse que j'ai pu connaître la ville de Bielefeld, découvrir toute une région de l'Allemagne et m'exercer dans une autre langue. Je vous remercie pour votre façon de voir plus loin et plus en avant. Merci Philippe d'avoir rendu possible multiples déplacements et conférences. Merci Max pour toute ton aide et ta constante présence dans cette aventure.

Bielefeld, 12.12.12

Dr. Julio RODRIGUEZ

Contents

1	Introduction	1
1.1	General Framework	1
1.2	Aim	1
1.3	Contributions	2
1.4	Organization	3
2	Time Delayed Interactions in Networks of Self-Adapting Hopf Oscillators ...	5
2.1	Introduction	5
2.2	Networks of HOPF Oscillators with Adaptive Mechanisms	7
2.2.1	Local Dynamics	7
2.2.2	Coupling Dynamics	7
2.2.3	Adaptive Mechanisms	8
2.3	Network's Dynamical System with Delay	8
2.3.1	Miscellaneous Remark: Delayed Stabilization Mechanism	12
2.4	Applications	12
2.5	Numerical Simulations	13
2.6	Conclusion	15
	Appendix	15
2.A	Stability Analysis for Case $k = 1$	15
3	Adaptation of Oscillatory Systems in Networks	
	- A Learning Signal Approach	17
3.1	Introduction	17
3.2	Networks of Periodic Stable Signals with Adaptive Mechanisms	19
3.2.1	Local Dynamics	19
3.2.2	Coupling Dynamics	19
3.2.3	Adaptive Mechanisms	21
3.3	Network's Dynamical System with Time Scale and Amplitude Adaptation	21
3.3.1	Miscellaneous Remark: Time Scale or Amplitude Adaptation Only	23
3.3.1.1	Amplitude Adaptation Only	23
3.3.1.2	Time scale Adaptation Only	24
3.4	Numerical Simulations	24
3.4.1	Time Scale and Amplitude Adaptation	25
3.4.2	Amplitude Adaptation Only	25
3.5	Conclusion	26
	Appendix	26
3.A	Convergence Towards Compact Set \mathbb{K}	26

4	Frequency Adaptation in Networks of Vibrating-Oscillatory Systems	31
4.1	Introduction	31
4.2	Networks of Damped Vibrational Systems and Phase Oscillators with Adaptive Mechanisms	35
4.2.1	Network of Vibrating-Oscillatory Systems	36
4.3	Network's Dynamical System	38
4.3.1	Adaptation	38
4.3.1.1	Adaptation in Homogenous q -DVSs	39
4.3.1.2	Adaptation in Heterogenous q_k -DVSs	41
4.3.2	Synchronization	42
4.3.2.1	Synchronization in Homogenous q -DVSs	42
4.3.2.2	Synchronization in Heterogenous q_k -DVSs	43
4.4	Summary	43
4.5	Numerical Simulations	44
4.5.1	Network of Homogenous q -DVSs and Heterogenous q_k -DVSs	44
4.5.2	Adaptation vs. Synchronization	45
4.6	Conclusions and Perspectives	47
	Appendix	47
4.A	Calculations for Equations (4.2), (4.3) and (4.4)	47
4.B	Verifying Properties For the Local Coupling Function in Example 2	49
4.C	Verifying Hypothesis For Coupling Potential E as Defined in Section 4.2.1	49
4.C.1	Properties For function W	50
4.C.2	Properties For function V	51
4.C.3	Verification of Hypothesis	52
4.D	Determining the $r_{c,k}$	53
5	Stochastic Parametric Resonance in Time-Dependent Networks of Adaptive Frequency Oscillators	55
5.1	Introduction	55
5.2	Network of Phase Oscillators with Time-dependent Adaptive Mechanisms	57
5.3	Network's Dynamical System with Random Switching Topologies	59
5.3.1	Stability Analysis	61
5.4	Numerical Simulations	65
5.5	Conclusions and Perspectives	65
	Appendix	66
5.A	Synchronized Solution	66
5.B	Proof of Convergence	68
5.C	Commuting Matrices	69
6	Noise Induced Temporal Patterns in Populations of Globally Coupled Oscillators	71
6.1	Introduction	71
6.2	KURAMOTO-SAKAGUCHI Model Driven by Super-Diffusive Noise	72
6.2.1	A None Gaussian, Super-Diffusive Noise	72
6.2.2	The Effect of The Non-Gaussian Noise	73
6.2.3	Extensions to More Complex Noise Sources	74
6.3	Noise Induced "Zig-Zagging" - a Case Study	75
6.4	Conclusion	77
	Appendix	77
6.A	Characterization of Full Synchronization via the Oder Parameter	77
7	Conclusions and Perspectives	79
7.1	Conclusions	79
7.2	Perspectives	80
	Appendix	81
7.A	Comparison Between Synchronization and Adaptation	82

References	85
Curriculum Vitae	89

Introduction

O mathématiques sévères, je ne vous ai pas oubliées, depuis que vos savantes leçons, plus douces que le miel, filtrèrent dans mon cœur, comme une onde rafraîchissante.

Comte de LAUTREAMONT

1.1 General Framework

Based on what has been presented in [42], a general framework of coupled heterogenous adapting local systems in a noisy environment with delay and time-dependent interactions is

$$\begin{aligned}
 \dot{\phi}_k(t) &= \mathbf{P}_k(\phi_k(t), r_k(t), \Omega_k(t)) - c_{\phi_k} \frac{\partial \mathcal{V}}{\partial \phi_k}(t, \phi(t-t), r(t-t)) + \mathbf{e}\Upsilon_k(t) \\
 \dot{r}_k(t) &= \underbrace{\mathbf{R}_k(\phi_k(t), r_k(t), \Omega_k(t))}_{\text{local dynamics}} - \underbrace{c_{r_k} \frac{\partial \mathcal{V}}{\partial r_k}(t, \phi(t-t), r(t-t))}_{\text{coupling dynamics}} \\
 \dot{\Omega}_k(t) &= \underbrace{\mathbf{A}_k(\phi_k(t-t), r_k(t-t))}_{\text{adaptive mechanisms}}
 \end{aligned} \quad k = 1, \dots, n, \quad (1.1)$$

where (ϕ_k, r_k) are the state variables, $(\mathbf{P}_k, \mathbf{R}_k)$ belonging to the class of PR systems (i.e. phase-radius systems, generally describing oscillatory motion), $\mathcal{V}(t, \phi, r) \geq 0$ is a time-dependent coupling potential, c_{ϕ_k} and c_{r_k} are coupling strengths, and $\Upsilon_k(t)$ is a noise source with noise intensity $\mathbf{e} \geq 0$. The adapting parameters are Ω_k , and their adaptation is governed by the adaptive mechanisms \mathbf{A}_k .

When $\mathbf{A}_k \equiv 0$ for all k , then $\Omega_k(t) = \bar{\Omega}_k$ for all t and k , and so they are fixed and constant parameters for the local dynamics. In this case, Equations (1.1) describes the classical framework of heterogenous local oscillatory motion coupled through delay and time-dependent interactions in a random environment for which observation of any type of emerging common dynamical pattern is of interest. Synchronization (i.e. oscillatory movement with the same frequency as its coupled neighbors) is by far the most studied and among the most captivating phenomena occurring in complex networks.

1.2 Aim

The main aim of this thesis is to study the resulting dynamics of System (1.1) with the adaptive mechanisms (i.e. $\mathbf{A}_k \not\equiv 0$) depending on delayed interactions or randomly switching networks.

Adaptation is a well establish research filed, as discussed in each chapter. The concept of adaptation, as well as the word itself, has many definitions and its meaning depends on the context. In this thesis, the general idea of adaptation can be expressed with the following example.

Consider Equations (1.1) with $A_k \equiv \mathbf{0}$ for all k , that is, local dynamics are equipped with fixed and constant parameters $\bar{\Omega}$. Suppose that the system admits a synchronized solution $S_{\Omega(t)} = (S_{1,\Omega(t)}, \dots, S_{n,\Omega(t)})$ (i.e. $S_{\Omega(t)}$ solve Equations (1.1) and all $S_{k,\Omega(t)}$ are periodic with the same period (i.e. synchronization)) and $\Omega = \{\Omega_1, \dots, \Omega_n\}$. For any other parameter set Λ not to distant from Ω (i.e. $0 \leq \|\Omega - \Lambda\| \ll 1$), one can suppose the existence of another synchronized solution $S_{\Lambda(t)}$. Denote by Ξ the set of all parameter set for which corresponds a synchronized solution of Equations (1.1). We say that adaptation occurs in the network if

- I among all the parameter sets in Ξ , there exists at least one, denoted as $\bar{\Omega}$, for which $Z(\bar{\Omega}) = \|\nabla V(S_{\bar{\Omega}(t)})\|$ is minimum over one period and
- II by letting the fixed and constant local parameters become time-dependent (i.e. $\Omega_k \rightsquigarrow \Omega_k(t)$) and have their own dynamics governed by functions A_k (now introduced in Equations (1.1)), the network dynamics behaves as

$$\lim_{t \rightarrow \infty} \Omega_k(t) = \bar{\Omega}_k \quad \text{and} \quad \lim_{t \rightarrow \infty} (\phi_k(t), r_k(t)) = S_{k,\bar{\Omega}(t)}. \quad (1.2)$$

Therefore, with this notion of adaptation, the aim is

- I to explicitly construct adaptive mechanisms A_k ,
- II determine the conditions for which Limits (1.2) hold,
- III determine the value of the set.

It is important to note that with this notion of adaptation, the idea of synchronization is preserved. However, in the case where $Z(\bar{\Omega})$ is zero (i.e. the synchronized solution $S_{\bar{\Omega}(t)}$ cancels the coupling dynamics), we note the following two important points

- I $S_{\bar{\Omega}(t)}$, by definition, is not influenced by V^1 . This implies that for any change in V (e.g. change in the network connections), the local dynamics are not perturbed.
- II If the coupling dynamics is removed, the local dynamics continue their common motion since in this case, it was not because of V that $S_{\bar{\Omega}(t)}$ is maintained.

In the first place, we continue to explore complex networks with adaptive mechanisms as done in [42], but here we investigate the influence of time delayed interactions, heterogenous local systems and stochastically switching networks. In a second part, we study the influence of a non-Gaussian, super diffusive environment on an assembly of ‘‘All-to-All’’ coupled phase oscillators.

1.3 Contributions

The original contributions of this thesis are summarized bellow.

Chapter 2 Whereas the dynamics of coupled HOPF oscillators with adapting frequency and amplitudes has been studied in [42], we here investigated the resulting dynamics for delayed adaptive mechanisms. The existence and conditions for converging towards a consensual oscillatory state are analytically given, as well as the asymptotic values for the consensual state. This contribution was published in [47]

Chapter 3 Based on adaptive attractor mechanisms presented in [42], we investigated shape adaptation in networks of periodic signals. Our approach is systematic, directly implantable for any signal given by its FOURIER series and, contrarily to what has be presented in [42], does not need beforehand any geometric information of the adapting attractor. Numerical experiments show that, under certain conditions, the local systems converge towards a consensual oscillatory state. The asymptotic values for this state are analytically determined.

¹ In a synchronization problem, $S_{\bar{\Omega}(t)}$ depends on the coupling potential V and on the parameter set Ω .

Chapter 4 Derived from potential robotic applications in [13, 41], we constructed an heterogenous complex system of interacting damped vibrating system and phase oscillators with frequency adaptive mechanisms. The existence of and convergence towards a consensual oscillatory state are analytically given, as well as the asymptotic values for the consensual state. We numerically investigated the network dynamics for a case without adaptation (i.e. synchronization) and for directed networks.

Chapter 5 Networks of frequency adaptive phase oscillators with deterministic time-dependent (continuous) connections have been investigated in [42]. We here explored the discrete stochastic switching version. For a class of network topologies and for predefined switching times, we analytically determined the conditions for destabilizing the network through parametric resonance phenomena.

Chapter 6 We introduced a new, non-Gaussian noise source in the KURAMOTO model with homogenous frequency oscillators. Using well-known results for the homogenous frequency KURAMOTO model driven by Gaussian noise, we were able to identify phase transitions and set up the corresponding bifurcation scenario. This contribution was published in [29, 30].

1.4 Organization

Each chapter is self-contained with its own Appendix, and hence any chapter can be read as an individual article. Based on the notation from Equations (1.1), the list bellow outlines the exact dynamical system that is investigated in each chapter.

Chapter 2 The system is composed of homogenous local dynamics - HOPF oscillators - coupled through a Laplacian potential with time-independent connections, and with adaptive mechanisms (i.e. $A_k \neq 0$) on the parameters controlling the frequency and radius of each HOPF oscillator. There are time delayed interactions (i.e. $\tau > 0$). There is no random environment (i.e. $e = 0$).

Chapter 3 The system is composed of homogenous local dynamics - Periodic Stable signals (PSS) - coupled through a general potential with time-independent connections, and with adaptive mechanisms (i.e. $A_k \neq 0$) on the parameters controlling the time scale and the shape of each PSS. There are no time delayed interactions (i.e. $\tau = 0$). There is no random environment (i.e. $e = 0$).

Chapter 4 The system is composed of heterogenous local dynamics - Damped Vibrating Systems (DVS) and Phase Oscillators (PO)² - coupled through a general potential with time-independent connections, and with adaptive mechanisms (i.e. $A_k \neq 0$) on the parameters controlling the frequency of the each PO. There are no time delayed interactions (i.e. $\tau = 0$). There is no random environment (i.e. $e = 0$).

Chapter 5 The system is composed of homogenous local dynamics - Phase Oscillators (PO) - coupled through a KURAMOTO-type potential with time-dependent - deterministic and stochastic switching - connections, and with adaptive mechanisms (i.e. $A_k \neq 0$) on the parameters controlling the frequency of each PO. There are no time delayed interactions (i.e. $\tau = 0$). There is no random environment (i.e. $e = 0$).

Chapter 6 The system is composed of homogenous local dynamics - Phase Oscillators (PO) - coupled through a KURAMOTO-type potential (“All-to-All” coupling) with time-independent connections, and with no adaptive mechanisms (i.e. $A_k \equiv 0$). There are no time delayed interactions (i.e. $\tau = 0$). There is a non-Gaussian random environment (i.e. $e > 0$).

² When these two units are coupled, they form Vibrating-Oscillatory Systems (VOS).

Time Delayed Interactions in Networks of Self-Adapting Hopf Oscillators

The farther back you can look, the farther forward you are likely to see.

Winston CHURCHILL

Abstract

A network of coupled limit cycle oscillators with delayed interactions is considered. The parameters characterizing the oscillator's frequency and limit cycle are allowed to self-adapt. Adaptation is due to time-delayed state variables that mutually interact via a network. The self-adaptive mechanisms ultimately drive all coupled oscillators to a consensual oscillatory state where the values of the parameters are identical for all local systems. They are analytically expressible. The interplay between the spectral properties of the coupling matrix and the time-delays determine the conditions for which convergence towards a consensual state takes place. Once reached, this consensual state subsists even if interactions are removed. In our class of models, the consensual values of the parameters neither depend on the delays nor on the network's topologies.

2.1 Introduction

The harmonic excitation of an elementary damped harmonic oscillator

$$\underbrace{\ddot{x}(t) + a\dot{x}(t) + fx(t)}_{\text{system}} = \underbrace{r \sin(\omega t)}_{\text{environment}} \quad (2.1)$$

with a, f, r and $\omega > 0$ produces the well known asymptotic response (c.f. [53])

$$x(t) = k \cos(\omega t - \vartheta) .$$

where k and ϑ depend on the control parameters a, r and ω . By construction, the oscillating environment here materialized by the input $r \sin(\omega t)$ is totally insensitive to the oscillator $x(t)$, implying that $x(t)$ in Equation (2.1) is slaved by the external forcing. The next stage of complexity is to replace the harmonic oscillator in Equation (2.1) by a LIENARD system

$$\ddot{x}(t) + R(x(t), \dot{x}(t)) + fx(t) = r \sin(\omega t) , \quad (2.2)$$

where $R(x(t), \dot{x}(t))$ is a nonlinear controller. In absence of external excitation in Equation (2.2) (i.e. when $r = 0$), we assume R to asymptotically drive the orbits towards a stable limit cycle which is independent of the initial conditions - the paradigmatic illustration being here the VAN DER POL oscillator. When $r \neq 0$ and for a suitably selected range of parameters, the time asymptotic response of Equation (2.2) can be qualitatively written as (c.f. [35, 25])

$$x(t) = S(t) \quad (2.3)$$

with $S(t)$ being a synchronized signal with the same periodicity as the environment (i.e. $S(t + \frac{2\pi}{w}) = S(t)$). By construction, the external forcing $r \sin(wt)$ in Equation (2.2) is, as before, insensitive to the LIENARD oscillator. In the resulting synchronized regime, the oscillator $x(t)$ is caught by the external excitation - in other words, the system adjusts itself to the environment but the environment remains insensible to the system. Observe that the dynamical response given by Equation (2.3) only subsists as long as $r \sin(wt)$ acts on the system. That is, as soon as the environment effect is removed (i.e. $r = 0$ in Equation (2.2)), the system (i.e. the limit cycle oscillator), after a transient time, recovers its original behavior - converges towards its limit cycle.

In our present paper, we shall extend the previous classical system-environment relationship in order to allow more realistic situations where mutual interactions permanently affect both the system and the environment. Such adaptive mechanisms can modify individual dynamics on a permanent basis. To stylize this new situation, the basic dynamics given by Equation (2.2) is modified as

$$\begin{aligned} \ddot{x}(t) + R(x(t), \dot{x}(t)) + f(t)x(t) &= r \sin(\omega(t)t), \\ \dot{f}(t) &= A^f(x(t), \dot{x}(t)) \quad \text{and} \quad \dot{\omega}(t) = A^\omega(x(t), \dot{x}(t)), \end{aligned} \quad (2.4)$$

where $f \rightsquigarrow f(t)$ and $w \rightsquigarrow \omega(t)$ are no longer constant parameters but variables of the global dynamics (and hence time-dependent) and the functions A^f and A^ω capture the mutual adaptation of the system-environment dipole. Hence, the system of Equations (2.4) has now to be considered globally - the system and its environment, are allowed to adaptively co-evolve.

The particular case of Equations (2.4) when $A^f \equiv 0$ (i.e. $f(t) := f$ for all t) has been studied in [13, 41]. This type of dynamical system provides a cornerstone of bio-inspired robotics where legs (or arms) of robots may be modeled by damped oscillators as Equation (2.1) (i.e. $R(x(t), \dot{x}(t)) = a\dot{x}(t)$). To ensure a maximum leg stride, the damped oscillators must be excited by $r \sin(\omega(t)t)$ at the damped oscillator's resonant frequency (i.e. $\omega(t) \simeq \sqrt{f}$ for all t). However, due to structural changes on the robot (adding load, lengthening legs), the resonant frequency of the damped oscillator has to be adjusted: $f \mapsto \bar{f}$. Hence, A^ω drives $\omega(t)$ towards the value \bar{f} to systematically guarantee the excitation at resonant frequency and thus maximum leg stride. Frequency adaptation (as well as amplitude adaption) is also important in movement assistance (e.g. retrain the nervous system, assist people with movement disorder) where robots and human beings must work in synchronous. An example of an exoskeleton for the human elbow was studied in [49].

The case where neither A^f nor A^ω are trivial has been covered in [44, 43], where the authors not only considered two adaptive coupled limit cycle oscillators, but n mutually interacting through a network. Here, self-adapting oscillators can be applied to robot formation modeling. Each individual robot belonging to a swarm, circulating around a specific point, adapts its angular velocity in order to lower the amount of exchanged information to maintain the formation. Self-adaptation in networks is also considered in [54], where here the control signals (and not the local systems) of the variables of the CPG adapt, and this, to quickly react to new situations and produce several different behavioral patterns.

Building on what has been done in previous contributions [13, 41, 44, 43], we here consider a network of limit cycle oscillators interaction with time-delayed state variables. The general form of our dynamical system in the phase-radius coordinates (i.e. polar coordinates ϕ_k and r_k) is

$$\begin{aligned} \dot{\phi}_k(t) &= P(\phi_k(t), r_k(t); \Omega_k) - c_k \underbrace{\frac{\partial V}{\partial \phi_k}}_{\text{coupling dynamics}}(\phi_{(t-t)}, r_{(t-t)}) \\ \dot{r}_k(t) &= \underbrace{R(\phi_k(t), r_k(t); \Omega_k)}_{\text{local dynamics}} - c_k \underbrace{\frac{\partial V}{\partial r_k}}_{\text{coupling dynamics}}(\phi_{(t-t)}, r_{(t-t)}) \quad k = 1, \dots, n, \end{aligned} \quad (2.5)$$

where P and R govern the local dynamics, $\phi = (\phi_1, \dots, \phi_n)$ and $r = (r_1, \dots, r_n)$ are the state variables, Ω_k is a parameter set determining the local characteristics and $c_k > 0$ are coupling

strengths. The coupling dynamics is the gradient of a potential V depending on state variables with time delay t . Adaptation of the local dynamics is accomplished by letting the constant parameters Ω_k become time-dependent (i.e. $\Omega_k \rightsquigarrow \Omega_k(t)$) with their own dynamics given by adaptive mechanisms A_k . Delays being ubiquitous in applications, their influence on adaptive processes is worth to be investigated and so, the general formalization is

$$\begin{aligned}\dot{\phi}_k(t) &= P(\phi_k(t), r_k(t), \Omega_k(t)) - c_k \frac{\partial V}{\partial \phi_k}(\phi(t-t), r(t-t)) \\ \dot{r}_k(t) &= \underbrace{R(\phi_k(t), r_k(t), \Omega_k(t))}_{\text{local dynamics}} - \underbrace{c_k \frac{\partial V}{\partial r_k}(\phi(t-t), r(t-t))}_{\text{coupling dynamics}} \quad k = 1, \dots, n. \\ \dot{\Omega}_k(t) &= \underbrace{A_k(\phi(t-t), r(t-t))}_{\text{adaptive mechanism}}\end{aligned}\tag{2.6}$$

We therefore confer to Ω_k the status of variables of the whole dynamical system. Let us remark that in this present contribution, adaptation occurs in the local systems. Note that in [52], the authors introduce, with the help of the speed-gradient method, an adaptive mechanism on the coupling constant that multiplies the delayed interactions.

This paper is organized as follows: In Section 2.2 we define the three components that together form the global system. We then discuss the dynamics of our model in Section 2.3. An application is presented in Section 2.4 which is then followed by some numerical experiments in Section 2.5. Finally we conclude in Section 2.6.

2.2 Networks of HOPF Oscillators with Adaptive Mechanisms

We now present explicitly the local and coupling dynamics as well as the adaptive mechanisms on which we shall focus on.

2.2.1 Local Dynamics

Each node of the network is equipped with a local dynamical system. In this contribution, a local system is a HOPF oscillator presented here in its polar coordinates

$$\begin{aligned}P(\phi_k, r_k; \Omega_k) &= \omega_k \\ R(\phi_k, r_k; \Omega_k) &= -(r_k^2 - r_k)r_k\end{aligned}\quad k = 1, \dots, n.\tag{2.7}$$

The state variables are (ϕ_k, r_k) and $\Omega_k = \{\omega_k, r_k\}$ are, for the time being, fixed and constant parameters. The parameter ω_k controls the frequency of the k^{th} oscillator given by the phase dynamics P . The radial dynamics R produces a stable circular limit cycle with radius $\sqrt{r_k}$.

2.2.2 Coupling Dynamics

Associated to a n vertex connected and undirected network, denote by A the weighted adjacency matrix with positive entries $a_{k,j} \geq 0$. Let L be the corresponding Laplacian matrix ($L := D - A$ where D is the diagonal matrix with $d_{k,k} := \sum_{j=1}^n a_{k,j}$). The coupling dynamics is given by the gradient of the positive semi-definite function

$$V(\phi, r) := \frac{1}{2} \langle r | L_{\cos} r \rangle = \frac{1}{2} \sum_{k=1}^n r_k \sum_{j=1}^n l_{k,j} r_j \cos(\phi_k - \phi_j) \geq 0$$

with $\phi = (\phi_1, \dots, \phi_n)$ and $r = (r_1, \dots, r_n)$ and where the matrix L_{\cos} has entries $l_{k,j} \cos(\phi_k - \phi_j)$. This matrix is positive semi-definite since all its eigenvalues are positive (i.e. nonnegative). This

is a direct application of ГЕРШГОРИН’s circle theorem [22]: for any eigenvalue ζ_{\cos} of L_{\cos} , there exists k such that

$$|\zeta_{\cos} - l_{k,k}| \leq \sum_{j \neq k}^n |l_{k,j} \cos(\phi_k - \phi_j)|$$

and so $|\zeta_{\cos} - l_{k,k}| \leq \sum_{j \neq k}^n |l_{k,j} \cos(\phi_k - \phi_j)| \leq \sum_{j \neq k}^n |l_{k,j}| = l_{k,k}$. Specifically, the coupling dynamics are

$$\begin{aligned} c_k \frac{\partial \mathcal{V}}{\partial \phi_k}(\phi, r) &= -c_k \sum_{j=1}^n l_{k,j} r_k r_j \sin(\phi_k - \phi_j) \\ c_k \frac{\partial \mathcal{V}}{\partial r_k}(\phi, r) &= c_k \sum_{j=1}^n l_{k,j} r_j \cos(\phi_k - \phi_j) \end{aligned} \quad k = 1, \dots, n, \quad (2.8)$$

where $c_k > 0$ are coupling strengths.

2.2.3 Adaptive Mechanisms

In this section, we now allow the fixed and constant parameters w_k and r_k to

- I become time dependent, i.e. $\Omega_k = \{w_k, r_k\} \rightsquigarrow (\omega_k(t), \rho_k(t)) = \Omega_k(t)$, for $k = 1, \dots, n$.
- II and each of them have their own dynamics, depending solely on the state variables ϕ and r , that is

$$A_k(\phi, r) = (A_k^\omega(\phi, r), A_k^r(\phi, r)) \quad \text{for } k = 1, \dots, n.$$

Among the numerous variants for changing the values of the parameter, we focus on those presented in [44, 43, 42], that is

$$\begin{aligned} A_k^\omega(\phi, r) &= s_k \sum_{j=1}^n l_{k,j} r_k r_j \sin(\phi_k - \phi_j) \\ A_k^r(\phi, r) &= -s_k \sum_{j=1}^n l_{k,j} r_j^2 \end{aligned} \quad k = 1, \dots, n, \quad (2.9)$$

where $l_{k,j}$ are the entries of L and s_k are “susceptibility constants”: the larger s_k is, the stronger is the influence on ω_k and ρ_k . Conversely, oscillators with small s_k are reluctant to modify their frequency and their limit cycle radius.

2.3 Network’s Dynamical System with Delay

We now discuss the resulting dynamics in presence of a time delay $t \geq 0$ affecting both, the coupling dynamics, and the adaptive mechanisms. We hence consider

$$\begin{aligned} \dot{\phi}_k(t) &= \omega_k(t) + c_k \sum_{j=1}^n l_{k,j} r_k(t-t) r_j(t-t) \sin(\phi_k(t-t) - \phi_j(t-t)) \\ \dot{r}_k(t) &= -(r_k(t)^2 - \rho_k(t)) r_k(t) - c_k \sum_{j=1}^n l_{k,j} r_j(t-t) \cos(\phi_k(t-t) - \phi_j(t-t)) \\ \dot{\omega}_k(t) &= s_k \sum_{j=1}^n l_{k,j} r_k(t-t) r_j(t-t) \sin(\phi_k(t-t) - \phi_j(t-t)) \\ \dot{\rho}_k(t) &= -s_k \sum_{j=1}^n l_{k,j} r_j(t-t)^2 \end{aligned} \quad k = 1, \dots, n. \quad (2.10)$$

For Equations (2.10), we have

Two Constants of Motion

The functions

$$J(\omega) = \sum_{j=1}^n \frac{\omega_j}{s_j}, \quad K(\rho) = \sum_{j=1}^n \frac{\rho_j}{s_j} \quad (2.11)$$

are constants of motion - in other words, if $\omega(t) = (\omega_1(t), \dots, \omega_n(t))$ and $\rho(t) = (\rho_1(t), \dots, \rho_n(t))$ are orbits of Equations (2.10), then

$$\frac{d[J(\omega(t))]}{dt} = \langle \nabla J(\omega(t)) | \dot{\omega}(t) \rangle = \frac{d[K(\rho(t))]}{dt} = \langle \nabla K(\rho(t)) | \dot{\rho}(t) \rangle = 0.$$

Existence of a Consensual Oscillatory State

We can explicitly exhibit a consensual oscillatory state. Indeed, for given ω_c and $\rho_c > 0$,

$$(\phi_k(t), r_k(t), \omega_k(t), \rho_k(t)) := (\omega_c t, \sqrt{\rho_c}, \omega_c, \rho_c) \quad (2.12)$$

for all $t \in [-t, 0] \cup \mathbb{R}_{\geq 0}$ is a consensual orbit of Equations (2.10).

Observe that in absence of the radial component r_k and without adaptation, Equations (2.10) yield the famous KURAMOTO model with delays [60, 39]¹.

In absence of time delay (i.e. $t = 0$) and under appropriate conditions (c.f. [42] for details), the adaptive mechanisms tune the value of frequencies ω_k and the radii ρ_k of the attractors so that the global dynamical system is driven into a consensual oscillatory state. In other words, we have the following limit

$$\lim_{t \rightarrow \infty} \|(\phi_k(t), r_k(t), \omega_k(t), \rho_k(t)) - (\omega_c t, \sqrt{\rho_c}, \omega_c, \rho_c)\| = 0 \quad \forall k \quad (2.13)$$

with constants ω_c and ρ_c and where $\|\cdot\|$ is the Euclidean norm. The consensual state is permanent (i.e. even if interactions are switched off, all local dynamics still oscillate with the same frequency and same amplitude). Let us now discuss the conditions for which Limit (2.13) holds when the global dynamics is affected by a time delay (i.e. $t > 0$).

Convergence Towards a Consensual Oscillatory State

The Limit (2.13) raises two issues - 1) the existence itself and 2) the limit values ω_c and ρ_c . For expository reasons, we first discuss the limit values and then the convergence conditions.

Limit Values - Thanks to the constant of motions in (2.11), we have

$$J(\omega(0)) = J(\omega(t)) \quad \forall t \quad \text{and} \quad K(\rho(0)) = K(\rho(t)) \quad \forall t,$$

with $\omega(t) = (\omega_1(t), \dots, \omega_n(t))$ and $\rho(t) = (\rho_1(t), \dots, \rho_n(t))$ orbits of Equations (2.10) with given initial conditions. Supposing that Limit (2.13) holds, we hence have

$$J(\omega(0)) = \lim_{t \rightarrow \infty} J(\omega(t)) = \omega_c \sum_{j=1}^n \frac{1}{s_j} \quad \text{and} \quad K(\rho(0)) = \lim_{t \rightarrow \infty} K(\rho(t)) = \rho_c \sum_{j=1}^n \frac{1}{s_j}$$

and so the asymptotic values are analytically expressed as

$$\omega_c = \frac{\sum_{j=1}^n \frac{\omega_j(0)}{s_j}}{\sum_{j=1}^n \frac{1}{s_j}} \quad \text{and} \quad \rho_c = \frac{\sum_{j=1}^n \frac{\rho_j(0)}{s_j}}{\sum_{j=1}^n \frac{1}{s_j}}. \quad (2.14)$$

¹ In these contributions, the authors considered the coupling dynamics with delay of the form: $\sum_{j=1}^n l_{k,j} \sin(\phi_k(t) - \phi_j(t-t))$, that is, delays concern the ‘‘exterior’’ variables ϕ_j and not the ‘‘local’’ variable ϕ_k . This can be done here for the coupling dynamics but not for the adaptive mechanism on ω_k , if we require J to be a constant of motion J .

It is important to emphasize that the consensual values ω_c and ρ_c do not depend on the network topology (i.e. not on L), nor on the initial conditions of the state variables (i.e. not on $(\phi_k(0), r_k(0))$) nor on the time delay (i.e. not on \mathbf{t}).

Convergence Conditions - To this aim we study the first order approximation of Equations (2.10) in the vicinity of Solution (2.12) and assume that linear stability analysis is sufficient to infer convergence conditions for the nonlinear system. Accordingly, we study the asymptotic behavior of the small perturbations $\epsilon_{\phi_k}(t)$, $\epsilon_{r_k}(t)$, $\epsilon_{\omega_k}(t)$ and $\epsilon_{\rho_k}(t)$ and write

$$(\phi_k(t), r_k(t), \omega_k(t), \rho_k(t)) = (\omega_c t + \epsilon_{\phi_k}(t), \sqrt{\rho_c} + \epsilon_{r_k}(t), \omega_c + \epsilon_{\omega_k}(t), \rho_c + \epsilon_{\rho_k}(t)).$$

Taking into account the constant of motions, we impose that

$$\sum_{j=1}^n \frac{\epsilon_{\omega_j}(0)}{s_j} = 0 \quad \text{and} \quad \sum_{j=1}^n \frac{\epsilon_{\rho_j}(0)}{s_j} = 0. \quad (2.15)$$

First Order Approximation

Rearranging the variables (i.e. the first n are the ϕ_k , the second n are the r_k , the third n are the ω_k and finally the last n are the ρ_k), the first order approximation of Equations (2.10) is

$$\begin{pmatrix} \dot{\epsilon}_{\phi} \\ \dot{\epsilon}_r \\ \dot{\epsilon}_{\omega} \\ \dot{\epsilon}_{\rho} \end{pmatrix} = \begin{pmatrix} \mathbf{0} & \mathbf{0} & Id & \mathbf{0} \\ \mathbf{0} & -2\rho_c Id & \mathbf{0} & \sqrt{\rho_c} Id \\ \mathbf{0} & \mathbf{0} & \mathbf{0} & \mathbf{0} \\ \mathbf{0} & \mathbf{0} & \mathbf{0} & \mathbf{0} \end{pmatrix} \begin{pmatrix} \epsilon_{\phi} \\ \epsilon_r \\ \epsilon_{\omega} \\ \epsilon_{\rho} \end{pmatrix} + \begin{pmatrix} -\rho_c [c] L & \mathbf{0} & \mathbf{0} & \mathbf{0} \\ \mathbf{0} & -[c] L & \mathbf{0} & \mathbf{0} \\ -\rho_c [s] L & \mathbf{0} & \mathbf{0} & \mathbf{0} \\ \mathbf{0} & -2\sqrt{\rho_c} [s] L & \mathbf{0} & \mathbf{0} \end{pmatrix} \begin{pmatrix} \check{\epsilon}_{\phi} \\ \check{\epsilon}_r \\ \check{\epsilon}_{\omega} \\ \check{\epsilon}_{\rho} \end{pmatrix} \quad (2.16)$$

with the $n \times n$ identity matrix Id , diagonal matrices $[c]$ and $[s]$ with, respectively, the coupling strengths and the susceptibility constants as entries and $\epsilon_{\phi} := (\epsilon_{\phi_1}, \dots, \epsilon_{\phi_n})$, $\epsilon_r := (\epsilon_{r_1}, \dots, \epsilon_{r_n})$, $\epsilon_{\omega} := (\epsilon_{\omega_1}, \dots, \epsilon_{\omega_n})$ and $\epsilon_{\rho} := (\epsilon_{\rho_1}, \dots, \epsilon_{\rho_n})$, and where the delayed perturbations are $\check{\epsilon}_{\phi} = \epsilon_{\phi}(t-t)$, $\check{\epsilon}_r = \epsilon_r(t-t)$, $\check{\epsilon}_{\omega} = \epsilon_{\omega}(t-t)$, $\check{\epsilon}_{\rho} = \epsilon_{\rho}(t-t)$.

Diagonalization

Suppose now that $[s] = \mathbf{q}[c]$ for some positive constant \mathbf{q} and let O denote an orthogonal matrix (i.e. $O^{\top} O = O O^{\top} = Id$) with real entries such that $O^{\top} [c]^{\frac{1}{2}} L [c]^{\frac{1}{2}} O = [\zeta]$, with $[\zeta]$ being a diagonal matrix with the eigenvalues of the symmetric matrix $[c]^{\frac{1}{2}} L [c]^{\frac{1}{2}}$ on its diagonal. The sign of these coincide with those of the eigenvalues of L : they are all strictly positive except for one that is zero. Hence, without loss of generality, one takes $\zeta_1 = 0$ and $\zeta_k > 0$ for $k = 2, \dots, n$.

Changing the basis of System (2.16) with a 4×4 bloc matrix (each bloc of size $n \times n$) with $O^{\top} [c]^{-\frac{1}{2}}$ on its diagonal, we can decompose the original system into $2n$ 2-dimensional systems of the form

$$\begin{pmatrix} \dot{\epsilon}_{\phi_k} \\ \dot{\epsilon}_{\omega_k} \end{pmatrix} = \begin{pmatrix} 0 & 1 \\ 0 & 0 \end{pmatrix} \begin{pmatrix} \epsilon_{\phi_k} \\ \epsilon_{\omega_k} \end{pmatrix} + \begin{pmatrix} -\rho_c \zeta_k & 0 \\ -\rho_c \mathbf{q} \zeta_k & 0 \end{pmatrix} \begin{pmatrix} \check{\epsilon}_{\phi_k} \\ \check{\epsilon}_{\omega_k} \end{pmatrix} \quad (2.17a)$$

$$\begin{pmatrix} \dot{\epsilon}_{r_k} \\ \dot{\epsilon}_{\rho_k} \end{pmatrix} = \begin{pmatrix} -2\rho_c & \sqrt{\rho_c} \\ 0 & 0 \end{pmatrix} \begin{pmatrix} \epsilon_{r_k} \\ \epsilon_{\rho_k} \end{pmatrix} + \begin{pmatrix} -\zeta_k & 0 \\ -2\sqrt{\rho_c} \mathbf{q} \zeta_k & 0 \end{pmatrix} \begin{pmatrix} \check{\epsilon}_{r_k} \\ \check{\epsilon}_{\rho_k} \end{pmatrix} \quad (2.17b)$$

with $\epsilon_{\phi} := O^{\top} [c]^{-\frac{1}{2}} \epsilon_{\phi}$ (respectively for $\epsilon_r, \epsilon_{\omega}, \epsilon_{\rho}$) and $\check{\epsilon}_{\phi} := O^{\top} [c]^{-\frac{1}{2}} \check{\epsilon}_{\phi}$ (respectively for $\check{\epsilon}_r, \check{\epsilon}_{\omega}, \check{\epsilon}_{\rho}$) for delayed perturbations obtained after the change of basis.

The case $k = 1$ is worked out in the Appendix 2.A. For $k \neq 1$, let us focus on the 2-dimensional systems and we rewrite Equations (2.17) as linear second order time delayed differential equations

$$\begin{aligned} \ddot{\epsilon}_{\phi_k}(t) + \rho_c \zeta_k \dot{\epsilon}_{\phi_k}(t-t) + \rho_c \mathbf{q} \zeta_k \epsilon_{\phi_k}(t-t) &= 0, \\ \ddot{\epsilon}_{r_k}(t) + 2\rho_c \dot{\epsilon}_{r_k}(t) + \zeta_k \dot{\epsilon}_{r_k}(t-t) + 2\rho_c \mathbf{q} \zeta_k \epsilon_{r_k}(t-t) &= 0. \end{aligned} \quad (2.18)$$

The convergence towards a consensual state is hence determined by the asymptotic stability of the zero solution of Equations (2.18). Stability follows if, and only if, all roots of the corresponding characteristic equations have strictly negative real parts (c.f. [8] for details). For Equations (2.17a), one can apply Theorem 3.3 in [14] which states that in this case the zero solution is asymptotically stable if and only if

$$\text{I} \quad \mathbf{t} \rho_c \zeta_k < \frac{\pi}{2} \quad (2.19a)$$

$$\text{II} \quad \frac{\mathbf{t}^2 \rho_c \mathbf{q} \zeta_k}{z^2} < \cos(z) \text{ where } z \text{ is the unique solution in }]0, \frac{\pi}{2}[\text{ of } \sin(z) = \frac{\mathbf{t} \rho_c \zeta_k}{z} \quad (2.19b)$$

for $k = 2, \dots, n$. We emphasize that the consensual value ρ_c influences the condition for convergence whereas it is not the case for ω_c . This leads to the idea that shaping the attractor is more delicate than tuning the angular velocity. This has been observed in [46].

Adaptation only on ω_k - If there is no adaptation on the radii (i.e. $\rho_k(t) := r$ for all k and t), then the Equations (2.17b) reduce to

$$\dot{\epsilon}_{r_k}(t) = -2r \epsilon_{r_k}(t) - \zeta_k \epsilon_{r_k}(t-t)$$

for which the zero solution is asymptotically stable provided (c.f. [33] for details)

$$4r^2 < \zeta_k^2 \quad \text{and} \quad \mathbf{t} < \check{\mathbf{t}} \quad \text{with} \quad \check{\mathbf{t}} = \frac{\cot^{-1}\left(\frac{-2r}{\sqrt{\zeta_k^2 - 4r^2}}\right)}{\sqrt{\zeta_k^2 - 4r^2}}. \quad (2.20)$$

The zero solution is unstable when $\mathbf{t} > \check{\mathbf{t}}$. Note that stability is guaranteed for any \mathbf{t} when $\zeta_k^2 < 4r^2$ or $\zeta_k^2 = 4r^2 \neq 0$.

No Time Delay in the Coupling Dynamics - If there is no time delay in the coupling dynamics (i.e. the coupling dynamics is defined as in Equations (2.8) with no delay), then Equations (2.18) become, for $k = 2, \dots, n$,

$$\ddot{\epsilon}_{\phi_k}(t) + \rho_c \zeta_k \dot{\epsilon}_{\phi_k}(t) + \rho_c \mathbf{q} \zeta_k \epsilon_{\phi_k}(t-t) = 0, \quad (2.21a)$$

$$\ddot{\epsilon}_{r_k}(t) + (2\rho_c + \zeta_k) \dot{\epsilon}_{r_k}(t) + 2\rho_c \mathbf{q} \zeta_k \epsilon_{r_k}(t-t) = 0. \quad (2.21b)$$

Invoking Theorem 3.5 in [14], the zero solution for Equations (2.21a) and Equations (2.21b) is asymptotically stable if and only if

$$\begin{aligned} \text{For Equations (2.21a): } -\mathbf{t}^2 \rho_c \mathbf{q} \zeta_k + (z^2 + \mathbf{t}^2 (\rho_c \zeta_k)^2) \cos(z) > 0 \text{ where } z \text{ is the} \\ \text{unique solution in }]0, \frac{\pi}{2}[\text{ of } z \sin(z) = \mathbf{t} \rho_c \zeta_k \cos(z) \end{aligned} \quad (2.22a)$$

$$\begin{aligned} \text{For Equations (2.21b): } -2\mathbf{t}^2 \rho_c \mathbf{q} \zeta_k + (z^2 + \mathbf{t}^2 (2\rho_c + \zeta_k)^2) \cos(z) > 0 \text{ where } z \text{ is the} \\ \text{unique solution in }]0, \frac{\pi}{2}[\text{ of } z \sin(z) = \mathbf{t} (2\rho_c + \zeta_k) \cos(z) \end{aligned} \quad (2.22b)$$

for $k = 2, \dots, n$.

Summary

For a network (with arbitrary topology but with symmetric, positive entries adjacency matrix) of HOPF oscillators (as defined in Section 2.2.1 by Equations (2.7)) interacting through time delayed KURAMOTO type coupling (as defined in Section 2.2.2 by Equations (2.8)) and with time delay adaptive mechanisms (as defined in Section 2.2.3 by Equations (2.9)) on the frequencies and amplitudes of the local systems - in other words, for Equations (2.10) - we have

I two constants of motions (c.f. (2.11))

- II the existence of a consensual oscillatory state (c.f. (2.12))
- III the consensual oscillatory state is linearly (i.e. locally) stable if all the roots of characteristic equations corresponding to Equations (2.18) have strictly negative real parts
- IV if there is no adaptation on the radii, the consensual oscillatory state is linearly (i.e. locally) stable if (2.19a), (2.19b) and (2.20) hold
- V if there is no delay in the coupling dynamics, the consensual oscillatory state is linearly (i.e. locally) stable if (2.22a) and (2.22b) hold

2.3.1 Miscellaneous Remark: Delayed Stabilization Mechanism

In this section we discuss the particular case arising when the delay is introduced only in the stabilization mechanism (i.e. dissipative part) of the local dynamics. The dynamical system is

$$\begin{aligned}
\dot{\phi}_k(t) &= \omega_k(t) + c_k \sum_{j=1}^n l_{k,j} r_k(t) r_j(t) \sin(\phi_k(t) - \phi_j(t)) \\
\dot{r}_k(t) &= -(r_k(t-t)^2 - \rho_k(t)) r_k(t) - c_k \sum_{j=1}^n l_{k,j} r_j(t) \cos(\phi_k(t) - \phi_j(t)) \\
\dot{\omega}_k(t) &= s_k \sum_{j=1}^n l_{k,j} r_k(t) r_j(t) \sin(\phi_k(t) - \phi_j(t)) \\
\dot{\rho}_k(t) &= -s_k \sum_{j=1}^n l_{k,j} r_j(t)^2
\end{aligned} \tag{2.23}$$

$k = 1, \dots, n.$

Equations (2.23) still admit the existence of a consensual oscillatory state and two constants of motion as in (2.11) and in (2.12) respectively. Linear stability analysis of the consensual state reduces to the study of

$$\ddot{\varepsilon}_{\phi_k}(t) + \rho_c \zeta_k \dot{\varepsilon}_{\phi_k}(t) + \rho_c \mathbf{q} \zeta_k \varepsilon_{\phi_k}(t) = 0, \tag{2.24a}$$

$$\ddot{\varepsilon}_{r_k}(t) + 2\rho_c \dot{\varepsilon}_{r_k}(t-t) + 2\rho_c \mathbf{q} \zeta_k \varepsilon_{r_k}(t) = 0, \tag{2.24b}$$

for $k = 2, \dots, n$. The zero solution for Equations (2.24a) is asymptotically stable. For Equations (2.24b), we apply Theorem 3.4 in [14] which states that in this case the zero solution is asymptotically stable if and only if

$$\text{I } \exists z \in \mathbb{Z}_{\geq 0} := \{0, 1, 2, \dots\} \text{ such that } (2z-1)\pi + \frac{\pi}{2} < \mathbf{t} \sqrt{2\rho_c \mathbf{q} \zeta_k} < 2z\pi + \frac{\pi}{2}$$

$$\text{II } 0 > -2\mathbf{t}\rho_c > \max \left\{ (2z-1)\pi + \frac{\pi}{2} - \frac{2\mathbf{t}^2 \rho_c \mathbf{q} \zeta_k}{(2z-1)\pi + \frac{\pi}{2}}, -(2z\pi + \frac{\pi}{2}) + \frac{2\mathbf{t}^2 \rho_c \mathbf{q} \zeta_k}{2z\pi + \frac{\pi}{2}} \right\}$$

for $k = 2, \dots, n$.

2.4 Applications

Conceptually, the problem of reliably distributing time and frequency among several spatial remote location is a “letmotiv” in applications ranging from basic metrology, navigation and position determination, signal processing, computer communications, energy distribution networks, swarms robotics, bioengineering, multi-agents systems, life sciences, acoustics and musical art to give but only a highly non-exhaustive list. Presently, a strong research impetus is devoted to complex interacting oscillating systems able to exhibit self-adaptive capabilities leading to a resilient consensual dynamic. Whatever the configurations under study, communication delays between the collection of interacting subparts of the global systems are physically unavoidable. Depending on the underlying time scales, delays do strongly affect the resulting dynamics. Our class of models explicitly study the influence of delays and in particular their destabilizing effects, that modify the instantaneous behavior. By an appropriate tuning of control parameters (e.g. susceptibility constants), our class of models offer, via a unique formalism, the possibility to continuously explore interacting configurations ranging from slave-master (i.e. system-environment relationship) to fully decentralized

regimes.

Alternatively, we may view this problematic in the context of soft controlled systems which presently receive a sustain attention [26]. Here, a swarm of agents is infiltrated by a lure agent (sometimes called a shill in economy). While the lure exhibits all the features of any ordinary agent, it can be externally controlled by an operator. As the interactions between the lure and any agent of the swarm remain unaffected (i.e. the lure remains incognito to ordinary agents), the external control of the lure can ultimately drive the whole population to a specific configuration. In our class of dynamics, a suitable choice of the susceptibility constant of a given local system (i.e. oscillator) may convert it into a shill. Indeed, in view of Equations (2.14), the ultimate consensual values ω_c and ρ_c are weighted averages. Such weighted averages can be made to strongly dependent on a very insensitive shill - stubborn to any external influence (i.e. with a very low susceptibility constant).

In absence of time delays, convergence towards a consensual state is observed even for large heterogeneities (widely dispersed initial frequencies and radii and large discrepancies among the susceptibility constants). Hence, a shill agent can be easily introduced. However, our present study shows, that time delays restrict the conditions for convergence towards a consensual state. As a consequence, the implementation of a lure is more delicate matter (i.e. here, the dynamics is far more sensitive to the value taken by the susceptibility constants).

2.5 Numerical Simulations

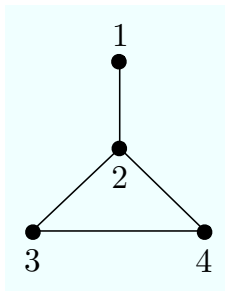


Fig. 2.1: Network topology

Adaptation on ω_k and ρ_k - We consider four HOPF oscillators interacting on a network with topology as in Figure 2.1. We choose the coupling strengths and susceptibility constants as $\{c_1, \dots, c_4\} = \{0.1, 2, 5, 3\}$ and $s_k = 0.8c_k$ for $k = 1, \dots, 4$ (i.e. $\mathbf{q} = 0.8$). The time delay is $\mathbf{t} = 0.1$. The initial function (i.e. history) is $(\phi_k(t), r_k(t), \omega_k(t), \rho_k(t)) = (t, 1, 1, 1)$ for $t \in [-\mathbf{t}, 0[$, having a jump at $t = 0$ with values $(\phi_k(0), r_k(0), \omega_k(0), \rho_k(0))$ that are randomly uniformly drawn from $] - 0.1, 0.1[\times] 0.9, 1.1[\times] 0.9, 1.1[\times] 0.9, 1.1[$ with the exception for $\omega_1(0) = 0.9$. The $\rho_k(0)$ are rescaled such that the consensual value ρ_c is one.

The resulting dynamics is shown in Figure 2.2. With the same initial conditions, we carry out another numerical simulation with here $\mathbf{t} = 0.12$. This violates Condition (2.19b) for $k = 4$ and hence the network does not converge towards a consensual state. This is shown in Figure 2.3.

Note that in Figure 2.2(a), the $\omega_k(0)$ converge close to 0.9, that is, close to the initial value $\omega_1(0)$. This because the first oscillator's susceptibility is "small" and hence it is this local system that acts as a shill. It interacts with its neighbor in the same way as they act with it. It can control the behavior of the network and this without being connected to all other local system.

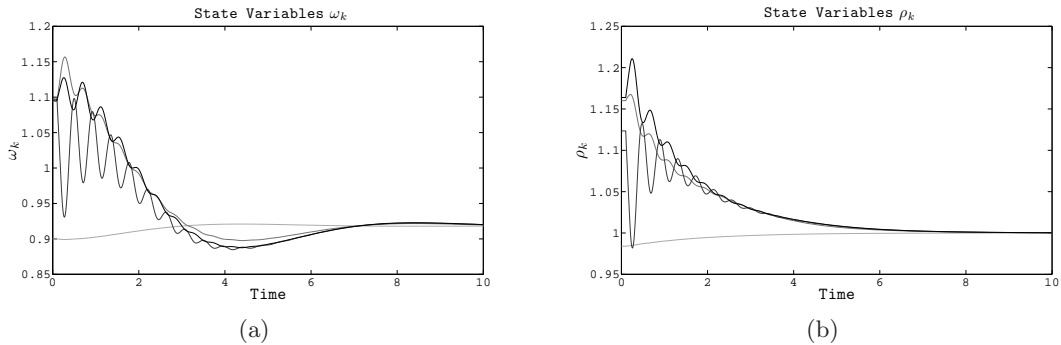


Fig. 2.2: Time evolution of ω_k (Figure 2.2(a)) and ρ_k (Figure 2.2(b)) for four HOPF oscillators, interacting through the network in Figure 2.1. In both figures, all variables converge towards a constant and common consensual value.

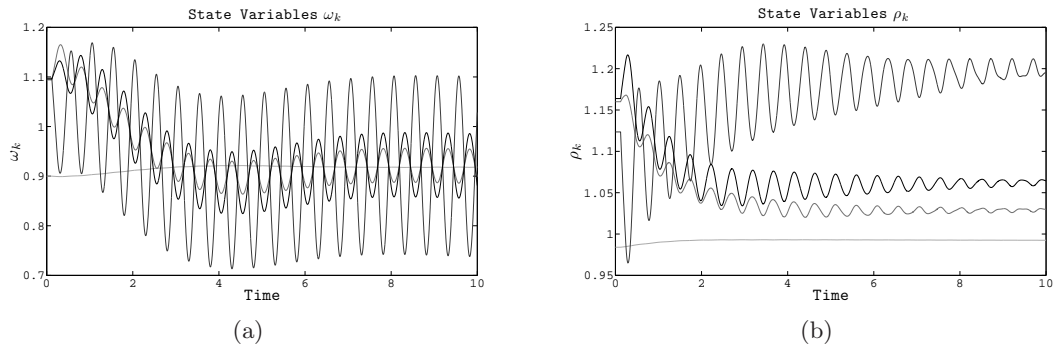


Fig. 2.3: Time evolution of ω_k (Figure 2.3(a)) and ρ_k (Figure 2.3(b)) for four HOPF oscillators, interacting through the network in Figure 2.1. In both figures, no common consensual value is reached.

In the extreme case, when $s_k = 0$ for all k (i.e. no adaptation), Equations (2.10) describe the dynamics of coupled oscillators with different limit cycles and frequencies and delayed interactions. For small frequency and attractor's shape heterogeneities, the network is able to synchronize. In this case (i.e. without adaptive mechanisms for ω_k and ρ_k), several numerical simulations show that for delayed time $t = 0.1175$ synchronization is not systematically attained (i.e. it depends on the initial conditions) - whereas it is attained in the absence of the time delay (i.e. $t = 0$). On the other hand, when the adaptive mechanisms are switched on (i.e. $s_k = 0.8c_k > 0$ for all k), a consensual state is reached - the linear stability criteria are still satisfied with $t = 0.1175$. Summarizing, here adaptation enhances the synchronization capability of the network.

Adaptation only on ω_k - Two HOPF oscillators, both having the same radius for the attractor (i.e. $\rho_k = r = 0.1$ for $k = 1, 2$), are coupled with coupling strengths and susceptibility constants as $\{c_1, c_2\} = \{1, 14\}$ and $s_k = c_k$ for $k = 1, 2$ (i.e. $q = 1$). The time delay is $t = 0.1057$. The initial function (i.e. history) is $(\phi_k(t), r_k(t), \omega_k(t)) = (t, \sqrt{0.1}, 1)$ for $t \in [-t, 0[$, having a jump at $t = 0$ with values $(\phi_k(0), r_k(0), \omega_k(0))$ that are randomly uniformly drawn from $] - 0.1, 0.1[\times]\sqrt{0.1} - 0.05, \sqrt{0.1} + 0.05[\times]0.9, 1.1[$. Under this configuration, Conditions (2.19) are satisfied (hence the zero solution of Equation (2.17a) is asymptotically stable) but not Condition (2.20) - the time delay is too large. Figure 2.4 displays the resulting dynamics. Observe that the radii do not converge towards their attractor. However, the oscillators still adapt their frequencies.

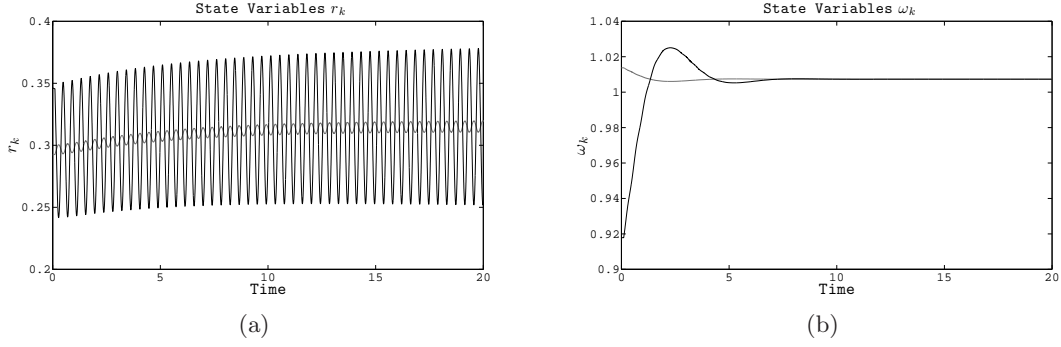


Fig. 2.4: Time evolution of r_k (Figure 2.4(a)) and ω_k (Figure 2.4(b)) for two HOPF oscillators. The two oscillators manage to adapt their frequencies while their radii do not converge towards their respective attractor.

2.6 Conclusion

It is more the rule than the exception that parameter adaptation in dynamical systems can be achieved via delayed mechanisms. This therefore converts ordinary differential equations arising in absence of delay to functional differential equations. Stability issues become more difficult to discuss since, dealing with functional differential equations, an infinite number of degrees of freedom is introduced into the dynamics. For the class of oscillatory networks with parametric adaptation we here considered, we are able to observe how the time delay affects the adaptation mechanisms. While it is intuitively expected, that large delays are likely to destabilize the dynamics, we are here able to analytically quantify the underlying critical delays. The analytical linear stability discussion is made possible since, for our class of dynamics, stability issues can be reduced to the study of two linear second order functional differential equations for which suitable theorems can be found. Finally, we emphasize that numerical simulations show that adaptation may enhance the emergence of common dynamical pattern whereas in classical synchronization, time delays may be too large for synchronous motion to be attained.

Appendix

2.A Stability Analysis for Case $k = 1$

Assuming that all perturbations $\varepsilon_{\phi_k}, \varepsilon_{r_k}, \varepsilon_{\omega_k}, \varepsilon_{\rho_k}, \check{\varepsilon}_{\phi_k}, \check{\varepsilon}_{r_k}, \check{\varepsilon}_{\omega_k}$ and $\check{\varepsilon}_{\rho_k}$ for $k = 2, \dots, n$ converge to zero, let us now study the case for $k = 1$. Here, $\zeta_1 = 0$ and so

$$\dot{\varepsilon}_{\phi_1} = \varepsilon_{\omega_1}, \quad \dot{\varepsilon}_{\omega_1} = 0 \quad \text{and} \quad \dot{\varepsilon}_{r_1} = -2\rho_c \varepsilon_{r_1} + \sqrt{\rho_c} \varepsilon_{\rho_1}, \quad \dot{\varepsilon}_{\rho_1} = 0$$

and therefore $\varepsilon_{\omega_1}(t) = \varepsilon_{\omega_1}(0)$ and $\varepsilon_{\rho_1}(t) = \varepsilon_{\rho_1}(0)$ for all t . Both of these constants $\varepsilon_{\omega_1}(0)$ and $\varepsilon_{\rho_1}(0)$ are zero. This is because the first orthonormal base vector (i.e. the normalized eigenvector for the eigenvalue $\zeta_1 = 0$) is $\mathfrak{C}(\frac{1}{\sqrt{c_1}}, \dots, \frac{1}{\sqrt{c_n}})$ (with $\mathfrak{C} := (\sum_{j=1}^n \frac{1}{c_j})^{-\frac{1}{2}}$) and the first coordinate of $O^\top[\mathfrak{c}]^{-\frac{1}{2}} \varepsilon_\omega$ and $O^\top[\mathfrak{c}]^{-\frac{1}{2}} \varepsilon_\rho$ is, respectively,

$$\varepsilon_{\omega_1}(0) = \mathfrak{C} \sum_{j=1}^n \frac{\varepsilon_{\omega_j}(0)}{c_j} = \mathfrak{C} \mathfrak{q} \sum_{j=1}^n \frac{\varepsilon_{\omega_j}(0)}{\mathfrak{s}_j} \quad \text{and} \quad \varepsilon_{\rho_1}(0) = \mathfrak{C} \sum_{j=1}^n \frac{\varepsilon_{\rho_j}(0)}{c_j} = \mathfrak{C} \mathfrak{q} \sum_{j=1}^n \frac{\varepsilon_{\rho_j}(0)}{\mathfrak{s}_j}$$

since we supposed that $\mathfrak{s}_j = \mathfrak{q}c_j$ for all j . These two sums are zero according to Equations (2.15). Therefore, $\dot{\varepsilon}_{r_1} = -2\rho_c \varepsilon_{r_1}$ (i.e. $\lim_{t \rightarrow \infty} \varepsilon_{r_1}(t) = 0$) and $\varepsilon_{\phi_1}(t) = \varepsilon_{\phi_1}(0)$ for all t . This allows to conclude that all perturbations $\varepsilon_{r_k}, \varepsilon_{\rho_k}$ and ε_{ω_k} decay for all k . We now need to study how the perturbations on the phases evolve. Since $\varepsilon_\phi = [\mathfrak{c}]^{\frac{1}{2}} O \varepsilon_\phi$, then

$$\lim_{t \rightarrow \infty} \epsilon_{\phi_k}(t) = \lim_{t \rightarrow \infty} \sqrt{c_k} \sum_{j=1}^n o_{k,j} \epsilon_{\phi_j}(t) = \sqrt{c_k} o_{k,1} \lim_{t \rightarrow \infty} \epsilon_{\phi_1}(t) = \mathfrak{E} \epsilon_{\phi_1}(0) = \mathfrak{E}^2 \sum_{j=1}^n \frac{\epsilon_{\phi_j}(0)}{c_j} = \frac{\sum_{j=1}^n \frac{\epsilon_{\phi_1}(0)}{c_j}}{\sum_{j=1}^n \frac{1}{c_j}}$$

since $\lim_{t \rightarrow \infty} \epsilon_{\phi_k}(t) = 0$ for $k = 2, \dots, n$, $o_{k,1} = \mathfrak{E} \frac{1}{\sqrt{c_k}}$ ($k = 1, \dots, n$) and the first coordinate of the product $O^\top[\mathbf{c}]^{-\frac{1}{2}} \epsilon_\phi$ is $\epsilon_{\phi_1}(0) = \mathfrak{E} \sum_{j=1}^n \frac{\epsilon_{\phi_j}(0)}{c_j}$. Hence all perturbations converge towards zero except those on the phase that all converge towards a constant (i.e. average phase perturbation). This corresponds to a phase shift.

Adaptation of Oscillatory Systems in Networks - A Learning Signal Approach

Dass der noch kaum zu Ende gedachte Gedanke, das noch feucht hingeschriebene Wort in derselben Sekunde schon Tausende Meilen weit empfangen, gelesen, verstanden werden kann und dass der unsichtbare Strom, der zwischen den beiden Polen der winzigen Voltaschen Säule schwingt, ausgedehnt zu werden vermag über die ganze Erde von ihrem einen bis zum anderen Ende.

Stefan ZWEIG

Abstract

We consider a complex system of n periodic signal generators interacting through the gradient of a coupling potential. Each local system has its own set of parameters Ω_k , characterizing the time scale of the signal and its shape (i.e. coefficients of a truncated FOURIER series). Due to additional coupling functions, the Ω_k are allowed to adapt (i.e. modify their values). The adaptive mechanisms, with the help of the usual state variable interactions, drive all local system towards a consensual oscillatory state where they all have a common, constant set of parameters Ω_c . Once reached, the consensual oscillatory state remains invariant to the coupling functions. This implies that if the interactions are removed, local system continue delivering the common and synchronized signal. It also means that any perturbation due to the coupling does not affect the local systems. This situation is to be contrasted with classical synchronization problems where common dynamical patterns are attained and maintained thanks to the interactions. Also, in synchronization, the set Ω_k is constant, implying that all local system converge back towards their individual behavior in the absence of interactions. The resulting value Ω_c is analytically calculated. It does not depend on the network's topology. However, the conditions for convergence do dependent on the connectivity of the network as well as on the coupling potential.

3.1 Introduction

Producing stable oscillatory motion is of great importance for a device delivering stable periodic signals. Due to its stability mechanism, the apparatus sends out signals that are not drastically altered even if it is placed in a noisy environment. However, structural changes within the device may occur (e.g. the stability mechanism may itself be perturbed), and these create permanent discrepancies, thus lowering the quality of the output signal. To overcome this problem, a signal can be coupled to another of its likes. As an example, consider two coupled signals $r_1(t)$ and $r_2(t)$ in the setup

$$\dot{r}_k = R(r_k; \Omega_k) - \frac{\partial V}{\partial r_k}(r_1, r_2) \quad k = 1, 2 \quad (3.1)$$

with the gradient of a potential V as coupling function. Here, the set of parameters $0 \neq \|\Omega_1 - \Omega_2\| \ll 1$, due to a structural change. Synchronizing signals may enhance the overall quality in the sense that now, under suitable conditions,

$$\lim_{t \rightarrow \infty} r_k(t) = r_{k,V}(t) \quad k = 1, 2$$

with signals $r_{k,V}(t)$ having the same periodicity t_V .

However, synchronized signals $r_{1,V}(t)$ and $r_{2,V}(t)$ only exit at the coast of maintaining the coupling - if the coupling vanishes (i.e. $V \equiv 0$), the two individual signals return, respectively, towards the signals produced by the vector fields $R(\cdot; \Omega_k)$ $k = 1, 2$. Furthermore, $r_{k,V}(t)$, and consequently period t_V , is subject to any change in the coupling: if V changes, the synchronized signals, as well as their periodic behavior, are perturbed.

One way to tackle this problem is to construct systems that can synchronize and simultaneously “adapt” local characteristics (i.e. Ω_k) in order to be

- I closer to their likes (i.e. reduce the difference $\|\Omega_1 - \Omega_2\|$)
- II less dependent on the coupling (i.e. find $\check{\Omega}_k$ such that $Z(\check{\Omega}_1, \check{\Omega}_2) = \|\nabla V(\check{r}_1(t), \check{r}_2(t))\|$ is minimum over a period and $\check{r}_k(t)$ solves Equations (3.1))

An optimum solution for I and II is when there exists a consensual parameter set $\Omega_c = \Omega_k$, $k = 1, 2$ such that $Z(\check{\Omega}_c, \check{\Omega}_c) = 0$. In this situation, if the coupling is removed, the devices continue to deliver the same signal. Furthermore, at this consensual state, any changes in the coupling does not affect the signals since they are now independent if it.

Technically, for local parameters Ω_k to adapt, they must become time-dependent (i.e. $\Omega_k \rightsquigarrow \Omega_k(t)$) and have their own dynamics. For n coupled signals, having each an additional phase variable controlling their time scale, the general complex networks dynamics is

$$\begin{aligned} \dot{\phi}_k &= P(\phi_k, r_k, \Omega_k) + \frac{\partial V}{\partial \phi_k}(\phi, r) \\ \dot{r}_k &= \underbrace{R(\phi_k, r_k, \Omega_k)}_{\text{local dynamics}} + \underbrace{\frac{\partial V}{\partial r_k}(\phi, r)}_{\text{coupling dynamics}} \quad k = 1, \dots, n \\ \dot{\Omega}_k &= \underbrace{A_k(\phi, r)}_{\text{adaptive mechanisms}} \end{aligned} \quad (3.2)$$

with $\phi = (\phi_1, \dots, \phi_n)$, $r = (r_1, \dots, r_n)$, and P and R belonging to the same class of PR systems (i.e. phase-radius systems). Adapting parameters in complex systems has long been a busy filed of research. Whereas in other contributions adaptation occurs in the coupling strength [36] or directly in the connections [18], Equations (3.2) describe adaptation in the local systems. As mentioned in [42], for local systems’ parameter adaptation, there exit two types: flow parameters controlling the frequency or time scale on an attractor, and geometric parameters determining the shape of the attracting set. Frequency or time scale controlling parameters have, in general, a high propensity for adaptation and have been well studied in [20, 56, 4, 45]. However, not much has been accomplished for shaping local attractors, which, by nature, is a more delicate task - as stated in [46].

In this paper, we present new adaptive mechanisms for modifying the local system’s attractor. Whereas in [46] the adaptive mechanisms implicitly depend on the parameter set Ω_k via a functional, ours solely depend¹ on the state variables ϕ_k and r_k . In [46], one needs to calculate or numerically compute an integral beforehand to know the sign of the function for the adaptive mechanism. Our approach is systematic for all parameters.

¹ Note that adaptive mechanisms should only dependent on the stat variables since, in practice, these are the only information available.

This contribution is organized as follows: We present individually the components of our network's dynamical system in Section 3.2. In Section 3.3 we discuss the resulting dynamics and present to related alternative to our system. Numerical simulations are reported in Section 3.4, and we conclude in Section 3.5.

3.2 Networks of Periodic Stable Signals with Adaptive Mechanisms

Consider a n -vertex connected and undirected network with positive adjacency entries. To each node corresponds a local dynamical system defined in Section 3.2.1. While the network topology (i.e. adjacency matrix) of the underlying network indicates if the k^{th} local system is connected to the j^{th} (and vice versa), it is the coupling dynamics discussed in Section 3.2.2 that describes how the neighboring local dynamics interact. Described in Section 3.2.3, supplementary interactions directly acting on the local systems' parameters will play the role of adaptive mechanisms. Let us now individually present each three dynamical components.

3.2.1 Local Dynamics

The local systems belong to the class of PR systems. We here focus on Periodic Stable Signals (PSS) which we define as

$$\begin{aligned} \text{P}(\phi_k, r_k; \Omega_k) &= \mathbf{w}_k \\ \text{R}(\phi_k, r_k; \Omega_k) &= \underbrace{-(r_k - \mathbf{F}_k(\phi_k))}_{\text{dissipative dynamics}} + \underbrace{\mathbf{F}'_k(\phi_k) \mathbf{w}_k}_{\text{oscillatory dynamics}} \quad k = 1, \dots, n \end{aligned} \quad (3.3)$$

with $\mathbf{F}_k(\phi_k) = \mathbf{u}_{k,0} + \sum_{s=1}^q \mathbf{u}_{k,s} \cos(s \phi_k) + \mathbf{v}_{k,s} \sin(s \phi_k)$. The set of parameters is $\Omega_k = \{\mathbf{w}_k, \mathbf{u}_{k,0}, \mathbf{u}_{k,1}, \mathbf{v}_{k,1}, \dots, \mathbf{u}_{k,q}, \mathbf{v}_{k,q}\}$. Parameter \mathbf{w}_k controls the time scale of the phase, which here oscillates uniformly (i.e. $\phi_k(t) = \mathbf{w}_k t + \varphi_k$). The rest of the parameters determine the shape of the stable periodic signal produced by a PSS. Stable here means that if the system endures a perturbation, it will converge back to its oscillatory motion and continue delivering the signal with its original shape given by the compact set $\mathbb{K}_k := \{(\phi, r) \in \mathbb{S}^1 \times \mathbb{R} \mid r - \mathbf{F}_k(\phi) = 0\}$. The convergence towards \mathbb{K}_k is discussed in Appendix 3.A. It is the dissipative dynamics that is responsible for driving the orbits towards \mathbb{K}_k . This term is the gradient (with respect to the variable r) of the potential $\frac{1}{2}(r - \mathbf{F}_k(\phi))^2$. It is seen as an energy controller that takes in and/or gives out energy (depending on the system's state) until it reaches its equilibrium state \mathbb{K}_k . On \mathbb{K}_k , the PSS's dynamics is governed by the oscillatory dynamics and so $\dot{r}_k(t) - \mathbf{F}'_k(\phi_k(t))\dot{\phi}_k(t) = 0$, which is consistence with Equation (3.3) when the dissipative dynamics is zero.

When $\mathbf{F}_k(\phi_k) = \mathbf{u}_{k,0}$, the PSS is a limit cycle oscillator with constant angular velocity and a circle of radius $\mathbf{u}_{k,0}$ as an attractor. As sketched in Figure 3.1, PSS may form more complicated and interesting attractors.

3.2.2 Coupling Dynamics

The coupling dynamics is here given by the gradient of a positive semi-definite coupling potential $\mathbf{V}(\phi, r) \geq 0$ (see Section 1.1.2 in [42] for precise definition). On \mathbf{V} , we have the following hypothesis

$$\phi = y\mathbf{1} \quad \text{and} \quad r = z\mathbf{1}, \quad y, z \in \mathbb{R} \quad \implies \quad \mathbf{V}(\phi, r) = 0$$

with $\phi = (\phi_1, \dots, \phi_n)$, $r = (r_1, \dots, r_n)$ and $\mathbf{1} = (1, \dots, 1)$. Bellow, we present two examples.

Example 1. Laplacian Potential Define \mathbf{V} as

$$\mathbf{V}(\phi, r) := \frac{1}{2} \langle r \mid L_{\cos} r \rangle = \frac{1}{2} \sum_{k=1}^n r_k \sum_{j=1}^n l_{k,j} r_j \cos(\phi_k - \phi_j) \geq 0$$

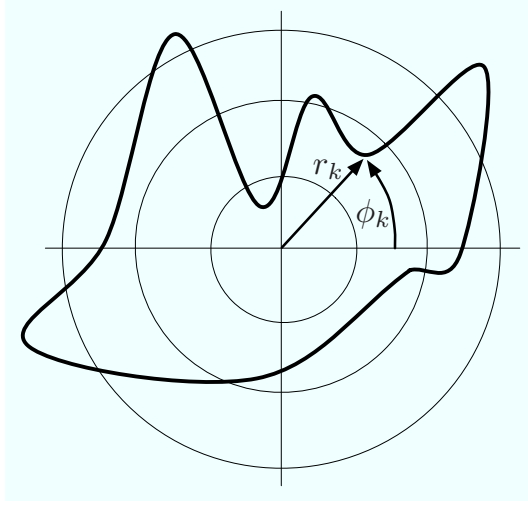


Fig. 3.1: Sketch of an attractor for a PSS. The dynamics evolves at a constant angular velocity $\dot{\phi}_k(t) = \omega_k t$ on the black thick curve.

with $\phi = (\phi_1, \dots, \phi_n)$ and $r = (r_1, \dots, r_n)$, and where the matrix L_{cos} has entries $l_{k,j} \cos(\phi_k - \phi_j)$ with L being the corresponding Laplacian matrix ($L := D - A$ where D is the diagonal matrix with $d_{k,k} := \sum_{j=1}^n a_{k,j}$). Matrix L_{cos} is positive semi-definite since, by ГЕРШГОРИН'S circle theorem [22], all its eigenvalues are positive (i.e. nonnegative). Explicitly, the coupling dynamics for this potential is

$$\begin{aligned} c_k \frac{\partial V}{\partial \phi_k}(\phi, r) &= -c_k \sum_{j=1}^n l_{k,j} r_k r_j \sin(\phi_k - \phi_j) \\ c_k \frac{\partial V}{\partial r_k}(\phi, r) &= c_k \sum_{j=1}^n l_{k,j} r_j \cos(\phi_k - \phi_j) \end{aligned} \quad k = 1, \dots, n,$$

where $c_k > 0$ are coupling strengths.

B Potential Define V as

$$V(\phi, r) := \frac{1}{2} \sum_{k,j=1}^n a_{k,j} (\mathbb{B}_{k,j}(\phi_k - \phi_j) + \mathbb{B}_{k,j}(r_k - r_j)) \geq 0$$

with edge weights $0 \leq a_{k,j} = a_{j,k}$, and where functions $\mathbb{B}_{k,j}$ satisfy $\mathbb{B}_{k,j}(x) \geq 0$, $\mathbb{B}_{k,j}(x) = 0 \Leftrightarrow x = 0$, $\mathbb{B}_{k,j}(x) = \mathbb{B}_{k,j}(-x)$ (i.e. even function) and $0 < \mathbb{B}_{k,j}''(0)$. As for the edge weights, we here impose $\mathbb{B}_{k,j} \equiv \mathbb{B}_{j,k}$. For the functions $\mathbb{B}_{k,j}$, one may take

$$\begin{aligned} \mathbb{B}_{k,j}(x) &= \frac{1}{2}x^2 & \text{Diffusion} & & \mathbb{B}_{k,j}(x) &= \cosh(x) - 1 \\ \mathbb{B}_{k,j}(x) &= 1 - \cos(x) & \text{KURAMOTO-type} & & \mathbb{B}_{k,j}(x) &= \log(\cosh(x)) \end{aligned}$$

Explicitly, the coupling dynamics for this potential is

$$\begin{aligned} c_k \frac{\partial V}{\partial \phi_k}(\phi, r) &= c_k \sum_{j=1}^n a_{k,j} \mathbb{B}'_{k,j}(\phi_k - \phi_j) \\ c_k \frac{\partial V}{\partial r_k}(\phi, r) &= c_k \sum_{j=1}^n a_{k,j} \mathbb{B}'_{k,j}(r_k - r_j) \end{aligned} \quad k = 1, \dots, n$$

with coupling strengths $c_k > 0$.

3.2.3 Adaptive Mechanisms

Here, adaptive mechanisms are additional interactions that modify the values of the local parameters. For this, the fixed and constant parameters Ω_k are now time-dependent (i.e. $\Omega_k = \{\mathbf{w}_k, \mathbf{u}_{k,0}, \mathbf{u}_{k,1}, \mathbf{v}_{k,1}, \dots, \mathbf{u}_{k,q}, \mathbf{v}_{k,q}\} \rightsquigarrow (\omega_k(t), \mu_{k,0}(t), \mu_{k,1}(t), \nu_{k,1}(t), \dots, \mu_{k,q}(t), \nu_{k,q}(t)) = \Omega_k(t)$, for $k = 1, \dots, n$) and each have their own dynamics, depending only on state variables ϕ and r that is, for all k , $\frac{\partial \mathbf{A}_k}{\partial \Omega_k} = \mathbf{0}$ with $\mathbf{0}$ a $2 + 2q$ dimensional vector of 0.

Time scale Adaptive Mechanisms

For adaptation on ω_k , we apply the same idea as developed in [46, 42] and so the explicit dynamics is

$$A_k^\omega(\phi, r) = -s_{\omega_k} \frac{\partial \mathcal{V}}{\partial \phi_k}(\phi, r) \quad k = 1, \dots, n,$$

where $s_{\omega_k} > 0$ are susceptibility constants, technically playing the role of coupling strengths but with the following interpretation: the smaller the value of s_{ω_k} , the less the PSS is willing to modify its value, and vice versa - the larger the value of s_{ω_k} , the more the PSS is willing to modify its value.

Amplitude Adaptive Mechanisms

Inspired by attractor-shaping mechanisms studied in [46, 42], we propose, for the PSS's $\mu_{k,0}$, $\mu_{k,s}$ and $\nu_{k,s}$, the following new adaptive mechanisms

$$\begin{aligned} A_k^{\mu_0}(\phi, r) &= -s_{\mu_{k,0}} \sum_{j=1}^n l_{k,j} r_j \frac{\partial F_j}{\partial \mu_{j,s}}(\phi_j) = -s_{\mu_{k,0}} \sum_{j=1}^n l_{k,j} r_j \\ A_k^{\mu_s}(\phi, r) &= -s_{\mu_{k,s}} \sum_{j=1}^n l_{k,j} r_j \frac{\partial F_j}{\partial \mu_{j,s}}(\phi_j) = -s_{\mu_{k,s}} \sum_{j=1}^n l_{k,j} r_j \cos(s\phi_j) \\ A_k^{\nu_s}(\phi, r) &= -s_{\nu_{k,s}} \sum_{j=1}^n l_{k,j} r_j \frac{\partial F_j}{\partial \nu_{j,s}}(\phi_j) = -s_{\nu_{k,s}} \sum_{j=1}^n l_{k,j} r_j \sin(s\phi_j) \end{aligned} \quad s = 1, \dots, q,$$

where $l_{k,j}$ are the entries of L and strictly positive $s_{\mu_{k,0}}$, $s_{\mu_{k,s}}$ and $s_{\nu_{k,s}}$ are susceptibility constants.

3.3 Network's Dynamical System with Time Scale and Amplitude Adaptation

Combining the individual components discussed in Section 3.2 yields the global dynamical system

$$\begin{aligned} \dot{\phi}_k &= \omega_k - c_k \frac{\partial \mathcal{V}}{\partial \phi_k}(\phi, r) \\ \dot{r}_k &= \underbrace{-(r_k - F_k(\phi_k)) + F'_k(\phi_k)\omega_k}_{\text{local dynamics}} - \underbrace{c_k \frac{\partial \mathcal{V}}{\partial r_k}(\phi, r)}_{\text{coupling dynamics}} \\ \dot{\omega}_k &= \underbrace{-s_{\omega_k} \frac{\partial \mathcal{V}}{\partial \phi_k}(\phi, r)}_{\text{time scale adaptive mechanisms}} \\ \dot{\mu}_{0,k} &= -s_{\mu_{k,0}} \sum_{j=1}^n l_{k,j} r_j \\ \dot{\mu}_{k,s} &= -s_{\mu_{k,s}} \sum_{j=1}^n l_{k,j} r_j \cos(s\phi_j) \\ \dot{\nu}_{k,s} &= \underbrace{-s_{\nu_{k,s}} \sum_{j=1}^n l_{k,j} r_j \sin(s\phi_j)}_{\text{amplitude adaptive mechanisms}} \end{aligned} \quad k = 1, \dots, n. \quad (3.4)$$

For Equations (3.4), we have $q + 1$ constants of motion, the existence of a consensual oscillatory state and the convergence towards it.

$q + 1$ Constants of Motion

The functions

$$J_{\mu_0}(\mu_0) = \sum_{k=1}^n \frac{\mu_{k,0}}{S_{\mu_{k,0}}}, \quad J_{\mu_s}(\mu_s) = \sum_{k=1}^n \frac{\mu_{k,s}}{S_{\mu_{k,s}}}, \quad J_{\nu_s}(\nu_s) = \sum_{k=1}^n \frac{\nu_{k,s}}{S_{\nu_{k,s}}} \quad s = 1, \dots, q \quad (3.5)$$

with $\mu_0 = (\mu_{0,1}, \dots, \mu_{0,n})$, $\mu_s = (\mu_{1,s}, \dots, \mu_{n,s})$ and $\nu_s = (\nu_{1,s}, \dots, \nu_{n,s})$ are constants of motion. Indeed, if $\mu_0(t)$, $\mu_s(t)$ and $\nu_s(t)$ for $s = 1, \dots, q$ are orbits of Equations (3.4), then

$$\begin{aligned} \frac{d[J_{\mu_0}(\mu_0(t))]}{dt} &= - \sum_{k=1}^n \left(\sum_{j=1}^n l_{k,j} r_j \right) = 0, & \frac{d[J_{\mu_s}(\mu_s(t))]}{dt} &= - \sum_{k=1}^n \left(\sum_{j=1}^n l_{k,j} r_j \cos(s\phi_j) \right) = 0 \\ \frac{d[J_{\nu_s}(\nu_s(t))]}{dt} &= - \sum_{k=1}^n \left(\sum_{j=1}^n l_{k,j} r_j \sin(s\phi_j) \right) = 0 \end{aligned}$$

by Lemma D.2 in [42]. If we further suppose that $\sum_{j=1}^n \frac{\partial V}{\partial \phi_j}(\phi, r) = 0$ for all (ϕ, r) (and this is true for both types of coupling potentials in Example 1), then Equations (3.4) admit another constant of motion, namely

$$J_{\omega}(\omega) = \sum_{j=1}^n \frac{\omega_j}{S_{\omega_j}} \quad (3.6)$$

with $\omega = (\omega_1, \dots, \omega_n)$.

Existence of a Consensual Oscillatory State

Equations (3.4) admit a consensual oscillatory state. Indeed, for given common constants $\Omega_c = (\omega_c, \mu_{c,0}, \mu_{c,1}, \nu_{c,1}, \dots, \mu_{c,q}, \nu_{c,q})$,

$$(\phi_k(t), r_k(t), \Omega_k(t)) := (\omega_c t, F_c(t), \Omega_c) \quad k = 1, \dots, n \quad (3.7)$$

is a consensual orbit of Equations (3.4), with here F_c taking the value Ω_c . Indeed, since points given by Equations (3.7) are extrema of the V , then the coupling dynamics and the adaptive time scale mechanisms are zero. Hence, $\omega_k(t)$ is a constant taking value ω_c for all k , and $(\phi_k(t), r_k(t)) = (\omega_c t, F_c(t))$ solves each local dynamics and cancels all amplitude adaptive mechanisms for all k . Therefore $(\mu_{k,0}(t), \mu_{k,1}(t), \nu_{k,1}(t), \dots, \mu_{k,q}(t), \nu_{k,q}(t))$ are constants taking, respectively, common values $(\mu_{c,0}, \mu_{c,1}, \nu_{c,1}, \dots, \mu_{c,q}, \nu_{c,q})$ for all k .

Convergence Towards a Consensual Oscillatory State

If perturbations are introduced in Equations (3.7), we have the following limit

$$\lim_{t \rightarrow \infty} \|(\phi_k(t), r_k(t), \Omega_k(t)) - (\omega_c t, F_c(t), \Omega_c)\| = 0 \quad \forall k \quad (3.8)$$

with constant Ω_c . This limit raises two problems: determining the limit values Ω_c and finding the conditions for convergence.

Limit Values - If the constant of motion in Equation (3.6) exists and if Limit (3.8) holds, then, thanks to all the other constants of motion in Equations (3.5), we have

$$\begin{aligned}
J_\omega(\omega(0)) &= \lim_{t \rightarrow \infty} J_\omega(\omega(t)) = J_\omega(\lim_{t \rightarrow \infty} \omega(t)) = J_\omega(\omega_c \mathbf{1}) = \omega_c \sum_{j=1}^n \frac{1}{s_{\omega_j}} \\
J_{\mu_0}(\mu_0(0)) &= \lim_{t \rightarrow \infty} J_{\mu_0}(\mu_0(t)) = J_{\mu_0}(\lim_{t \rightarrow \infty} \rho(t)) = J_{\mu_0}(\mu_{c,0} \mathbf{1}) = \mu_{c,0} \sum_{j=1}^n \frac{1}{s_{\mu_{j,0}}} \\
J_{\mu_s}(\mu_s(0)) &= \lim_{t \rightarrow \infty} J_{\mu_s}(\mu_s(t)) = J_{\mu_s}(\lim_{t \rightarrow \infty} \mu_s(t)) = J_{\mu_s}(\mu_{c,s} \mathbf{1}) = \mu_{c,s} \sum_{j=1}^n \frac{1}{s_{\mu_{j,s}}} \quad s = 1, \dots, q. \\
J_{\nu_s}(\nu_s(0)) &= \lim_{t \rightarrow \infty} J_{\nu_s}(\nu_s(t)) = J_{\nu_s}(\lim_{t \rightarrow \infty} \nu_s(t)) = J_{\nu_s}(\nu_{c,s} \mathbf{1}) = \nu_{c,s} \sum_{j=1}^n \frac{1}{s_{\nu_{j,s}}}
\end{aligned}$$

Hence, the consensual values of Ω_c are analytically expressed as

$$\omega_c = \frac{\sum_{j=1}^n \frac{\omega_j(0)}{s_{\omega_j}}}{\sum_{j=1}^n \frac{1}{s_{\omega_j}}}, \quad \mu_{c,0} = \frac{\sum_{j=1}^n \frac{\mu_{j,0}(0)}{s_{\mu_{j,0}}}}{\sum_{j=1}^n \frac{1}{s_{\mu_{j,0}}}}, \quad \mu_{c,s} = \frac{\sum_{j=1}^n \frac{\mu_{j,s}(0)}{s_{\mu_{j,s}}}}{\sum_{j=1}^n \frac{1}{s_{\mu_{j,s}}}}, \quad \nu_{c,s} = \frac{\sum_{j=1}^n \frac{\nu_{j,s}(0)}{s_{\nu_{j,s}}}}{\sum_{j=1}^n \frac{1}{s_{\nu_{j,s}}}} \quad s = 1, \dots, q. \quad (3.9)$$

Convergence Conditions - To prove the convergence in Limit (3.8), one can linearize Equations (3.4) around a consensual oscillatory state. In general, the resulting $n(4+2q) \times n(4+2q)$ Jacobian depends explicitly on time (since evaluated on a consensual oscillatory state) and therefore FLOQUET exponents have to be computed. Note that for certain coupling potentials \mathbf{V} and assumptions on the coupling strengths and susceptibility constants, the Jacobian can be diagonalized in order to reduce the computation of FLOQUET exponents to n systems, each of size $n(4+2q) \times n(4+2q)$.

We emphasize that numerous numerical simulations show that Limit (3.8) holds - and this for different topologies, coupling potential and values of coupling strengths and susceptibility constants. For these numerical experiments, the coupling strengths were set around one and susceptibility constants around 0.1.

Remark: Adaptation

Here, adaptation is to be interpreted as an asymptotic stability problem, which is directly related to the study of Limit (3.8). Indeed, for initially different PSS, if Limit (3.8) holds, then the adaptive mechanisms, with the help of the coupling dynamics, drive all the local systems towards a consensual oscillatory state as defined in Equations (3.7). Once this state is reached, the coupling dynamics, as well as the adaptive mechanisms, may be removed - and all PSS will still continue to deliver the same signal with the same time scale (i.e. local system are no longer dependent on their environment to produce common dynamical patterns). This is because the values Ω_k have been permanently modified (i.e. $\lim_{t \rightarrow \infty} \Omega_k(t) = \Omega_c$). If the adaptive mechanisms are not switched on initially, dynamical patterns may occur (due to the coupling dynamics) - but these are maintained because of the network interactions. If the interactions are removed, all PSS converge back towards their own shape, which is determined by \mathbb{K}_k and their own time scale, given by w_k .

With the adaptive mechanisms as defined in Section 3.2.3, the consensual values Ω_c only depend on the susceptibility constants and the initial values $\Omega_k(0)$, but not on the network topology (i.e. not on $a_{k,j}$) or the initial conditions ($\phi_k(0), r_k(0)$).

3.3.1 Miscellaneous Remark: Time Scale or Amplitude Adaptation Only

We present here two alternatives of System (3.4). One alternative concerns amplitude r_k adaptation only (Section 3.3.1.1), whereas the other deals with time scale ω_k adaptation only (Section 3.3.1.2).

3.3.1.1 Amplitude Adaptation Only

Consider Equations (3.4) with no phases ϕ_k (and hence no time scale adaptive mechanisms), and for each local PSS, let $\phi_k(t) = t$ for all k . The system becomes

$$\begin{aligned}
\dot{r}_k &= \underbrace{-(r_k - F_k(t)) + \dot{F}_k(t)}_{\text{local dynamics}} - \underbrace{c_k \frac{\partial V}{\partial r_k}(r)}_{\text{coupling dynamics}} \\
\dot{\mu}_{0,k} &= -s_{\mu_{k,0}} \sum_{j=1}^n l_{k,j} r_j & k = 1, \dots, n. \\
\dot{\mu}_{k,s} &= -s_{\mu_{k,s}} \cos(st) \frac{\partial V}{\partial r_k}(r) & s = 1, \dots, q \\
\dot{\nu}_{k,s} &= \underbrace{-s_{\nu_{k,s}} \sin(st) \frac{\partial V}{\partial r_k}(r)}_{\text{amplitude adaptive mechanisms}}
\end{aligned} \tag{3.10}$$

with $F_k(t) = \sum_{s=1}^q \mu_{k,s} \cos(st) + \nu_{k,s} \sin(st)$. Note that for Equations (3.10) we still have $q + 1$ constants of motion (as given in Equations (3.5)), the existence of a consensual oscillatory state $(r_k(t), \Omega_k(t)) := (F_c(t), \Omega_c)$ for $k = 1, \dots, n$, and the convergence towards it (i.e. $\lim_{t \rightarrow \infty} \|(r_k(t), \Omega_k(t)) - (F_c(t), \Omega_c)\| = 0 \quad \forall k$) as observed by numerous numerical simulations.

A priori, Equations (3.10) describe a system where adaptation only occurs on the shape of the local attractors. However, by adequately setting the value of one or several constants of motion in Equations (3.5), one can cancel the asymptotic values of the corresponding coefficients. Thus, by changing the shape of the signal, one can change its frequency.

3.3.1.2 Time scale Adaptation Only

We here remark that PSS (i.e. belonging to the class of PR System) can be slightly modified in order to be seen as Ortho-Gradient (OG) systems. For a precise definition and examples, see Section 1.1.1 in [42]. Briefly, OG systems are characterized by dissipative dynamics that are orthogonal to their canonical - or here, oscillatory - dynamics. Let us consider the following network of PSS that are also OG systems, and where there is only time scale adaptation

$$\begin{aligned}
\dot{\phi}_k &= \omega_k + (r_k - F(\phi_k))F'(\phi_k) - \underbrace{c_k \frac{\partial V}{\partial \phi_k}(\phi)}_{\text{coupling dynamics}} \\
\dot{r}_k &= \underbrace{\omega_k F'(\phi_k) - (r_k - F(\phi_k))}_{\text{local dynamics}} & k = 1, \dots, n. \\
\dot{\omega}_k &= \underbrace{-s_{\omega_k} \frac{\partial V}{\partial \phi_k}(\phi)}_{\text{time scale adaptive mechanisms}}
\end{aligned} \tag{3.11}$$

As shown in Lemma 1.1 in [42], each local dynamics in Equations (3.11), taken individually, possesses its own attractor given by \mathbb{K} . Networks of OG systems with adapting angular velocities have been studied. For the particular type of coupling dynamics and time scale adaptive mechanisms (i.e. only on variables ϕ_k), one can directly apply Proposition 2.2 in [42] to show that System (3.11) converges towards a consensual oscillatory state with consensual value ω_c as in Equations (3.9). For this convergence, one needs to suppose that $\langle \mathbf{1} | \nabla V(\phi) \rangle = 0$ for all ϕ and to make a technical hypothesis on V .

3.4 Numerical Simulations

We report two sets of numerical simulations one with time scale and amplitude adaptation (refer to Section 3.4.1) and one with amplitude adaptation only (refer to Section 3.4.2).

3.4.1 Time Scale and Amplitude Adaptation

We consider 39 PSSs as in Equations (3.4) with network topology as in Figure 3.2(a). Here, each PSS is given by $F_k(\phi) = \sum_{s=1}^3 \mu_{k,s} \cos(s\phi) + \nu_{k,s} \sin(s\phi)$ for $k = 1, 2$ (i.e. $s = 3$). The coupling strengths and the susceptibility constants are $c_k = 1$, $s_{\omega_k} = s_{\mu_{k,0}} = s_{\mu_{k,s}} = 0.1$ for $k = 1, \dots, 39$ and $s = 1, 2, 3$. A Laplacian potential, as in Example 1, is used for the coupling dynamics. The initial conditions $(r_k(0), \phi_k(0), \omega_k(0), \mu_{k,0}(0), \mu_{k,1}(0), \nu_{k,1}(0), \mu_{k,2}(0), \nu_{k,2}(0), \mu_{k,3}(0), \nu_{k,3}(0))$ are randomly uniformly drawn from $]F_k(0) - 0.225, F_k(0) + 0.225[\times]-0.225, 0.225[\times]1 - 0.225, 1 + 0.225[\times]2 - 0.225, 2 + 0.225[\times]5 - 0.225, 5 + 0.225[\times] - 3 - 0.225, -3 + 0.225[\times] - 7 - 0.225, -7 + 0.225[\times] - 5 - 0.225, -5 + 0.225[\times] - 3 - 0.225, -3 + 0.225[\times]7 - 0.225, 7 + 0.225[$.

The resulting dynamics for the variables r_k and ω_k is shown in Figure 3.3 and for variables $\mu_{k,s}$ and $\nu_{k,s}$ for $s = 1, 2, 3$ in Figure 3.4. Note that the variables r_k converge quickly to a common signal where as the variables Ω_k take more time to converge towards their asymptotic values. This is due to a relatively strong coupling strength compared to the susceptibility constants. For this set up, we have always observed converges towards a consensual oscillatory state. With the same set up, but with a network as in Figure 3.2(b), convergence was not observed for all numerical experiments as we report in Figures 3.5 and 3.6. However, for the exact the same initial conditions as in Figures 3.5 and 3.6, if all adaptive mechanisms are switched off (i.e. all susceptibility constants are zero), the network is still able to synchronize as shown in Figure 3.7.

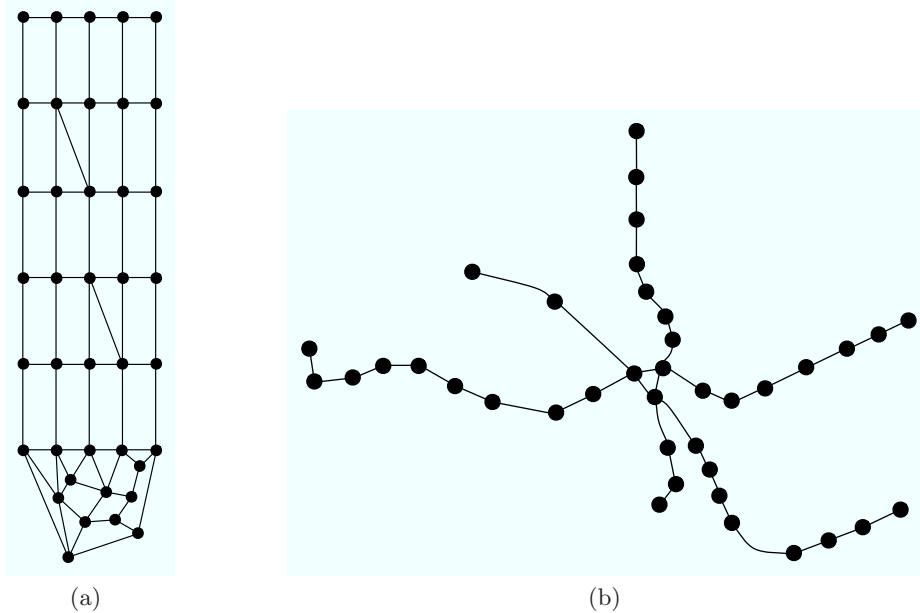


Fig. 3.2: Two 39-vertex Network Topologies, “Manhattan” (Figure 3.2(a)) and Київське Метро (Figure 3.2(b)).

3.4.2 Amplitude Adaptation Only

Two PSSs with amplitude adaptation only as in Equations (3.10) are considered, with here $F_k(t) = \sum_{s=1}^3 \mu_{k,s} \cos(st) + \nu_{k,s} \sin(st)$ for $k = 1, 2$ (i.e. $s = 3$). The coupling strengths and the susceptibility constants are $c_k = 2$, $s_{\omega_k} = s_{\mu_{k,0}} = s_{\mu_{k,s}} = 0.5$ for $k = 1, 2$ and $s = 1, 2, 3$. The coupling potential is $V(r) := \frac{(r_1 - r_2)^2}{2}$. The initial conditions $(r_k(0), \mu_{k,0}(0))$ are randomly uniformly drawn from $]F_k(0) - 0.2, F_k(0) + 0.2[\times]0.8, 1.1[$ for $k = 1, 2$, $(\mu_{1,3}(0), \nu_{1,3}(0), \mu_{2,3}(0), \nu_{2,3}(0))$ are randomly uniformly

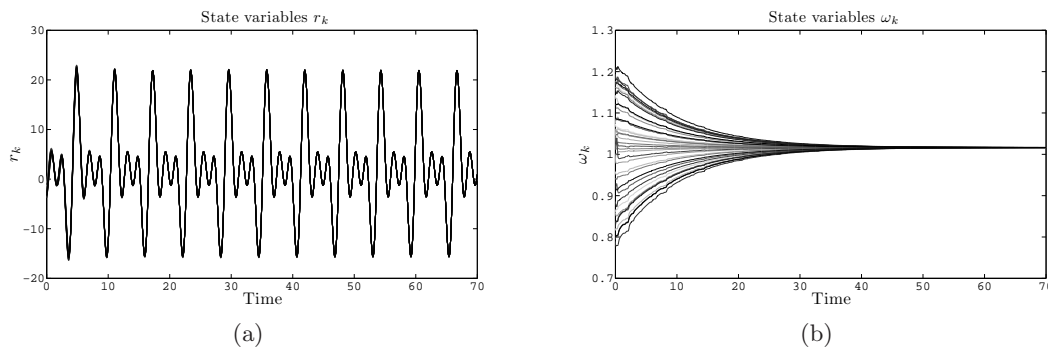


Fig. 3.3: Time evolution of r_k (Figure 3.3(a)) and ω_k (Figure 3.3(b)) for 39 PSSs, interacting through the network in Figure 3.2(a).

drawn from $]2.8 - 0.2, 3.2[\times]4.8, 5.2[\times]4.8, 5.2[\times] - 7.2, -6.8[$, $(\mu_{1,1}(0), \nu_{1,1}(0), \mu_{1,2}(0), \nu_{1,2}(0)) = (2, -2, -1, 1)$ and $(\mu_{2,1}(0), \nu_{2,1}(0), \mu_{2,2}(0), \nu_{2,2}(0)) = (-2, 2, 1, -1)$.

The resulting dynamics for the variables r_k , $\mu_{k,1}$ and $\nu_{k,2}$ is shown in Figure 3.8. For $t \in [0, 15]$, the coupling dynamics and the adaptive mechanisms are switched off and so each PSS generates its individual signal. Because of the choice of the initial conditions $(\mu_{k,s}(0), \nu_{k,s}(0))$ $k, s = 1, 2$, the asymptotic values are $(\mu_{c,s}(0), \nu_{c,s}(0)) = (0, 0)$ for $s = 1, 2$, and so both amplitudes $r_1(t)$ $r_2(t)$ converge towards $F_c(t) = \mu_{c,3} \cos(3t) + \nu_{c,3} \sin(3t)$ (i.e. FOURIER series with mode $\cos(3t)$ and $\sin(3t)$ only). As a consequence, $F_c(t)$ has a higher frequency than any of the two signals before interactions are switched on. This is observed in Figure 3.8(a) where the two signals have a larger period in the interval $[0, 15]$ than when they are close to $F_c(t)$.

3.5 Conclusion

PSS form a suitable class of system to investigate interaction of multi signal dynamics. Whereas adapting the time scale is a fairly straightforward procedure, shaping the attractor is more complicated. Nevertheless, our dynamical systems show that this can be implemented in a robust manner. The adaptive mechanisms dependent solely on the state variables and no pre-calculations or information on the curvature of the attractor is needed.

The asymptotic values from the resulting dynamics are analytically calculable. The network's topology and the nature of the coupling potential itself directly influence the conditions for attaining a consensual oscillatory state. Determining basins of attraction with respects to the connectivity and coupling functions are still open questions.

Apart from investigating the resulting dynamics for directed network connections with time-dependent edges, perspective works also include merging two adapting PSS communities - one belonging to the class of systems given by Equations (3.4), and the other described by Systems (3.10).

Appendix

3.A Convergence Towards Compact Set \mathbb{K}

The convergence towards the compact set $\mathbb{K} := \{(\phi, r) \in \mathbb{S}^1 \times \mathbb{R} \mid r - F(\phi) = 0\}$ follows from ЛЯПУНОВ's second method with ЛЯПУНОВ function

$$L(\phi, r) = \frac{1}{2}(r - F(\phi))^2 \geq 0.$$

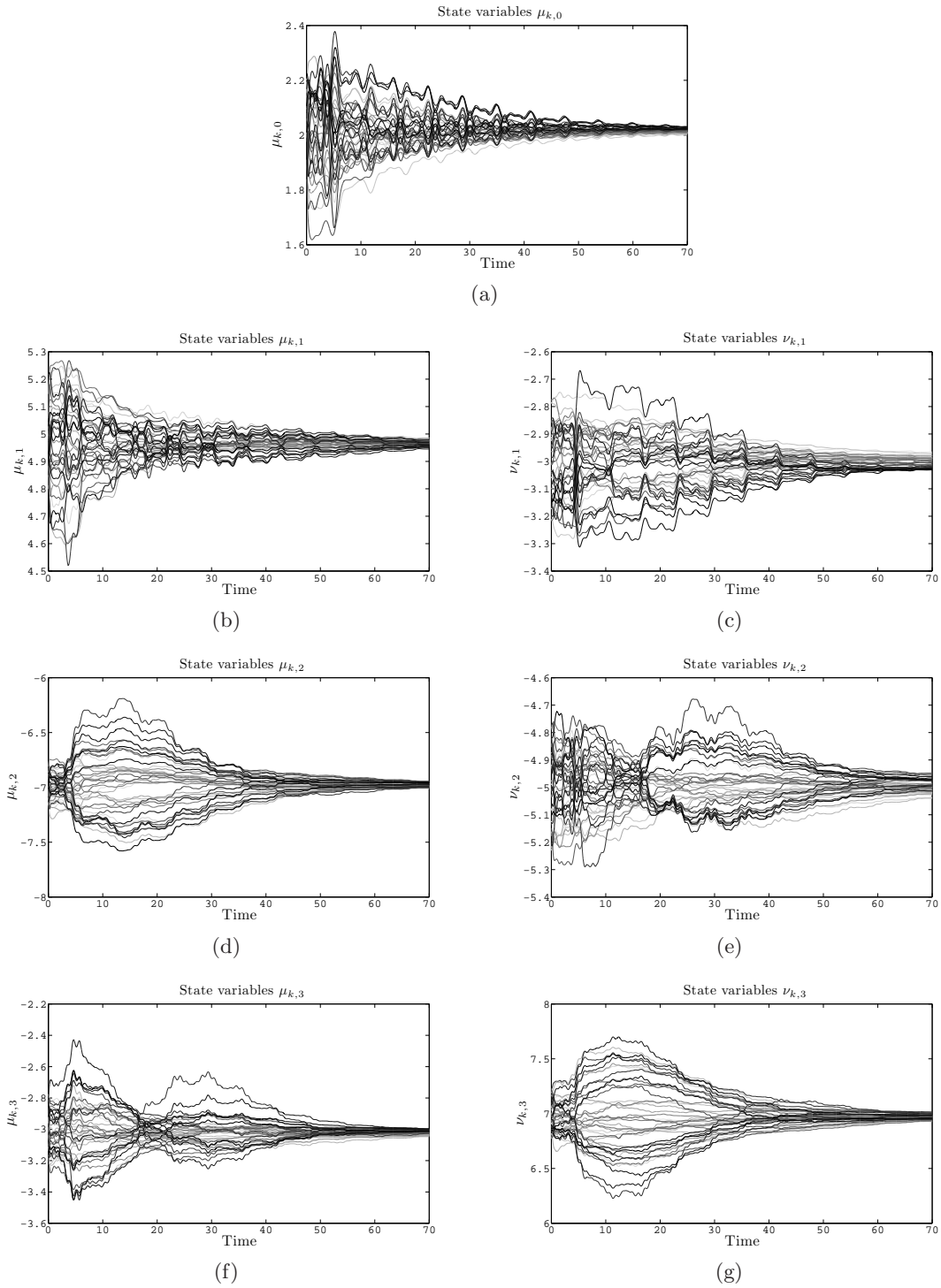


Fig. 3.4: Time evolution of $\mu_{k,0}$ (Figure 3.4(a)), $\mu_{k,1}$ and $\nu_{k,1}$ (Figures 3.4(b) & 3.4(c)), $\mu_{k,2}$ and $\nu_{k,2}$ (Figures 3.4(d) & 3.4(e)) and $\mu_{k,3}$ and $\nu_{k,3}$ (Figures 3.4(f) & 3.4(g)) for 39 PSSs, interacting through the network in Figure 3.2(a).

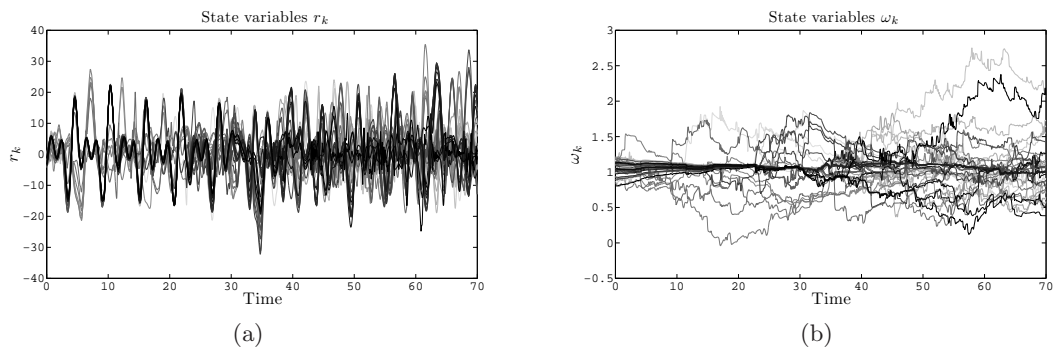


Fig. 3.5: Time evolution of r_k (Figure 3.5(a)) and ω_k (Figure 3.5(b)) for 39 PSSs, interacting through the network in Figure 3.2(b).

By construction, we have that $\mathbb{K} = \{(\phi, r) \in \mathbb{S}^1 \times \mathbb{R} \mid \mathbf{L}(\phi, r) = 0\}$. Computing the time derivative

$$\begin{aligned}
 \langle \nabla \mathbf{L}(\phi, r) \mid (\dot{\phi}, \dot{r}) \rangle &= -(r - \mathbf{F}(\phi)) \mathbf{F}'(\phi) \dot{\phi} + (r - \mathbf{F}(\phi)) \dot{r} \\
 &= -(r - \mathbf{F}(\phi)) \mathbf{F}'(\phi) \mathbf{w} + (r - \mathbf{F}(\phi)) (- (r - \mathbf{F}(\phi)) + \mathbf{F}'(\phi) \mathbf{w}) \\
 &= -(r - \mathbf{F}(\phi))^2.
 \end{aligned}$$

Hence, $\langle \nabla \mathbf{L}(\phi, r) \mid (\dot{\phi}, \dot{r}) \rangle < 0$ for all $(\phi, r) \in (\mathbb{S}^1 \times \mathbb{R}) \setminus \mathbb{K}$.

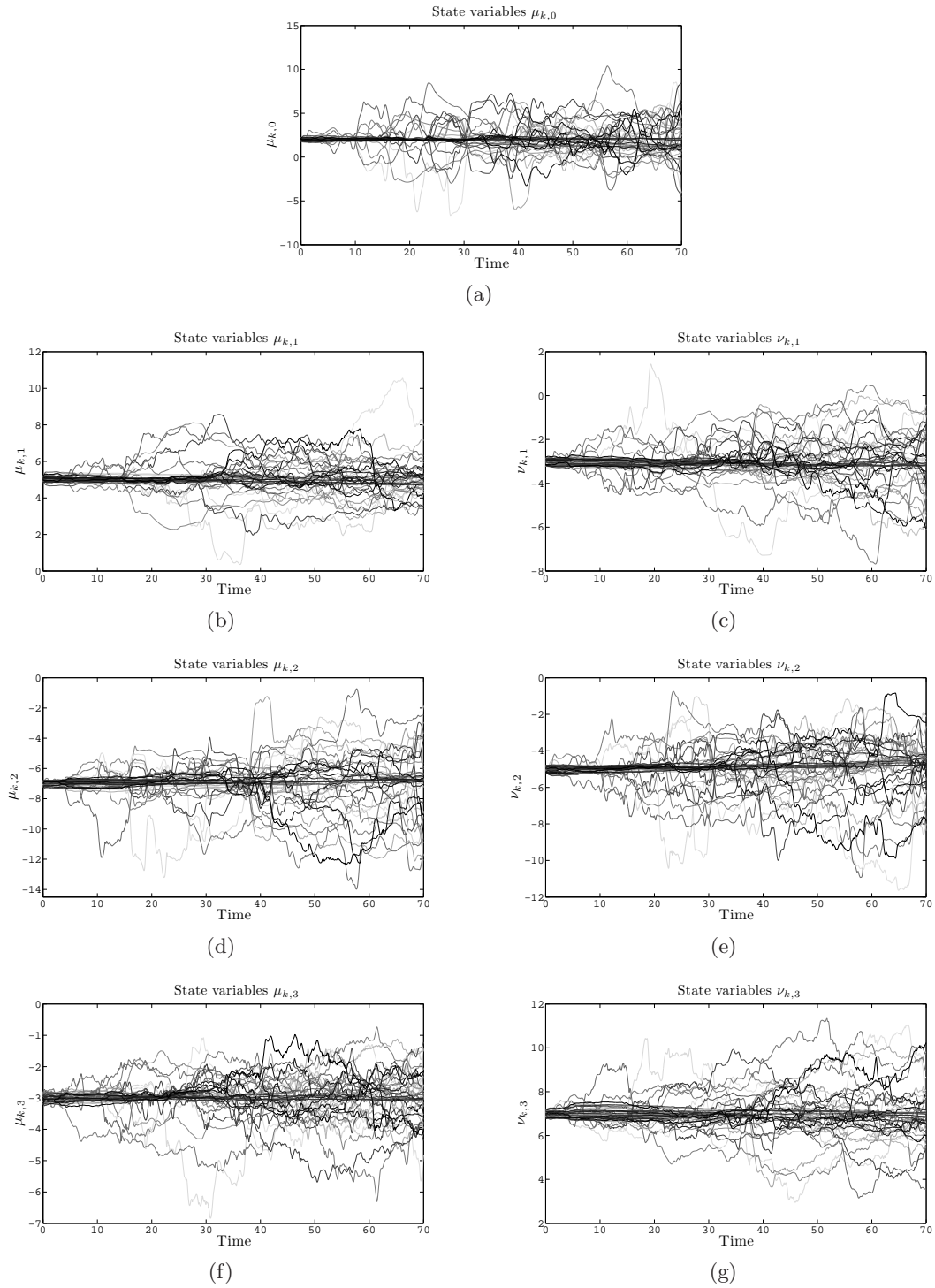


Fig. 3.6: Time evolution of $\mu_{k,0}$ (Figure 3.6(a)), $\mu_{k,1}$ and $\nu_{k,1}$ (Figures 3.6(b) & 3.6(c)), $\mu_{k,2}$ and $\nu_{k,2}$ (Figures 3.6(d) & 3.6(e)) and $\mu_{k,3}$ and $\nu_{k,3}$ (Figures 3.6(f) & 3.6(g)) for 39 PSSs, interacting through the network in Figure 3.2(b).

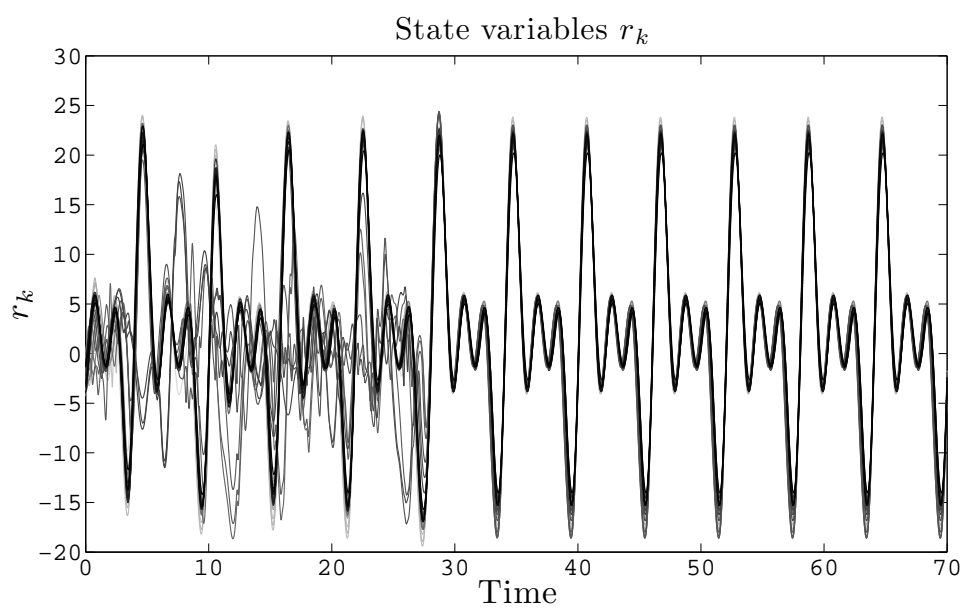


Fig. 3.7: Time evolution of r_k for 39 PSSs with all their adaptive mechanisms switched off (i.e. all susceptibility constants are zero), interacting through the network in Figure 3.2(b).

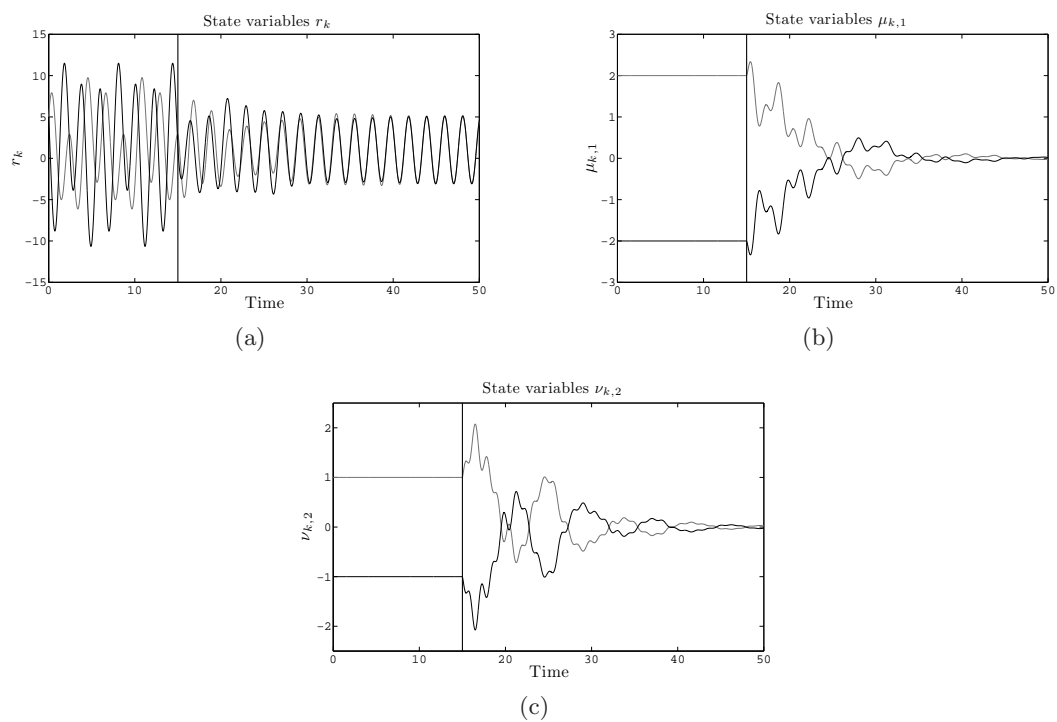


Fig. 3.8: Time evolution of r_k (Figure 3.8(a)), $\mu_{k,1}$ (Figure 3.8(b)) and $\nu_{k,2}$ (Figure 3.8(c)) for two PSSs. Coupling dynamics and adaptive mechanisms are switched on at $t = 15$ (black solid line).

Frequency Adaptation in Networks of Vibrating-Oscillatory Systems

Mais toute une plage vibrante de soleil se pressait
derrière moi.

Albert CAMUS

Abstract

We study a complex system composed of damped vibrational systems and phase oscillators interacting through heterogenous coupling functions. We introduce adaptive mechanisms that modify the value of each parameter controlling the phase oscillator's frequency. Thanks to the adaptive mechanisms and the coupling dynamics, the system converges towards a common oscillatory state in which all phase oscillators share a constant and common frequency - and continue to oscillate as such even if all interactions are removed. For comparison's sake, the same system is considered without the adaptive mechanisms. In both cases and for undirected networks, the common frequency of all heterogenous local systems is independent of the underlying connecting topology and is analytically calculated. In some cases, the convergence is proven analytically - in other cases, numerical simulations show the emergence of common dynamical patterns. We report numerical simulations displaying the adaptive mechanisms' transient and corroborate the asymptotic theoretical assertions.

4.1 Introduction

The theory of vibrational systems models the dynamics of periodic motion, commonly found in different parts of robots and automatic machines. As typical examples, consider arms or legs of a robot or devices in production chains with pick-and-place mechanisms.

Consider a robot dog as sketched in Figure 4.1(a) and concentrate on one of its legs, outlined in Figure 4.1(b). Broadly put, the leg's motion corresponds to an elementary damped vibrating system (DVS) described by Equation (4.1) with fixed parameters q and f depending on engineering contingencies.

$$\begin{aligned}\dot{\theta} &= q \\ \dot{r} &= -fr .\end{aligned}\tag{4.1}$$

For the leg to move, it must be set into motion by an engine. From a dynamical system point of view, this can be conceptualized via a DVS being "entrained" by an external phase oscillator (PO) $\phi(t) = \omega t$ as in

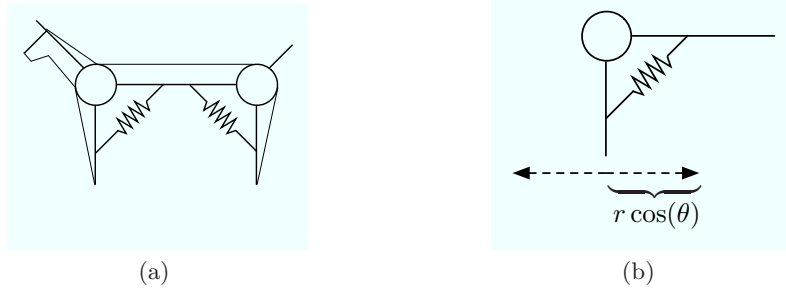


Fig. 4.1: Qualitative sketch of a robot dog (Figure 4.1(a)) and one of its legs (Figure 4.1(b)).

$$\text{Entrainment} \quad \begin{cases} \dot{\theta} = \mathbf{q} - r \sin(\theta - \phi) \\ \dot{r} = -fr + r \cos(\theta - \phi) \\ \dot{\phi} = \mathbf{w} \end{cases} \quad (4.2)$$

with fixed parameter \mathbf{w} controlling the frequency and the “entrained solution” being

$$\theta(t) = \mathbf{w}t + \vartheta \quad r(t) = \bar{r} \quad \phi(t) = \mathbf{w}t + \varphi$$

with $\vartheta = \frac{1}{2} \sin^{-1}(2(\mathbf{q} - \mathbf{w})f) + \varphi$, $\varphi = \phi(0) \in [0, 2\pi[$ and $\bar{r} = \frac{\sqrt{1-2(\mathbf{q}-\mathbf{w})f} + \sqrt{1+2(\mathbf{q}-\mathbf{w})f}}{2f}$ (see Appendix 4.A). The coupling of a DVS with a PO as in Equation 4.2 is here known as a vibrating-oscillatory system (VOS): “vibrating” refers to the DVS and “oscillatory” to the PO. It is well known from the theory of vibrational systems¹ that for the dog to move with maximum leg stride - or equivalently, for maximum amplitude response r - the DVS must be entrained (i.e. forced/excited) at its resonance frequency (here setting the value of \mathbf{w} to equal \mathbf{q}).

However, fixing \mathbf{w} to its appropriate value once and for all is not realistic. Indeed, depending on the environment, DVSs may endure structural changes, implying that the values of \mathbf{q} and f will be modified. As an example, consider the case represented in Figure 4.2. The robot dog in Figure 4.1(a) is sent out to collect and bring back a box of bottles. On its way towards its target (i.e. collecting the box of bottles), each PO’s frequency is set at its corresponding DVS’s resonant frequency, and hence guaranteeing maximum leg stride. However, once the robot is loaded (i.e. with a box of bottles on its back), the values of \mathbf{q} and f change due to the new setting. Hence, on its way back, each PO is no longer entraining its corresponding DVS at its resonant frequency, and therefore maximum leg stride is no longer attained.

We are therefore faced with the following problem

If \mathbf{q} changes, what can be done to its corresponding PO (i.e. to $\dot{\phi} = \mathbf{w}$) to ensure resonance?

A first approach is to feed information from the DVS back to its PO in order to “synchronize” the phases θ and ϕ . For this, we consider a VOS of the form

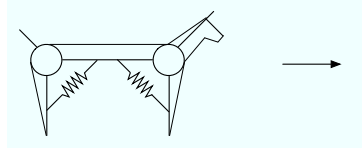
$$\text{Synchronization} \quad \begin{cases} \dot{\theta} = \mathbf{q} - r \sin(\theta - \phi) \\ \dot{r} = -fr + \cos(\theta - \phi) \\ \dot{\phi} = \mathbf{w} - r \sin(\phi - \theta) \end{cases} \quad (4.3)$$

with the “synchronized solution” being

$$\theta(t) = \frac{\mathbf{q} + \mathbf{w}}{2} t + \vartheta \quad r(t) = \bar{r} \quad \phi(t) = \frac{\mathbf{q} + \mathbf{w}}{2} t + \varphi$$

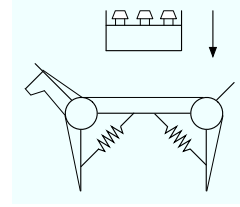
¹ It can also be seen directly from the entrained solution.

Going to target
 $q = w$



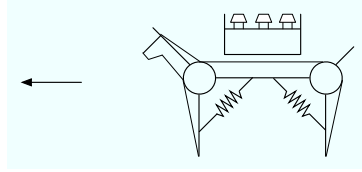
(a)

Loading
 $q \mapsto \check{q}$
 $f \mapsto \check{f}$



(b)

Coming back
 $\check{q} \neq w$



(c)

Fig. 4.2: The robot dog on its way to collect the box of bottles (Figure 4.2(a)) - value of w set to q , guaranteeing maximum leg stride. The box of bottles is loaded on the robot dog's back (Figure 4.2(b)) - change in values of $q \mapsto \check{q}$ and $f \mapsto \check{f}$. The robot dog comes back (Figure 4.2(c)) - value w does not equal new value \check{q} , maximum leg stride is no longer attained.

with $\vartheta = \frac{\theta(0)+\phi(0)}{2} + \frac{1}{4} \sin^{-1}((q-w)f)$, $\varphi = \frac{\theta(0)+\phi(0)}{2} + \frac{1}{4} \sin^{-1}((w-q)f)$ and $\bar{r} = \frac{\sqrt{1-(q-w)f} + \sqrt{1+(q-w)f}}{2f}$ (see Appendix 4.A). Although there is a gain in amplitude response from the entrained solution, maximum leg stride is not attained, and this because

$$\lim_{t \rightarrow \infty} \dot{\phi}(t) = \frac{q+w}{2} \neq q.$$

Note also that if $|q-w|$ is too large (i.e. a considerable structural change occurs, here the heavy load), then phase synchronization is no longer possible.

To overcome this problem and to follow what has been proposed in [13, 41], let the PO adapt its frequency to the value q . That is, consider a VOS with an adaptive frequency mechanism

$$\text{Adaptation} \quad \begin{cases} \dot{\theta} = q - r \sin(\theta - \phi) \\ \dot{r} = -fr + \cos(\theta - \phi) \\ \dot{\phi} = \omega \\ \dot{\omega} = \underbrace{-r \sin(\phi - \theta)}_{\text{adaptive frequency mechanisms}} \end{cases} \quad (4.4)$$

with the “adapted solution” being

$$\theta(t) = qt + \vartheta \quad r(t) = \frac{1}{f} \quad \phi(t) = qt + \varphi \quad \omega(t) = q$$

with $\vartheta = \varphi = \theta(0) + \phi(0) - q$. Not only do the phases θ and ϕ have the same frequency q , but they are also fully synchronized (i.e. in phase). As a consequence, $r(t) = \frac{1}{f}$, which corresponds to its maximum amplitude, leading to the maximum leg stride. A ЛЯПУНОВ function (see Appendix

4.B) proves that for initially different $\omega(0) := \mathbf{w} \neq \mathbf{q}$, then $\lim_{t \rightarrow \infty} \omega(t) = \mathbf{q}$.

Hence, the PO entrains its DVS at resonant frequency, thus guaranteeing maximum amplitude response. Furthermore, once this state is reached, the adaptive frequency mechanisms $r \sin(\theta - \phi)$ can be removed and the PO will still continue to force its DVS at frequency \mathbf{q} . This means that the PO permanently modified its frequency. This has to be contrasted with the phase synchronization approach, where the synchronized frequency $\frac{\mathbf{q} + \mathbf{w}}{2}$ is maintained only via persistent coupling.

Modifying the values of parameters through additional network interactions has attracted much attention as a research field. In the context of networks of coupled dynamical systems, different types of adaptation may exist. Tuning the coupling strength [36] or modifying the underlying topology for enhancing synchronization [18] are among the generic examples directly involving network characteristics. At the level of the local systems, adaptation may occur for frequency or time scale controlling parameters [20, 56, 21, 45] or for shaping the local attractors [46].

There have been recent publications on frequency adaptation in noisy [57], time delayed [47], or time-dependent [42] environments. However, in all these contributions, the authors considered a collection of interacting homogeneous local systems (i.e. same functional determining local dynamics). In the present contribution, our goal has been to explore frequency adaptation in a collection of interacting local units which are divided into two distinct communities. The general form of the dynamical system discussed is

$$\begin{aligned}
\dot{\theta}_k &= \underbrace{P_1(\theta_k, r_k; \Delta_k)}_{\text{local dynamics (type 1)}} - \mathbf{a}_k \underbrace{\frac{\partial E}{\partial \theta_k}}_{\text{coupling dynamics}}(\theta, r, \phi, h) \\
\dot{r}_k &= \underbrace{R_1(\theta_k, r_k; \Delta_k)}_{\text{local dynamics (type 1)}} - \mathbf{b}_k \underbrace{\frac{\partial E}{\partial r_k}}_{\text{coupling dynamics}}(\theta, r, \phi, h) \\
\dot{\phi}_k &= \underbrace{P_2(\phi_k, h_k, \Omega_k)}_{\text{local dynamics (type 2)}} - \mathbf{c}_k \underbrace{\frac{\partial E}{\partial \phi_k}}_{\text{coupling dynamics}}(\theta, r, \phi, h) \quad k = 1, \dots, n \\
\dot{h}_k &= \underbrace{R_2(\phi_k, h_k, \Omega_k)}_{\text{local dynamics (type 2)}} - \mathbf{d}_k \underbrace{\frac{\partial E}{\partial h_k}}_{\text{coupling dynamics}}(\theta, r, \phi, h) \\
\dot{\Omega}_k &= \underbrace{A_k(\theta, r, \phi, h)}_{\text{adaptive mechanisms}}
\end{aligned} \tag{4.5}$$

with $\theta = (\theta_1, \dots, \theta_n)$, $r = (r_1, \dots, r_n)$, $\phi = (\phi_1, \dots, \phi_n)$, $h = (h_1, \dots, h_n)$, and (P_1, R_1) and (P_2, R_2) belonging, respectively, to the same class of PR systems (i.e phase-radius system for which one has limit cycle oscillators, damped vibrational systems, etc ...) - and where $E(\theta, r, \phi) \geq 0$ is a coupling potential. While the parameters Δ_k of the first community (i.e. local dynamics (type 1)) are fixed and constant, the parameters Ω_k of the second community (i.e. local dynamics (type 2)) are time-dependent and have their own dynamics governed by the adaptive mechanisms A_k (i.e. they acquire the status of variables of the global dynamics).

For Equations (4.5), when the first community is removed (i.e. $P_1 \equiv R_1 \equiv 0$), the complex systems reduces to a homogenous collection of self-adapting PR for which a general framework has been considered in [42]. On the other hand, when the second community is removed (i.e. $P_2 \equiv R_2 \equiv 0$), Equations (4.5) describe the classical framework of interacting homogeneous units (with different parameters), for which the observation of emergence of dynamical patterns is of interest. Hence, the natural idea arises of merging the two communities. Heterogenous complex systems where each component adapts at least one of its local parameters have been analytically discussed in [45]. Closely related to the present note, All-to-All coupled switches and phase oscillators with adapting frequencies have been studied in [21], where synchronization features similar to homogenous cases are observed. The aim here is therefore to investigate the dynamics of a community that not only interacts and adapts among itself but must also interact and adapt to the other community, and

this via arbitrary network topologies.

This contribution is organized as follows: In Section 4.2, we give explicit forms of the three components of the local dynamics, coupling dynamics and adaptive mechanisms. Together, these components form the global dynamical system of interest for which Section 4.3 provides analytical asymptotic behaviors for different regimes. Numerical simulations are presented in Section 4.5. We conclude and discuss perspective works in Section 4.6.

4.2 Networks of Damped Vibrational Systems and Phase Oscillators with Adaptive Mechanisms

The general form of the dynamical system we focus on is

$$\begin{aligned}
\dot{\theta}_k &= \mathbf{q}_k && - \mathbf{a}_k \frac{\partial \mathbf{E}}{\partial \theta_k}(\theta, r, \phi) \\
\dot{r}_k &= \underbrace{-\mathbf{f}_k r_k}_{\text{local dynamics (DVS)}} && - \mathbf{U}_k(\theta, r, \phi) \\
\dot{\phi}_k &= \underbrace{\omega_k}_{\text{local dynamics (PO)}} && - \underbrace{\mathbf{c}_k \frac{\partial \mathbf{E}}{\partial \phi_k}(\theta, r, \phi)}_{\text{coupling dynamics}} \quad k = 1, \dots, n \\
\dot{\omega}_k &= \underbrace{-\mathbf{s}_k \frac{\partial \mathbf{E}}{\partial \phi_k}(\theta, r, \phi)}_{\text{adaptive mechanisms}}
\end{aligned} \tag{4.6}$$

with $\theta = (\theta_1, \dots, \theta_n)$, $r = (r_1, \dots, r_n)$ and $\phi = (\phi_1, \dots, \phi_n)$ and the constituting elements are local dynamics, coupling dynamics and adaptive mechanisms.

Local Dynamics Consider a $2n$ -vertex network where n vertices are endowed with a damped vibrating system (DVS) - local dynamics (type 1), - and the n other vertices have a phase oscillator (PO) - local dynamics (type 2)

$$\begin{aligned}
\dot{\theta}_k &= \mathbf{q}_k && \dot{\phi} = \omega_k \\
\dot{r}_k &= -\mathbf{f}_k r_k && k = 1, \dots, n.
\end{aligned}$$

damped vibrating system (DVS) phase oscillator (PO)

Here, \mathbf{q}_k and $0 < \mathbf{f}_k$ are fixed and constant parameters controlling, respectively, the frequency of the vibrations and its relaxations rate. The ω_k are variables of the global system with their own dynamics determined by the adaptive mechanisms (see below). For the local dynamics (Type 2), the radius dynamics is here $\mathbf{R}_2 \equiv 0$.

Coupling Dynamics The interactions between the phases θ_k and ϕ_k are characterized by the respective coordinates of a coupling potential $\mathbf{E}(\theta, r, \phi) \geq 0$. The r_k are coupled through the vertex-dependent function \mathbf{U}_k defined as

$$\mathbf{U}_k(\theta, r, \phi) = -(\mathbf{f}_k r_k + \mathbf{b}_k \frac{\partial \mathbf{E}}{\partial r_k}(\theta, r, \phi)) \quad k = 1, \dots, n.$$

Here, $\mathbf{a}_k, \mathbf{b}_k, \mathbf{c}_k > 0$ are coupling strengths. On \mathbf{E} we make the following hypothesis

Hypothesis 1

I For $r_k > 0$,

$$\theta_k = \phi_j \quad \text{and} \quad r_k = \frac{\mathbf{b}_k}{\mathbf{f}_k} \quad \forall k, j \quad \iff \quad \mathbf{E}(\theta, r, \phi) = 0$$

- II $\sum_{k=1}^n \left(\frac{\partial \mathbf{E}}{\partial \theta_k}(\theta, r, \phi) + \frac{\partial \mathbf{E}}{\partial \phi_k}(\theta, r, \phi) \right) = 0 \quad \forall (\theta, r, \phi)$
 III for $\bar{\lambda} = (\bar{\theta}_1, \dots, \bar{\theta}_n, \frac{b_1}{f_1}, \dots, \frac{b_n}{f_n}, \bar{\phi}_1, \dots, \bar{\phi}_n)$ with $\bar{\theta}_k = \bar{\phi}_j \quad \forall k, j$, suppose that

$$\theta_k = \phi_j \quad \text{and} \quad r_k = 0 \quad \forall k, j \quad \iff \quad \langle \lambda | \mathfrak{D}^2 \mathbf{E}(\bar{\lambda}) \lambda \rangle = 0$$

with $\lambda = (\theta, r, \phi)$ and where \mathfrak{D}^2 is the second total derivative operator

Adaptive Mechanisms Inspired by the adaptive mechanisms studied in [42], the frequency of each PO adapts via the partial derivative of \mathbf{E} with respect to ϕ_k . Fixed and constant susceptibility constants $0 < \mathbf{s}_k$ are technically the same as \mathbf{c}_k but have another interpretation. For “small”-valued \mathbf{s}_k , the PO is unwilling to change its frequency. On the other hand, “large”-valued \mathbf{s}_k correspond to a PO that is willing to modify its frequency.

Note that System (4.6) can be rewritten in a compact form as

$$\begin{aligned} \dot{\theta}_k &= \mathbf{q}_k - \mathbf{a}_k \frac{\partial \mathbf{E}}{\partial \theta_k}(\theta, r, \phi) \\ \dot{r}_k &= -\mathbf{b}_k \frac{\partial \mathbf{E}}{\partial \phi_k}(\theta, r, \phi) \\ \dot{\phi}_k &= \omega_k - \mathbf{c}_k \frac{\partial \mathbf{E}}{\partial \phi_k}(\theta, r, \phi) \\ \dot{\omega}_k &= -\mathbf{s}_k \frac{\partial \mathbf{E}}{\partial \phi_k}(\theta, r, \phi) \end{aligned} \quad k = 1, \dots, n. \quad (4.7)$$

Equations (4.7) encompass coupled vibrating-oscillatory systems (VOS) which we discuss below.

4.2.1 Network of Vibrating-Oscillatory Systems

Defining the coupling potential as

$$\mathbf{E}(\theta, r, \phi) = \sum_{k=1}^n \mathbf{Q}_k(\theta_k, r_k, \phi_k) + \mathbf{W}(\theta, r) + \mathbf{V}(\phi),$$

System (4.7) becomes

$$\begin{aligned} \dot{\theta}_k &= \mathbf{q}_k - \mathbf{a}_k \frac{\partial \mathbf{Q}_k}{\partial \theta_k}(\theta_k, r_k, \phi_k) - \mathbf{a}_k \frac{\partial \mathbf{W}}{\partial \theta_k}(\theta, r) \\ \dot{r}_k &= -\mathbf{b}_k \frac{\partial \mathbf{Q}_k}{\partial r_k}(\theta_k, r_k, \phi_k) - \mathbf{b}_k \frac{\partial \mathbf{W}}{\partial r_k}(\theta, r) \\ \dot{\phi}_k &= \underbrace{\omega_k - \mathbf{c}_k \frac{\partial \mathbf{Q}_k}{\partial \phi_k}(\theta_k, r_k, \phi_k)}_{\text{vibrating-oscillatory system}} - \underbrace{\mathbf{c}_k \frac{\partial \mathbf{V}}{\partial \phi_k}(\theta, r)}_{\text{network interactions}} \quad k = 1, \dots, n. \quad (4.8) \\ \dot{\omega}_k &= -\underbrace{\mathbf{s}_k \left(\frac{\partial \mathbf{Q}_k}{\partial \phi_k}(\theta_k, r_k, \phi_k) + \frac{\partial \mathbf{V}}{\partial \phi_k}(\phi) \right)}_{\text{adaptive mechanisms}} \end{aligned}$$

DVSs and POs are locally coupled to create vibrating-oscillatory systems (VOS). In this framework, Equations (4.8) is to be seen as a n -vertex network where each node is endowed with a VOS. For a collection of coupled VOS, we further suppose that the functions \mathbf{Q}_k fulfill the following properties:

Hypothesis 2

$$\mathbf{Q}_k(\theta_k, r_k, \phi_k) \geq 0 \quad \forall (\theta_k, r_k, \phi_k)$$

II for $r_k > 0$

$$\theta_k = \phi_k \quad \text{and} \quad r_k = \frac{b_k}{f_k} \iff \mathbf{Q}_k(\theta_k, r_k, \phi_k) = 0$$

III for all k , $\frac{\partial \mathbf{Q}_k}{\partial \theta_k}(\theta_k, r_k, \phi_k) = -\frac{\partial \mathbf{Q}_k}{\partial \phi_k}(\theta_k, r_k, \phi_k) \quad \forall (\theta_k, r_k, \phi_k)$

IV $-b_k \frac{\partial \mathbf{Q}_k}{\partial r_k}(\theta_k, r_k, \phi_k) = -f_k r_k + Y_k(\theta_k, r_k, \phi_k)$

V for $\bar{\lambda}_k := (\bar{\theta}_k, \frac{b_k}{f_k}, \bar{\phi}_k)$ with $\bar{\theta}_k = \bar{\phi}_k$,

$$\theta_k = \phi_k \quad \text{and} \quad r_k = 0 \iff \langle \lambda_k | \mathfrak{D}^2 \mathbf{Q}_k(\bar{\lambda}_k) \lambda_k \rangle = 0$$

with $\lambda_k = (\theta_k, r_k, \phi_k)$ and where $\mathfrak{D}^2 \mathbf{Q}_k(\bar{\lambda}_k)$ is the 3×3 Hessian of \mathbf{Q}_k evaluated at $(\bar{\theta}_k, \frac{b_k}{f_k}, \bar{\phi}_k)$

We now present an example of local coupling function \mathbf{Q}_k .

Example 2. Define \mathbf{Q}_k as

$$\mathbf{Q}_k(\theta_k, r_k, \phi_k) = S\left(\sqrt{\frac{f_k}{b_k}} r_k, \sqrt{\frac{f_k}{b_k}} \frac{b_k}{f_k}, \theta_k, \phi_k\right) = \frac{1}{2} \left(\frac{f_k}{b_k} r_k^2 + \frac{b_k}{f_k} - 2r_k \cos(\theta_k - \phi_k) \right)$$

with

$$S(x, y, \theta, \phi) = \frac{1}{2} \left\langle \begin{pmatrix} x \\ y \end{pmatrix} \middle| \begin{pmatrix} 1 & -\cos(\theta - \phi) \\ -\cos(\theta - \phi) & 1 \end{pmatrix} \begin{pmatrix} x \\ y \end{pmatrix} \right\rangle$$

for real numbers x, y , and θ and ϕ belonging to \mathbb{S}^1 .

The properties in Hypothesis 2 are explicitly verified in Appendix 4.B. Additionally to the local interaction, both the DVS and PO interact with their likes (and only with their likes) through their own n -vertex network via the gradients of $W(\theta, r)$ and $V(\phi)$ respectively. To picture this, consider the sketch in Figure 4.3.

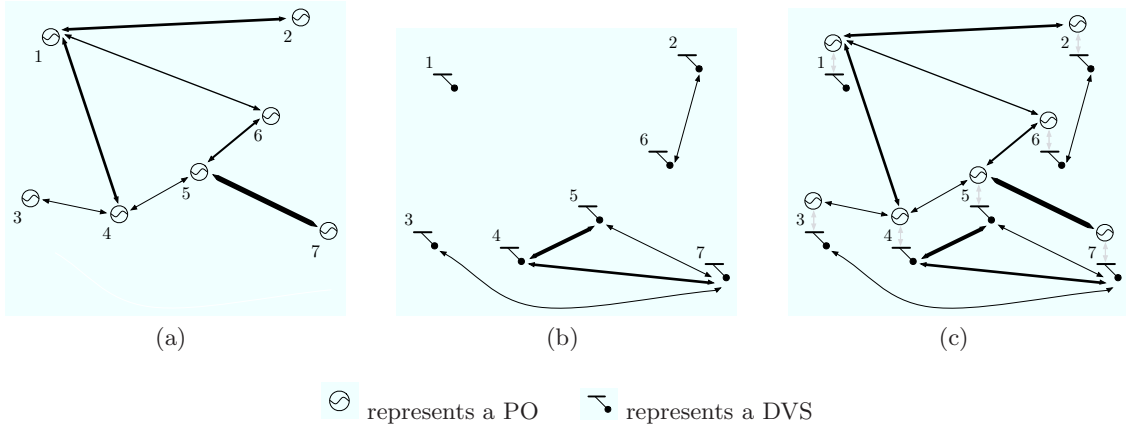


Fig. 4.3: A connected network characterizing the interactions for the PO (Figure 4.3(a)). An unconnected network characterizing the interactions for the DVS (Figure 4.3(b)). Each PO is coupled to one (and only one) DVS (gray arrows) forming a VOS-interacting network (Figure 4.3(c)).

We now present an explicit example for W and V that, together with the \mathbf{Q}_k , fulfill Hypothesis 1 (refer to Appendix 4.C).

Example 3. Define W and V as

$$W(\theta, r) = \frac{1}{2} \left(\sum_{\substack{k=1 \\ j>k}}^n a_{k,j} S\left(\frac{r_k f_k}{b_k}, \frac{r_j f_j}{b_j}, \theta_k, \theta_j\right) \right) \quad \text{and} \quad V(\phi) = \sum_{k,j=1}^n a_{k,j}^\phi B_{k,j}(\phi_k - \phi_j) \geq 0$$

with edge weights $0 \leq a_{k,j} = a_{j,k}$, function S defined as in Example 2, other edge weights $0 \leq a_{k,j}^\phi = a_{j,k}^\phi$ and where functions $B_{k,j}$ satisfy $B_{k,j}(x) \geq 0$, $B_{k,j}(x) = 0 \Leftrightarrow x = 0$, $B_{k,j}(x) = B_{k,j}(-x)$ (i.e. even function) and $0 < B''_{k,j}(0)$. As for the edge weights, we here impose $B_{k,j} \equiv B_{j,k}$. For the functions $B_{k,j}$, one may take

$$\begin{aligned} B_{k,j}(x) &= \frac{1}{2}x^2 & \text{Diffusion} & & B_{k,j}(x) &= \cosh(x) - 1 \\ B_{k,j}(x) &= 1 - \cos(x) & \text{KURAMOTO-type} & & B_{k,j}(x) &= \log(\cosh(x)) . \end{aligned}$$

With Examples 2 and 3, System (4.8) becomes

$$\begin{aligned} \dot{\theta}_k &= \mathbf{q}_k - \mathbf{a}_k r_k \sin(\theta_k - \phi_k) & + & & \mathbf{a}_k \sum_{j=1}^n l_{k,j} r_k r_j \frac{f_k}{b_k} \frac{f_j}{b_j} \sin(\theta_k - \theta_j) \\ \dot{r}_k &= -f_k r_k - b_k \cos(\theta_k - \phi_k) & - & & b_k \sum_{j=1}^n l_{k,j} r_j \frac{f_k}{b_k} \frac{f_j}{b_j} \cos(\theta_k - \theta_j) \\ \dot{\phi}_k &= \underbrace{\omega_k - c_k r_k \sin(\phi_k - \theta_k)}_{\text{vibrating-oscillatory system}} & - & & \underbrace{c_k \sum_{j=1}^n a_{k,j}^\phi B'_{k,j}(\phi_k - \phi_j)}_{\text{network interactions}} & \quad k = 1, \dots, n, \quad (4.9) \\ \dot{\omega}_k &= -\underbrace{s_k \left(\sum_{j=1}^n a_{k,j}^\phi B'_{k,j}(\phi_k - \phi_j) \right)}_{\text{adaptive mechanisms}} \end{aligned}$$

where $l_{k,j}$ are the entries of the associated Laplacian matrix (i.e. $l_{k,j} = -a_{k,j} \leq 0$ and $l_{k,k} = \sum_{j \neq k}^n a_{k,j}$). As mentioned above, Equations (4.9) describe the dynamics of two interacting networks merged together. Through one adjacency matrix (with entries $a_{k,j}$), DVS are coupled among themselves just as the POs interact with their likes via another adjacency (with entries $a_{k,j}^\phi$). Each DVS is coupled to one and only one PO (via its corresponding Q_k function).

4.3 Network's Dynamical System

We now analytically discuss some dynamics belonging to System (4.7). We distinguish between adaptation and synchronization. For both, we analyze the system for a collection of homogeneous q-DVSs and heterogeneous \mathbf{q}_k -DVSs.

4.3.1 Adaptation

In this section we study Equations (4.7) when $s_k > 0$ for all k . Remark that in this case, System (4.7) possesses a ‘‘pseudo’’ constant of motion.

‘‘Pseudo’’ Constant of Motion

If $\theta_k(t)$ and $\omega_k(t)$ solve Equations (4.8) for all k , then

$$\sum_{k=1}^n \left(\frac{\theta_k(t)}{\mathbf{a}_k} + \frac{\omega_k(t)}{s_k} \right) = \left(\sum_{k=1}^n \frac{\mathbf{q}_k}{\mathbf{a}_k} \right) t + \mathbf{K}$$

with $\mathbf{K} := \sum_{k=1}^n \left(\frac{\theta_k(0)}{\mathbf{a}_k} + \frac{\omega_k(0)}{\mathbf{s}_k} \right)$. Indeed, calculating the derivative with respect to t gives (omitting the arguments of the functions)

$$\sum_{k=1}^n \left(\frac{\dot{\theta}_k(t)}{\mathbf{a}_k} + \frac{\dot{\omega}_k(t)}{\mathbf{s}_k} \right) = \sum_{k=1}^n \left(\frac{\mathbf{q}_k}{\mathbf{a}_k} - \frac{\partial \mathbf{E}}{\partial \theta_k} - \frac{\partial \mathbf{E}}{\partial \phi_k} \right) = \sum_{k=1}^n \frac{\mathbf{q}_k}{\mathbf{a}_k} - \sum_{k=1}^n \frac{\partial \mathcal{W}}{\partial \theta_k} + \frac{\partial \mathcal{W}}{\partial \phi_k}$$

and by Hypothesis 1 II we have $\sum_{k=1}^n \frac{\partial \mathcal{W}}{\partial \theta_k} + \frac{\partial \mathcal{W}}{\partial \phi_k} = 0$.

4.3.1.1 Adaptation in Homogenous q-DVSs

Here we study Equations (4.7) when all DVSs have the same vibrating frequency (i.e. $\mathbf{q} = \mathbf{q}_k$ for all k). We first discuss the existence of a consensual oscillatory state, then the convergence towards it.

Existence of a Consensual Oscillatory State

Due to the left-hand side implication in Hypothesis 1 I, $\theta_k(t) = \phi_j(t)$ and $r_k(t) = \frac{\mathbf{b}_k}{\mathbf{f}_k}$ for all k, j and t is an extremum of \mathbf{E} , so that it cancels the coupling dynamics. Therefore, Equations (4.8) possess a consensual oscillatory state of the form

$$(\theta_k(t), r_k(t), \phi_k(t), \omega_k(t)) = \left(\mathbf{q} t, \frac{\mathbf{b}_k}{\mathbf{f}_k}, \mathbf{q} t, \mathbf{q} \right). \quad (4.10)$$

As stated in [42, 45], adaptation can be interpreted as a stability problem of a particular state. Therefore, we want to study the asymptotic stability of Orbit (4.10). That is, if the network interactions and adaptive mechanisms are switched on, do we have

$$\lim_{t \rightarrow \infty} |\theta_k(t) - \phi_k(t)| = 0, \quad \lim_{t \rightarrow \infty} |\phi_j(t) - \phi_k(t)| = 0, \quad \lim_{t \rightarrow \infty} r_k(t) = \frac{\mathbf{b}_k}{\mathbf{f}_k} \quad \text{and} \quad \lim_{t \rightarrow \infty} \omega_k(t) = \mathbf{q} \quad \forall k, j? \quad (4.11)$$

In the context of a network of VOSs, Limit (4.11) is interpreted as follows: once a consensual state is reached, all VOSs oscillate with the same frequency \mathbf{q} and this even if network interactions and adaptive mechanisms are removed. Hence, from an array of homogenous DVSs and coupled POs with initially different frequencies, network interactions and adaptive mechanisms drive the global system towards a synchronized oscillating state where each individual VOS no longer depends on its environment to maintain synchronization.

Convergence Towards a Consensual Oscillatory State

The convergence is proven in Lemma 1. For this lemma, we need to define the nonempty and compact set

$$\mathbb{K} := \{(\theta, r, \phi, \omega) \in (\mathbb{S}^1)^n \times \mathbb{R}_{\geq 0}^n \times (\mathbb{S}^1)^n \times \mathbb{R}^n \mid (\theta, r, \phi) \in \mathbb{M} \text{ and } \omega = \mathbf{q}\},$$

where \mathbb{M} is the consensual compact submanifold defined as

$$\mathbb{M} := \{(\theta, r, \phi) \in (\mathbb{S}^1)^n \times \mathbb{R}_{\geq 0}^n \times (\mathbb{S}^1)^n \mid \mathbf{M}(\theta, r, \phi) = 0\}$$

with $\mathbf{M}(\theta, r, \phi) = (\hat{L}(\theta, \phi)^\top, r - \frac{\mathbf{b}}{\mathbf{f}})$, and where \hat{L} is an $(2n-1) \times 2n$ matrix with $\hat{l}_{k,k} = 2n-1$ for $k = 1, \dots, 2n-1$, and where all other entries are -1 , and $\frac{\mathbf{b}}{\mathbf{f}} = \left(\frac{\mathbf{b}_1}{\mathbf{f}_1}, \dots, \frac{\mathbf{b}_n}{\mathbf{f}_n} \right)^\top$. An element λ in \mathbb{M} is such that

$$\theta_k = \phi_j, \quad r_k = \frac{\mathbf{b}_k}{\mathbf{f}_k} \quad \text{and} \quad \omega_k = \mathbf{q} \quad \forall k, j.$$

Lemma 1. *For coupling potentials \mathbf{E} in Equations (4.8) fulfilling Hypothesis 1, then there exists a neighborhood \mathbb{U} of \mathbb{K} such that all orbits $(\theta(t), r(t), \phi(t), \omega(t))$ solving Equations (4.8) (here $\mathbf{q} = \mathbf{q}_k$ for all k) with initial conditions in \mathbb{U} converge towards \mathbb{K} .*

Proof. The convergence towards \mathbb{K} follows from ЛЯПУНОВ's second method with ЛЯПУНОВ function

$$\mathbb{L}(\theta, r, \phi, \omega) = \mathbb{E}(\theta, r, \phi) + \frac{1}{2} \sum_{k=1}^n \frac{(\omega_k - \mathbf{q})^2}{s_k} \geq 0 .$$

We then have that $\mathbb{K} = \{(\theta, r, \phi, \omega) \in (\mathbb{S}^1)^n \times \mathbb{R}_{\geq 0}^n \times (\mathbb{S}^1)^n \times \mathbb{R}^n \mid \mathbb{L}(\theta, r, \phi, \omega) = 0\}$. The time derivation of $\frac{d[\mathbb{L}(\theta(t), r(t), \phi(t), \omega(t))]}{dt}$ is (omitting the dependence on time and the arguments of the functions)

$$\langle \nabla \mathbb{L}(\theta, r, \phi, \omega) \mid (\dot{\theta}, \dot{r}, \dot{\phi}, \dot{\omega})^\top \rangle = \sum_{k=1}^n \frac{\partial \mathbb{L}}{\partial \theta_k} \dot{\theta}_k + \sum_{k=1}^n \frac{\partial \mathbb{L}}{\partial r_k} \dot{r}_k + \sum_{k=1}^n \frac{\partial \mathbb{L}}{\partial \phi_k} \dot{\phi}_k + \sum_{k=1}^n \frac{\partial \mathbb{L}}{\partial \omega_k} \dot{\omega}_k$$

with

$$\begin{aligned} \sum_{k=1}^n \frac{\partial \mathbb{L}}{\partial \theta_k} \dot{\theta}_k &= \sum_{k=1}^n \frac{\partial \mathbb{E}}{\partial \theta_k} \cdot (\mathbf{q} - \mathbf{a}_k \frac{\partial \mathbb{E}}{\partial \theta_k}) = \mathbf{q} \sum_{k=1}^n \frac{\partial \mathbb{E}}{\partial \theta_k} - \sum_{k=1}^n \mathbf{a}_k \left(\frac{\partial \mathbb{E}}{\partial \theta_k} \right)^2 , \\ \sum_{k=1}^n \frac{\partial \mathbb{L}}{\partial r_k} \dot{r}_k &= \sum_{k=1}^n \frac{\partial \mathbb{E}}{\partial r_k} \cdot \left(-\mathbf{b}_k \frac{\partial \mathbb{E}}{\partial r_k} \right) = - \sum_{k=1}^n \mathbf{b}_k \left(\frac{\partial \mathbb{E}}{\partial r_k} \right)^2 , \\ \sum_{k=1}^n \frac{\partial \mathbb{L}}{\partial \phi_k} \dot{\phi}_k &= \sum_{k=1}^n \frac{\partial \mathbb{E}}{\partial \phi_k} \cdot \left(\omega_k - \mathbf{c}_k \frac{\partial \mathbb{E}}{\partial \phi_k} \right) = \sum_{k=1}^n \omega_k \frac{\partial \mathbb{E}}{\partial \phi_k} - \sum_{k=1}^n \mathbf{c}_k \left(\frac{\partial \mathbb{E}}{\partial \phi_k} \right)^2 , \\ \sum_{k=1}^n \frac{\partial \mathbb{L}}{\partial \omega_k} \dot{\omega}_k &= \sum_{k=1}^n \frac{(\omega_k - \mathbf{q})}{s_k} \cdot \left(-s_k \right) \frac{\partial \mathbb{E}}{\partial \phi_k} = - \sum_{k=1}^n \omega_k \frac{\partial \mathbb{E}}{\partial \phi_k} + \mathbf{q} \sum_{k=1}^n \frac{\partial \mathbb{E}}{\partial \phi_k} . \end{aligned}$$

Hence

$$\langle \nabla \mathbb{L}(\theta, r, \phi, \omega) \mid (\dot{\theta}, \dot{r}, \dot{\phi}, \dot{\omega})^\top \rangle = - \sum_{k=1}^n \left(\mathbf{a}_k \left(\frac{\partial \mathbb{E}}{\partial \theta_k} \right)^2 + \mathbf{b}_k \left(\frac{\partial \mathbb{E}}{\partial r_k} \right)^2 + \mathbf{c}_k \left(\frac{\partial \mathbb{E}}{\partial \phi_k} \right)^2 \right) + \underbrace{\mathbf{q} \sum_{k=1}^n \left(\frac{\partial \mathbb{E}}{\partial \phi_k} + \frac{\partial \mathbb{E}}{\partial \theta_k} \right)}_{=0} \leq 0 .$$

The last inequality is zero if and only if $\nabla \mathbb{E}(\theta, \phi, r) = \mathbf{0}$. Therefore, to guarantee strict negativity, we need to prove the existence of a neighborhood \mathbb{U}_λ of \mathbb{M} such that $\nabla \mathbb{F}(\theta, r, \phi) \neq \mathbf{0}$ for all $(\theta, r, \phi) \in \mathbb{U}_\lambda \setminus \mathbb{M}$. Such neighborhood exists (see Corollary E.2 in [45]) if, for all $\bar{\lambda} \in \mathbb{M}$, we have

$$\ker(\mathfrak{D}^2 \mathbb{E}(\bar{\lambda})) = \ker(\mathbb{M}(\bar{\lambda})) ,$$

where $\ker(\mathfrak{D}^2 \mathbb{E}(\bar{\lambda}))$ is the kernel of the $3n \times 3n$ Hessian of \mathbb{E} evaluated at $\bar{\lambda}$, and $\ker(\mathbb{M}(\bar{\lambda}))$ is the kernel of the submanifold \mathbb{M} evaluated at $\bar{\lambda}$. We now verify the equality between the kernels.

Since

$$\mathfrak{D} \mathbb{M}(\bar{\lambda}) = \mathbf{0} \iff \hat{L}(\theta, \phi)^\top = \mathbf{0} \quad \text{and} \quad Id r = \mathbf{0}$$

with $n \times n$ identity matrix Id , then, by definition of \hat{L} , we have $\ker(\mathbb{M}(\bar{\lambda})) = \{\theta_k = \phi_j \text{ and } r_k = 0 \forall k, j\}$.

Since $\mathfrak{D}^2 \mathbb{E}(\bar{\lambda})$ is positive semi-definite (because $\bar{\lambda}$ is a minimum of \mathbb{E}) and symmetric, then $\ker(\mathfrak{D}^2 \mathbb{E}(\bar{\lambda})) = \{\lambda \in (\mathbb{S}^1)^n \times \mathbb{R}_{\geq 0}^n \times (\mathbb{S}^1)^n \mid \langle \lambda \mid \mathfrak{D}^2 \mathbb{E}(\bar{\lambda}) \lambda \rangle = 0\}$. By hypothesis, we have

$$\langle \lambda \mid \mathfrak{D}^2 \mathbb{E}(\bar{\lambda}) \lambda \rangle = 0 \iff \lambda = (\theta, r, \phi) \quad \text{such that} \quad \theta_k = \phi_j \quad \text{and} \quad r_k = 0 \quad \forall k, j ,$$

and so

$$\lambda \in \ker(\mathfrak{D}^2 \mathbb{E}(\bar{\lambda})) \iff \lambda \in \ker(\mathbb{M}(\bar{\lambda})) .$$

Finally, take a neighborhood \mathbb{U}_ω of $\{\omega \in \mathbb{R}^n \mid \omega = \mathbf{q}\}$ and define \mathbb{U} as $\mathbb{U} := \mathbb{U}_\lambda \times \mathbb{U}_\omega$. □

Remark I

Numerical simulations show that if the symmetric hypothesis of the networks is relaxed directly in Equations (4.9) (i.e. precisely, the $a_{k,j}$ and $a_{k,j}^\phi$ are no longer symmetric), the dynamics still converges towards a consensual oscillatory state: that is, Limit (4.11) still holds.

4.3.1.2 Adaptation in Heterogenous \mathbf{q}_k -DVSs

We here consider Equations (4.7) where the DVSs have vertex-dependent vibrating frequencies \mathbf{q}_k . We discuss the existence of a consensual oscillatory state. The convergence towards it has been numerically observed.

Existence of a Consensual Oscillatory State

If the complex system possesses a consensual oscillatory state, then by definition we have, for $k = 1, \dots, n$,

$$\theta_k(t) = \mathbf{q}_c t + \vartheta_k, \quad r_k(t) = r_{c,k}, \quad \phi_k(t) = \mathbf{q}_c t + \varphi_k, \quad \omega_k(t) = \mathbf{q}_c$$

with phase shifts ϑ_k and φ_k . Note that the following conditions are necessary in order for the global system to possess a consensual oscillatory state.

- I $\frac{\partial E}{\partial \theta_k}(\mathbf{q}_c t + \vartheta_k, r_{c,k}, \mathbf{q}_c t + \varphi_k) = \frac{\mathbf{q}_k - \mathbf{q}_c}{\mathbf{a}_k}$ for all k and t
- II $\frac{\partial E}{\partial r_k}(\mathbf{q}_c t + \vartheta_k, r_{c,k}, \mathbf{q}_c t + \varphi_k) = 0$ for all k and t
- III $\frac{\partial E}{\partial \phi_k}(\mathbf{q}_c t + \vartheta_k, r_{c,k}, \mathbf{q}_c t + \varphi_k) = 0$ for all k and t

Let us determine the value \mathbf{q}_c . By the ‘‘pseudo’’ constant of motion, we have

$$\sum_{k=1}^n \frac{\mathbf{q}_k}{\mathbf{a}_k} = \sum_{k=1}^n \left(\frac{\dot{\theta}_k(t)}{\mathbf{a}_k} + \frac{\dot{\omega}_k(t)}{\mathbf{s}_k} \right) = \sum_{k=1}^n \frac{\mathbf{q}_c}{\mathbf{a}_k} \iff \mathbf{q}_c = \frac{\sum_{k=1}^n \frac{\mathbf{q}_k}{\mathbf{a}_k}}{\sum_{k=1}^n \frac{1}{\mathbf{a}_k}}.$$

Remark I

Numerical simulations show that if the symmetric hypothesis of the networks is relaxed directly in Equations (4.9) (i.e. precisely, the $a_{k,j}$ and $a_{k,j}^\phi$ are no longer symmetric), the dynamics still converges towards a consensual oscillatory state. That is, Limit (4.11) still holds. However, the value of the consensual frequency is no longer \mathbf{q}_c (i.e. $\lim_{t \rightarrow \infty} \omega_k(t) = \tilde{\mathbf{q}}_c \neq \mathbf{q}_c$).

Remark II

When E is taken as in Section 4.2.1 with local coupling functions defined as in Example (2) and with $W \equiv 0$, the system becomes

$$\begin{aligned} \dot{\theta}_k &= \mathbf{q}_k - \mathbf{a}_k r_k \sin(\theta_k - \phi_k) \\ \dot{r}_k &= -\mathbf{f}_k r_k + \mathbf{b}_k \cos(\theta_k - \phi_k) \\ \dot{\phi}_k &= \omega_k - \mathbf{c}_k (r_k \sin(\phi_k - \theta_k) - \frac{\partial \mathcal{V}}{\partial \phi_k}(\phi)) \quad k = 1, \dots, n, \\ \dot{\omega}_k &= -\mathbf{s}_k (r_k \sin(\phi_k - \theta_k) - \frac{\partial \mathcal{V}}{\partial \phi_k}(\phi)) \end{aligned} \tag{4.12}$$

and the $r_{c,k}$ for the consensual oscillatory state are analytically determined (see Appendix 4.D for details) as either $O_k^+(\mathbf{q}_c)$ or $O_k^-(\mathbf{q}_c)$ with

$$O_k^\pm(x) = \sqrt{\frac{1 \pm \sqrt{1 - 4\left(\frac{\mathbf{f}_k}{\mathbf{b}_k}\right)^2 \left(\frac{\mathbf{q}_k - x}{\mathbf{a}_k}\right)^2}}{2\left(\frac{\mathbf{f}_k}{\mathbf{b}_k}\right)^2}} \quad k = 1, \dots, n. \tag{4.13}$$

In numerical simulation, it has been observed that the $r_k(t)$ converge towards $O_k^+(\mathbf{q}_c)$ instead of $O_k^-(\mathbf{q}_c)$. Note that we have $O_k^-(\mathbf{q}_c) \leq O_k^+(\mathbf{q}_c) \leq \frac{\mathbf{b}_k}{\mathbf{f}_k}$ since

$$\left(\frac{\mathbf{b}_k}{\mathbf{f}_k}\right)^2 = \frac{1 + 1}{2\left(\frac{\mathbf{f}_k}{\mathbf{b}_k}\right)^2} = \frac{1 + \sqrt{1 - 4\left(\frac{\mathbf{f}_k}{\mathbf{b}_k}\right)^2 \left(\frac{\mathbf{q}_k - \mathbf{q}_c}{\mathbf{a}_k}\right)^2}}{2\left(\frac{\mathbf{f}_k}{\mathbf{b}_k}\right)^2}.$$

Refer to Appendix 4.D to see that $0 \leq \sqrt{1 - 4\left(\frac{\mathbf{f}_k}{\mathbf{b}_k}\right)^2 \left(\frac{\mathbf{q}_k - \mathbf{q}_c}{\mathbf{a}_k}\right)^2} \leq 1$.

4.3.2 Synchronization

In this section we study Equations (4.7) when $s_k = 0$ for all k . Remark that in this case, System (4.7) possesses a “pseudo” constant of motion.

“Pseudo” Constant of Motion

If $\theta_k(t)$ and $\phi_k(t)$ solve Equations (4.8) for all k , then

$$\sum_{k=1}^n \left(\frac{\theta_k(t)}{a_k} + \frac{\phi_k(t)}{c_k} \right) = \left(\sum_{k=1}^n \left(\frac{q_k}{a_k} + \frac{w_k}{c_k} \right) \right) t + \mathbf{K}$$

with $\mathbf{K} := \sum_{k=1}^n \left(\frac{\theta_k(0)}{a_k} + \frac{\phi_k(0)}{c_k} \right)$. Indeed, calculating the derivative with respect to t gives (omitting the arguments of the functions)

$$\sum_{k=1}^n \left(\frac{\dot{\theta}_k(t)}{a_k} + \frac{\dot{\phi}_k(t)}{c_k} \right) = \sum_{k=1}^n \left(\frac{q_k}{a_k} + \frac{w_k}{c_k} - \frac{\partial E}{\partial \theta_k} - \frac{\partial E}{\partial \phi_k} \right) = \sum_{k=1}^n \left(\frac{q_k}{a_k} + \frac{w_k}{c_k} \right) - \sum_{k=1}^n \frac{\partial W}{\partial \theta_k} + \frac{\partial W}{\partial \phi_k}$$

and by Hypothesis 1 II, we have $\sum_{k=1}^n \frac{\partial W}{\partial \theta_k} + \frac{\partial W}{\partial \phi_k} = 0$.

4.3.2.1 Synchronization in Homogenous q-DVSs

Here we study Equations (4.7) when all DVSs have the same vibrating frequency (i.e. $q = q_k$ for all k). We discuss the existence of a synchronized oscillatory state. The convergence towards it has been numerically observed.

Existence of a Synchronized Oscillatory State

If the complex system possesses a synchronized state, then, by definition, we have, for $k = 1, \dots, n$,

$$\theta_k(t) = \bar{q} t + \vartheta_k, \quad r_k(t) = \bar{r}_k, \quad \phi_k(t) = \bar{q} t + \varphi_k$$

with phase shifts ϑ_k and φ_k . Note that the following conditions are necessary in order for the global system to possess a synchronized oscillatory state.

- I $\frac{\partial E}{\partial \theta_k}(\bar{q} t + \vartheta_k, \bar{r}_k, \bar{q} t + \varphi_k) = \frac{q - \bar{q}}{a_k}$ for all k and t
- II $\frac{\partial E}{\partial r_k}(\bar{q} t + \vartheta_k, \bar{r}_k, \bar{q} t + \varphi_k) = 0$ for all k and t
- III $\frac{\partial E}{\partial \phi_k}(\bar{q} t + \vartheta_k, \bar{r}_k, \bar{q} t + \varphi_k) = \frac{w_k - \bar{q}}{c_k}$ for all k and t

Let us determine the value \bar{q} . By the “pseudo” constant of motion, we have

$$\sum_{k=1}^n \left(\frac{q}{a_k} + \frac{w_k}{c_k} \right) = \sum_{k=1}^n \left(\frac{\dot{\theta}_k(t)}{a_k} + \frac{\dot{\phi}_k(t)}{c_k} \right) = \sum_{k=1}^n \left(\frac{\bar{q}}{a_k} + \frac{\bar{q}}{c_k} \right) \iff \bar{q} = \frac{q \sum_{k=1}^n \frac{1}{a_k} + \sum_{k=1}^n \frac{w_k}{c_k}}{\sum_{k=1}^n \left(\frac{1}{a_k} + \frac{1}{c_k} \right)}$$

Remark I

When E is taken as in Section 4.2.1 with local coupling functions defined as in Example (2) and with $W \equiv 0$, the \bar{r}_k for the synchronized oscillatory state are analytically determined as either $O_k^+(\bar{q})$ or $O_k^-(\bar{q})$ (see Equation (4.13)). In numerical simulation, it has been observed that the $r_k(t)$ converge towards $O_k^+(\bar{q})$ instead of $O_k^-(\bar{q})$.

4.3.2.2 Synchronization in Heterogenous \mathbf{q}_k -DVSs

We here consider Equations (4.7) where the DVSs have vertex-dependent vibrating frequencies \mathbf{q}_k . We discuss the existence of a synchronized oscillatory state. The convergence towards it has been numerically observed.

Existence of a Synchronized Oscillatory State

If the complex system possesses a synchronized state, then by definition we have, for $k = 1, \dots, n$,

$$\theta_k(t) = \mathbf{q}_s t + \vartheta_k, \quad r_k(t) = r_{s,k}, \quad \phi_k(t) = \mathbf{q}_s t + \varphi_k$$

with phase shifts ϑ_k and φ_k . Note that the following conditions are necessary in order for the global system to possess a synchronized oscillatory state.

- I $\frac{\partial \mathbf{E}}{\partial \theta_k}(\mathbf{q}_s t + \vartheta_k, r_{s,k}, \mathbf{q}_s t + \varphi_k) = \frac{\mathbf{q}_k - \mathbf{q}_s}{\mathbf{a}_k}$ for all k and t
- II $\frac{\partial \mathbf{E}}{\partial r_k}(\mathbf{q}_s t + \vartheta_k, r_{s,k}, \mathbf{q}_s t + \varphi_k) = 0$ for all k and t
- III $\frac{\partial \mathbf{E}}{\partial \phi_k}(\mathbf{q}_s t + \vartheta_k, r_{s,k}, \mathbf{q}_s t + \varphi_k) = \frac{\mathbf{w}_k - \mathbf{q}_s}{\mathbf{c}_k}$ for all k and t

Let us determine the value \mathbf{q}_s . By the ‘‘pseudo’’ constant of motion, we have

$$\sum_{k=1}^n \left(\frac{\mathbf{q}_k}{\mathbf{a}_k} + \frac{\mathbf{w}_k}{\mathbf{c}_k} \right) = \sum_{k=1}^n \left(\frac{\dot{\theta}_k(t)}{\mathbf{a}_k} + \frac{\dot{\phi}_k(t)}{\mathbf{c}_k} \right) = \sum_{k=1}^n \left(\frac{\mathbf{q}_s}{\mathbf{a}_k} + \frac{\mathbf{q}_s}{\mathbf{c}_k} \right) \iff \mathbf{q}_s = \frac{\sum_{k=1}^n \left(\frac{\mathbf{q}_k}{\mathbf{a}_k} + \frac{\mathbf{w}_k}{\mathbf{c}_k} \right)}{\sum_{k=1}^n \left(\frac{1}{\mathbf{a}_k} + \frac{1}{\mathbf{c}_k} \right)}.$$

Remark I

When \mathbf{E} is taken as in Section 4.2.1 with local coupling functions defined as in Example (2) and with $\mathbf{W} \equiv 0$, the \bar{r}_k for the synchronized oscillatory state are analytically determined as either $\mathbf{O}_k^+(\mathbf{q}_s)$ or $\mathbf{O}_k^-(\mathbf{q}_s)$ (see Equation (4.13)). In numerical simulation, it has been observed that the $r_k(t)$ converge towards $\mathbf{O}_k^+(\mathbf{q}_s)$ instead of $\mathbf{O}_k^-(\mathbf{q}_s)$.

4.4 Summary

Table 4.1 summarizes the asymptotics of Equations (4.7) for the different cases and under different assumptions.

		Adaptation		Synchronization		
		General \mathbf{E}	\mathbf{E} as in Section 4.2.1	General \mathbf{E}	\mathbf{E} as in Section 4.2.1	
Homogenous \mathbf{q} -DVS	U.N.	1	1	U.N.	6	7
	D.N.	2	2	D.N.	8	8
Heterogenous \mathbf{q}_k -DVS	U.N.	3	4	U.N.	9	10
	D.N.	5	5	D.N.	11	11

Table 4.1: Summarizing Asymptotic Dynamics for System (4.7). U.N. and D.N. stand, respectively, for undirected and directed networks.

Legend (COS and SOS stand, respectively, for consensual oscillatory state and synchronized oscillatory state)

- 1 Convergence towards COS as defined in Section 4.3.1.1 is analytically proven (i.e. Limit (4.11) holds).
- 2 Convergence towards COS as defined in Section 4.3.1.1 is numerically observed (i.e. Limit (4.11) holds).
- 3 Convergence towards COS as defined in Section 4.3.1.2 with $\mathbf{q}_c = \frac{\sum_{k=1}^n \frac{q_k}{a_k}}{\sum_{k=1}^n \frac{1}{a_k}}$ is numerically observed.
- 4 Convergence towards COS as defined in Section 4.3.1.2 with $\mathbf{q}_c = \frac{\sum_{k=1}^n \frac{q_k}{a_k}}{\sum_{k=1}^n \frac{1}{a_k}}$ and $\bar{r}_k = \mathbf{O}_k^+(\mathbf{q}_c)$ is numerically observed.
- 5 Convergence towards COS as defined in Section 4.3.1.2 but here $\mathbf{q}_c \neq \frac{\sum_{k=1}^n \frac{q_k}{a_k}}{\sum_{k=1}^n \frac{1}{a_k}}$ is numerically observed.
- 6 Convergence towards SOS as defined in Section 4.3.2.1 with $\bar{\mathbf{q}} = \frac{q \sum_{k=1}^n \frac{1}{a_k} + \sum_{k=1}^n \frac{w_k}{c_k}}{\sum_{k=1}^n \left(\frac{1}{a_k} + \frac{1}{c_k} \right)}$ is numerically observed.
- 7 Convergence towards SOS as defined in Section 4.3.2.1 with $\bar{\mathbf{q}} = \frac{q \sum_{k=1}^n \frac{1}{a_k} + \sum_{k=1}^n \frac{w_k}{c_k}}{\sum_{k=1}^n \left(\frac{1}{a_k} + \frac{1}{c_k} \right)}$ and $\bar{r}_k = \mathbf{O}_k^+(\bar{\mathbf{q}})$ is numerically observed.
- 8 Convergence towards SOS as defined in Section 4.3.2.1 but here $\bar{\mathbf{q}} \neq \frac{q \sum_{k=1}^n \frac{1}{a_k} + \sum_{k=1}^n \frac{w_k}{c_k}}{\sum_{k=1}^n \left(\frac{1}{a_k} + \frac{1}{c_k} \right)}$ is numerically observed.
- 9 Convergence towards SOS as defined in Section 4.3.2.2 with $\mathbf{q}_s = \frac{\sum_{k=1}^n \left(\frac{q_k}{a_k} + \frac{w_k}{c_k} \right)}{\sum_{k=1}^n \left(\frac{1}{a_k} + \frac{1}{c_k} \right)}$ is numerically observed.
- 10 Convergence towards SOS as defined in Section 4.3.2.2 with $\mathbf{q}_s = \frac{\sum_{k=1}^n \left(\frac{q_k}{a_k} + \frac{w_k}{c_k} \right)}{\sum_{k=1}^n \left(\frac{1}{a_k} + \frac{1}{c_k} \right)}$ and $\bar{r}_k = \mathbf{O}_k^+(\mathbf{q}_s)$ is numerically observed.
- 11 Convergence towards SOS as defined in Section 4.3.2.2 but here $\mathbf{q}_s \neq \frac{\sum_{k=1}^n \left(\frac{q_k}{a_k} + \frac{w_k}{c_k} \right)}{\sum_{k=1}^n \left(\frac{1}{a_k} + \frac{1}{c_k} \right)}$ is numerically observed.

4.5 Numerical Simulations

We report two sets of numerical simulations. The first compares the transient and asymptotic dynamics between seven homogenous \mathbf{q} -DVSs and heterogenous \mathbf{q}_k -DVSs with undirected and directed networks (refer to Section 4.5.1). The second compares the basin of attraction towards a consensual state of two coupled VOSs with and without adaptation (refer to Section 4.5.2).

4.5.1 Network of Homogenous \mathbf{q} -DVSs and Heterogenous \mathbf{q}_k -DVSs

Here, $n = 7$, and the network is defined as in Figure 4.3(c). The friction parameters are $f_k = 1 + 0.1(k - 1)$. The coupling strengths are chosen as $a_k = 0.3$, $b_k = 1$ for all k , $c_k = 0.2$ for $k = 1, 2, 3$, $c_4 = 0.15$, $c_k = 0.1$ for $k = 5, 6, 7$, and the susceptibility constants as $s_1 = 0.1$ and $s_k = 0.7 + 0.1(k - 2)$ for $k = 2, \dots, 7$. The coupling function is $\mathbf{B}_{k,j}(x) = \sinh(x)$ for all k, j . The initial conditions $(\theta_k(0), r_k(0), \phi_k(0), \omega_k(0))$ are randomly uniformly drawn from $]-0.1, 0.1[\times]0.9, 1.1[\times]-0.1, 0.1[\times]0.9, 1.1[$.

For the network of homogenous \mathbf{q} -DVSs, the frequencies are set as $\mathbf{q}_k = 1$ for all k , and for the network of heterogenous \mathbf{q}_k -DVSs, the frequencies are $\mathbf{q}_k = 0.91 + 0.3(k - 1)$ for $k = 1, \dots, 7$ and so $\mathbf{q}_c = 1$. For both cases, all ω_k should converge towards one, and this is observed in Figure 4.4(a) and Figure 4.4(b).

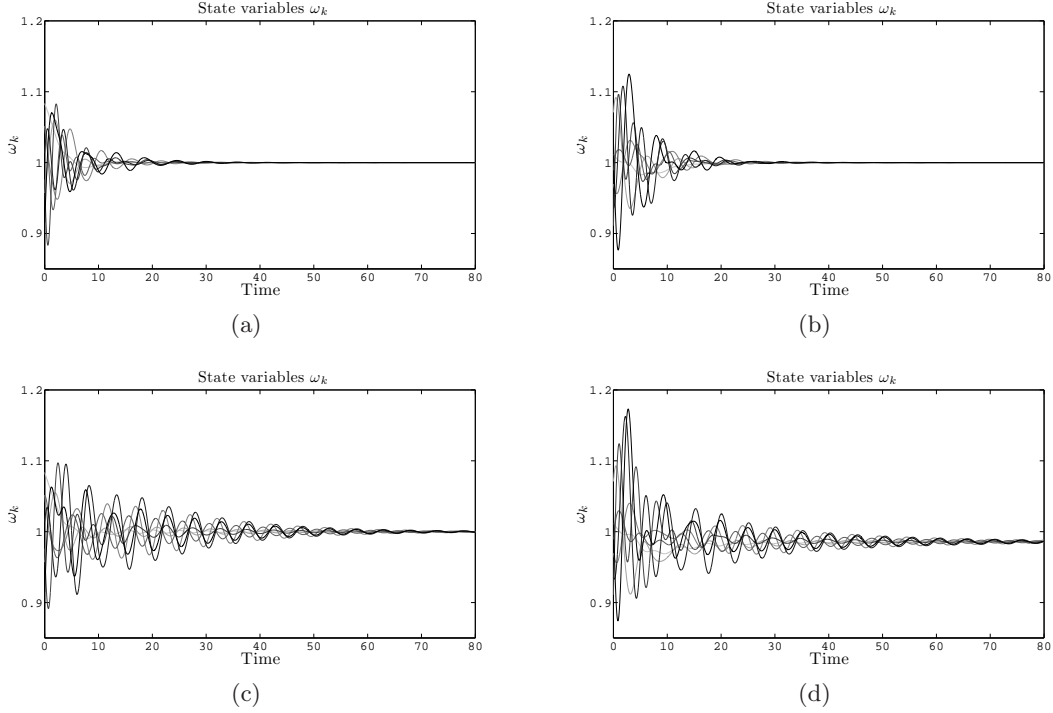


Fig. 4.4: Time evolution of ω_k for seven homogenous \mathbf{q} -DVSs (Figure 4.4(a)) and for seven heterogenous \mathbf{q}_k -DVSs, interacting through an undirected network as in Figure 4.3(c).

With the same configuration, another numerical integration is carried out, this time with a directed network as in Figure 4.5. The resulting dynamics for ω_k in a collection of homogenous \mathbf{q} -DVSs and heterogenous \mathbf{q}_k -DVSs is shown in Figures 4.4(c) and 4.4(d). Note that in Figure 4.4(d) the asymptotic value of any ω_k is not equal to one. As mentioned in Sections 4.3.1.1 and 4.3.1.2, numerical experiments show that for a directed network of homogenous \mathbf{q} -DVSs, Limit (4.11) holds, while for a directed network of heterogenous \mathbf{q}_k -DVSs, the ω_k converge towards a constant value which is, in general, not equal to \mathbf{q}_c .

4.5.2 Adaptation vs. Synchronization

Here, we consider two VOSs with only the POs are coupled (i.e. $a_{1,2} = a_{2,1} = 0$ and $a_{1,2}^\phi = a_{2,1}^\phi = 1$). The parameters and coupling strengths are $\mathbf{q}_1 = 0.9$ and $\mathbf{q}_2 = 1.1$, and $\mathbf{f}_1 = \mathbf{f}_2 = \mathbf{a}_1 = \mathbf{a}_2 = \mathbf{b}_1 = \mathbf{b}_2 = \mathbf{c}_1 = \mathbf{c}_2 = 1$. The coupling function is $\mathbf{B}(x) = \sin(x)$. The initial conditions $(\theta_k(0), r_k(0), \phi_k(0))$ are randomly uniformly drawn from $] - 0.1, 0.1[\times] 0.9, 1.1[\times] - 0.1, 0.1[$ and $\omega(0)_1 = -0.15$ and $\omega(0)_2 = 2.15$.

For the first numerical experiment, the two VOSs are allowed to adapt their frequencies, and here the susceptibility constants are $\mathbf{s}_k = 1$ for $k = 1, 2$. The resulting dynamics for r_k and ω_k is displayed in Figures 4.6(a) and 4.6(b). Figure 4.6(c) shows the resulting dynamics when the two VOSs do not adapt their frequencies (i.e. here $\mathbf{s}_k = 0$ for $k = 1, 2$ and so $w_1 := \omega(0)_1 = -0.15$ and $w_2 := \omega(0)_2 = 2.15$). For both situations, $\mathbf{q}_c = \bar{\mathbf{q}} = 1$.

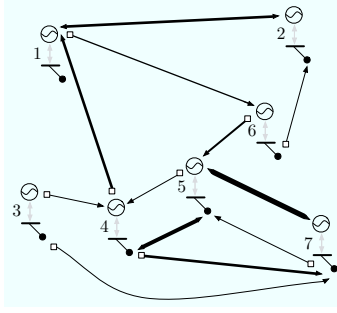


Fig. 4.5: Directed Network Topology. The cubes at the end of the edges indicate that there is no interaction with the vertex in question. For example, PO 5 interacts with PO 4, but PO 4 does not interact with PO 5 (i.e. PO 4 receives information from PO 5 but not vice versa).

Observe in Figure 4.6 that for this parameter setting and with these initial conditions, the two coupled VOSs are still able to adapt their frequencies and converge towards a consensual oscillatory state. However, if they are not allowed to adapt, the amplitudes r_k do not converge towards a common and constant value, but rather towards a common oscillatory state. Still in the non-adapting case and when $B(x) = \cosh(x) - 1$, it has been observed that the two VOSs do synchronize with frequency \bar{q} , and that the two r_k converge towards the common value $\bar{r} = \sqrt{\frac{1+\sqrt{0.96}}{2}}$. However, when $B(x) = \log(\cosh(x))$, the VOSs do not synchronize. We observe the following: $\lim_{t \rightarrow \infty} \dot{\theta}_1(t) = \lim_{t \rightarrow \infty} \dot{\phi}_1(t) = m_1$ and $\lim_{t \rightarrow \infty} \dot{\theta}_2(t) = \lim_{t \rightarrow \infty} \dot{\phi}_2(t) = m_2$, and the r_k converge to a common and constant value just under one (but which is not \bar{r}).

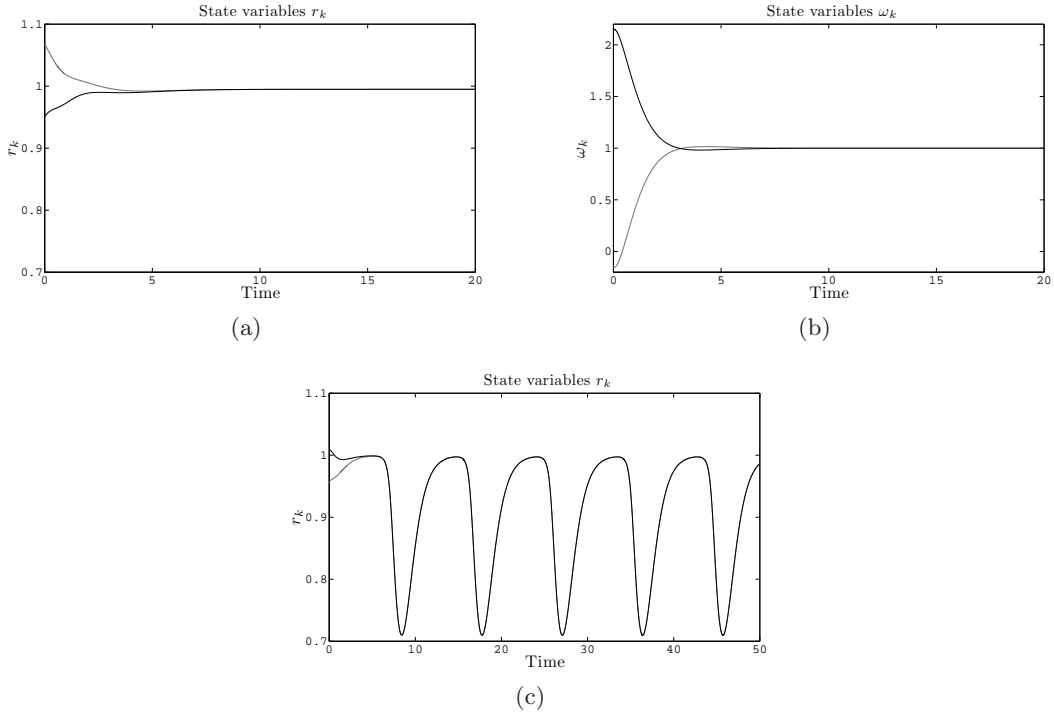


Fig. 4.6: Time evolution of r_k and ω_k for two heterogeneous \mathbf{q}_k -DVSs with adapting frequencies (Figure 4.6(a) & 4.6(b)), and time evolution of r_k for two heterogeneous \mathbf{q}_k -DVSs with no adaptation (Figure 4.6(c)).

4.6 Conclusions and Perspectives

We study a complex system composed of heterogenous local systems with qualitatively different dynamics. The two different communities merged into one interacting complex network grasp two well-known phenomena: synchronization and adaptation. Indeed, Equations (4.7) characterize phase synchronization with the coupled θ_k variables. At the same time, these equations express an adaptive frequency behavior with variables ω_k . Therefore, for such systems, one can speak of the “plastic” (i.e. synchronization) and “elastic” (i.e. adaptation) capabilities of the network to produce common dynamical patterns. Plastic, since it concerns a synchronization problem: common dynamical patterns are attained and maintained thanks to the coupling dynamics - remove the interaction and all local systems converge back towards their individual behavior. Elastic since it deals with an adaptation approach: common dynamical patterns are attained thanks to the coupling dynamics, but coupling is no longer needed in order to maintain the common dynamics - remove the interactions and local systems self-perpetuate the common dynamical pattern.

In VOS networks with homogenous q-DVSs, adaptation leads the system to converge towards a state where all DVSs are entrained with maximum amplitude. Here, it is important to note that this consensual oscillatory state does not depend on the coupling dynamics. Hence, once this state is reached, any changes in network topology will not perturb the local system. This is not true for all three other cases, where the consensual or synchronized state does depend on the network connections and thus a change in the environment automatically causes a disturbance for the local dynamics.

Perspective works include a rigorous study of advantages and disadvantages of adaptive frequency systems compared to phase synchronization systems. Also, as occurring in nature, time-dependent connections in networks should be implemented. As discussed in [42], parametric resonance phenomena may occur in networks of adaptive frequency oscillators.

Appendix

4.A Calculations for Equations (4.2), (4.3) and (4.4)

We verify that the entrained solution solves Equation 4.2. Since² $\cos(\frac{1}{2}\sin^{-1}(x)) = \frac{1}{2}(\sqrt{1-x} + \sqrt{1+x})$, then $\frac{1}{f}\cos(\frac{1}{2}\sin^{-1}(2(q-w)f)) = \frac{1}{2f}(\sqrt{1-2(q-w)f} + \sqrt{1+2(q-w)f})$ and so $\bar{r} = \frac{1}{f}\cos(\frac{1}{2}\sin^{-1}(2(q-w)f))$. By direct computation, we have

$$\begin{aligned}\dot{\theta} = w &\leftrightarrow q - \frac{1}{f}\cos(\frac{1}{2}\sin^{-1}(2(q-w)f))\sin(\frac{1}{2}\sin^{-1}(2(q-w)f)) = q - \frac{\sin(\sin^{-1}(2(q-w)f))}{2f} \\ &= q - q + w = w \\ \dot{r} = 0 &\leftrightarrow -f\frac{1}{f}\cos(\frac{1}{2}\sin^{-1}(2(q-w)f)) + \cos(\frac{1}{2}\sin^{-1}(2(q-w)f)) = 0 \\ \dot{\phi} = w &\leftrightarrow w\end{aligned}$$

which concludes the verification.

We verify that the synchronized solution solves Equation 4.3. First note that for any orbits $\theta(t)$ and $\phi(t)$ solving Equation (4.3), then $\dot{\theta}(t) + \dot{\phi}(t) = q - r(t)\sin(\theta(t) - \phi(t)) + w - r(t)\sin(\phi(t) - \theta(t)) = q + w$. Hence, the system possesses a “pseudo” constant of motion $\theta(t) + \phi(t) = (q + w)t + \mathbf{K}$ with

² Since $\cos(\frac{1}{2}y) = \pm\sqrt{\frac{1}{2}(1+\cos(y))}$ and $\cos(\sin^{-1}(z)) = \sqrt{1-z^2}$, then $\cos(\frac{1}{2}\sin^{-1}(x)) = \sqrt{\frac{1}{2}(1+\sqrt{1-x^2})}$ for $x \in [0, 1]$, which equals $\frac{1}{2}(\sqrt{1-x} + \sqrt{1+x})$ for $x \in [0, 1]$ because

$$\left(\frac{1}{2}(\sqrt{1-x} + \sqrt{1+x})\right)^2 = \frac{1}{4}(2 + 2\sqrt{1-x^2}) = \frac{1}{2}(1 + \sqrt{1-x^2}).$$

$\mathbf{K} = \theta(0) + \phi(0)$. The synchronized solution is consistent with the “pseudo” constant of motion since

$$\begin{aligned}\theta(t) + \phi(t) &= \frac{\mathbf{q} + \mathbf{w}}{2} t + \frac{\theta(0) + \phi(0)}{2} + \frac{1}{4} \sin^{-1}((\mathbf{q} - \mathbf{w})\mathbf{f}) \\ &\quad + \frac{\mathbf{q} + \mathbf{w}}{2} t + \frac{\theta(0) + \phi(0)}{2} + \frac{1}{4} \sin^{-1}((\mathbf{w} - \mathbf{q})\mathbf{f}) \\ &= (\mathbf{q} + \mathbf{w})t + \theta(0) + \phi(0) .\end{aligned}$$

Here, $\theta(t) - \phi(t) = \frac{1}{4} \sin^{-1}((\mathbf{q} - \mathbf{w})\mathbf{f}) - \frac{1}{4} \sin^{-1}((\mathbf{w} - \mathbf{q})\mathbf{f}) = \frac{1}{2} \sin^{-1}((\mathbf{q} - \mathbf{w})\mathbf{f})$ and so, by direct computation, we have

$$\begin{aligned}\dot{\theta} = \frac{\mathbf{q} + \mathbf{w}}{2} &\leftrightarrow \mathbf{q} - \frac{1}{f} \cos\left(\frac{1}{2} \sin^{-1}((\mathbf{q} - \mathbf{w})\mathbf{f})\right) \sin\left(\frac{1}{2} \sin^{-1}((\mathbf{q} - \mathbf{w})\mathbf{f})\right) = \mathbf{q} - \frac{\sin(\sin^{-1}((\mathbf{q} - \mathbf{w})\mathbf{f}))}{2f} \\ &= \mathbf{q} - \frac{\mathbf{q}}{2} + \frac{\mathbf{w}}{2} = \frac{\mathbf{q} + \mathbf{w}}{2} \\ \dot{r} = 0 &\leftrightarrow -f \frac{1}{f} \cos\left(\frac{1}{2} \sin^{-1}((\mathbf{q} - \mathbf{w})\mathbf{f})\right) + \cos\left(\frac{1}{2} \sin^{-1}((\mathbf{q} - \mathbf{w})\mathbf{f})\right) = 0 \\ \dot{\phi} = \frac{\mathbf{q} + \mathbf{w}}{2} &\leftrightarrow \mathbf{w} - \frac{1}{f} \cos\left(\frac{1}{2} \sin^{-1}((\mathbf{q} - \mathbf{w})\mathbf{f})\right) \sin\left(\frac{-1}{2} \sin^{-1}((\mathbf{q} - \mathbf{w})\mathbf{f})\right) = \mathbf{q} + \frac{\sin(\sin^{-1}((\mathbf{q} - \mathbf{w})\mathbf{f}))}{2f} \\ &= \mathbf{w} + \frac{\mathbf{q}}{2} - \frac{\mathbf{w}}{2} = \frac{\mathbf{q} + \mathbf{w}}{2}\end{aligned}$$

which concludes the verification.

We verify that the adapted solution solves Equation 4.4. First note that for any orbits $\theta(t)$ and $\omega(t)$ solving Equation (4.4), then $\dot{\theta}(t) + \dot{\omega}(t) = \mathbf{q} - r(t) \sin(\theta(t) - \phi(t)) - r(t) \sin(\phi(t) - \theta(t)) = \mathbf{q}$. Hence, the system possesses a “pseudo” constant of motion $\theta(t) + \omega(t) = \mathbf{q}t + \mathbf{K}$ with $\mathbf{K} = \theta(0) + \omega(0)$. The adapted solution is consistent with the “pseudo” constant of motion since $\theta(t) + \omega(t) = \mathbf{q}t + \vartheta + \mathbf{q} = \mathbf{q}t + (\theta(0) + \omega(0) - \mathbf{q}) + \mathbf{q} = \mathbf{q}t + \mathbf{K}$. By direct computation, we have

$$\begin{aligned}\dot{\theta} = \mathbf{q} &\leftrightarrow \mathbf{q} - \frac{1}{f} \sin(\mathbf{q}t + \vartheta - \mathbf{w}t + \varphi) = \mathbf{q} \\ \dot{r} = 0 &\leftrightarrow -f \frac{1}{f} + \cos(\mathbf{q}t + \vartheta - \mathbf{w}t + \varphi) = 0 \\ \dot{\phi} = \mathbf{q} &\leftrightarrow \mathbf{q} \\ \dot{\omega} = 0 &\leftrightarrow = -\frac{1}{f} \sin(\mathbf{q}t + \varphi - \mathbf{w}t + \vartheta) = 0\end{aligned}$$

which concludes the verification.

The adapted solution is asymptotically stable and it is proven by ЛЯПУНОВ’s second method. Define the nonempty compact set

$$\mathbb{M} = \{(\theta, r, \phi, \omega) \in \mathbb{S}^1 \times \mathbb{R} \times \mathbb{S}^1 \times \mathbb{R} \mid \theta - \phi = 0, r - \frac{1}{f} = 0, \omega - \mathbf{q} = 0\} ,$$

let \mathbf{F} be the vector field of Equation (4.4) (i.e. $\mathbf{F}(\theta, r, \phi, \omega) = (\mathbf{q} - r \sin(\theta - \phi), -fr + \cos(\theta - \phi), \omega, -r \sin(\phi - \theta))$) and define a ЛЯПУНОВ function as

$$\mathbf{L}(\theta, r, \phi, \omega) = \frac{f}{2} \left\langle \begin{pmatrix} r \\ \frac{1}{f} \end{pmatrix} \mid \begin{pmatrix} 1 & -\cos(\theta - \phi) \\ -\cos(\theta - \phi) & 1 \end{pmatrix} \begin{pmatrix} r \\ \frac{1}{f} \end{pmatrix} \right\rangle + \frac{1}{2} (\omega - \mathbf{q})^2 .$$

defined on $\mathbb{S}^1 \times \mathbb{R}_{\geq 0} \times \mathbb{S}^1 \times \mathbb{R}$. Function \mathbf{L} is positive because $\begin{pmatrix} 1 & -\cos(\theta - \phi) \\ -\cos(\theta - \phi) & 1 \end{pmatrix}$ is positive semi-definite since its eigenvalues are $1 \pm \cos(\theta - \phi)$. Let us determine the real numbers x, y , and the θ and ϕ belonging to \mathbb{S}^1 that satisfy

$$\left\langle \begin{pmatrix} x \\ y \end{pmatrix} \mid \begin{pmatrix} 1 & -\cos(\theta - \phi) \\ -\cos(\theta - \phi) & 1 \end{pmatrix} \begin{pmatrix} x \\ y \end{pmatrix} \right\rangle = 0 . \quad (4.14)$$

We consider the three following cases

$\theta, \phi \in [0, 2\pi[$ and $\theta - \phi \neq \pi$ nor $\theta - \phi \neq 0$ Here, the matrix in Equation (4.14) has two eigenvalues that are strictly positive and so this implies that $x = y = 0$.

$\theta - \phi = \pi$ In this case, Equation (4.14) becomes $(x + y)^2 = 0$ and so $x = -y$.

$\theta - \phi = 0$ In this case, Equation (4.14) becomes $(x - y)^2 = 0$ and so $x = y$.

Since \mathbb{L} is defined for $r \geq 0$ and from the analysis of Equation (4.14), we have $\mathbb{M} = \{(\theta, r, \phi, \omega) \in \mathbb{S}^1 \times \mathbb{R}_{\geq 0} \times \mathbb{S}^1 \times \mathbb{R} \mid \mathbb{L}(\theta, r, \phi, \omega) = 0\}$. By direct computation, we have

$$\begin{aligned} \langle \nabla \mathbb{L}(\theta, r, \phi, \omega) \mid \mathbb{F}(\theta, r, \phi, \omega) \rangle &= r \sin(\theta - \phi)(\mathbf{q} - r \sin(\theta - \phi)) + (\mathbf{f}r - \cos(\theta - \phi))(-\mathbf{f}r + \cos(\theta - \phi)) \\ &\quad + r \sin(\phi - \theta)\omega + (\omega - \mathbf{q})(-r \sin(\phi - \theta)) \\ &= -r^2 \sin(\theta - \phi)^2 - (\mathbf{f}r - \cos(\theta - \phi))^2 \leq 0. \end{aligned}$$

Therefore $\langle \nabla \mathbb{L}(\theta, r, \phi, \omega) \mid \mathbb{F}(\theta, r, \phi, \omega) \rangle = 0$ if and only if

$$r \sin(\theta - \phi) = 0 \quad \text{and} \quad \mathbf{f}r - \cos(\theta - \phi) = 0.$$

If $r = 0$, then $\cos(\theta - \phi) = 0$, which implies that $\theta \equiv \phi \pmod{\frac{\pi}{2}}$ or $\theta \equiv \phi \pmod{\frac{3\pi}{2}}$. If $r > 0$, the $\sin(\theta - \phi) = 0$, which implies that $\theta \equiv \phi \pmod{2\pi}$ or $\theta \equiv \phi \pmod{\pi}$ and so either $r = \frac{1}{\mathbf{f}}$ or $r = \frac{-1}{\mathbf{f}}$ (excluded since $r \geq 0$). Therefore, there are only three points outside \mathbb{M} for which $\langle \nabla \mathbb{L}(\theta, r, \phi, \omega) \mid \mathbb{F}(\theta, r, \phi, \omega) \rangle = 0$, and so \mathbb{M} is asymptotically stable (refer to Appendix A in [42] for definition).

4.B Verifying Properties For the Local Coupling Function in Example 2

Let us verify the properties. We here drop the index k .

[I] The matrix in function \mathbb{S} is positive semi-definite since its eigenvalues are $1 \pm \cos(\theta - \phi)$.

[II] \Rightarrow For $\theta = \phi$ and $r = \frac{\mathbf{b}}{\mathbf{f}}$, we have $\cos(\theta - \phi) = 1$ and so

$$\mathbb{Q}(\theta, r, \phi) = \frac{1}{2\mathbf{b}}(\mathbf{f} \frac{\mathbf{b}^2}{\mathbf{f}^2} + \frac{\mathbf{b}^2}{\mathbf{f}} - 2 \frac{\mathbf{b}}{\mathbf{f}} \mathbf{b}) = \frac{1}{2\mathbf{b}}(\frac{\mathbf{b}^2}{\mathbf{f}} + \frac{\mathbf{b}^2}{\mathbf{f}} - 2 \frac{\mathbf{b}^2}{\mathbf{f}}) = 0.$$

\Leftarrow By the analysis done with Equation (4.14) we have $\theta = \phi$ and $r = \frac{\mathbf{b}}{\mathbf{f}}$.

[III] & [IV] By direct computation, we have

$$\begin{aligned} \frac{\partial \mathbb{Q}}{\partial \theta}(\theta, r, \phi) &= r \sin(\theta - \phi) = -\frac{\partial \mathbb{Q}}{\partial \phi}(\theta, r, \phi) \quad \text{and} \\ -\mathbf{b} \frac{\partial \mathbb{Q}}{\partial r}(\theta, r, \phi) &= -\mathbf{b}(\frac{\mathbf{f}}{\mathbf{b}}r - \cos(\theta - \phi)) = -\mathbf{f}r + \mathbf{b} \cos(\theta - \phi). \end{aligned}$$

[V] For $\bar{\lambda} := (\bar{\theta}, \frac{\mathbf{b}}{\mathbf{f}}, \bar{\phi})$ with $\bar{\theta} = \bar{\phi}$, we have

$$\mathfrak{D}^2 \mathbb{Q}(\bar{\lambda}) = \begin{pmatrix} \frac{\mathbf{b}}{\mathbf{f}} & 0 & -\frac{\mathbf{b}}{\mathbf{f}} \\ 0 & \frac{\mathbf{f}}{\mathbf{b}} & 0 \\ -\frac{\mathbf{b}}{\mathbf{f}} & 0 & \frac{\mathbf{b}}{\mathbf{f}} \end{pmatrix}$$

and so (with $\lambda = (\theta, r, \phi)$), $0 = \langle \lambda \mid \mathfrak{D}^2 \mathbb{Q}(\bar{\lambda}) \lambda \rangle = \frac{\mathbf{b}}{\mathbf{f}}(\theta - \phi)^2 + \frac{\mathbf{f}}{\mathbf{b}}r^2$ is equivalent to $\theta = \phi$ and $r = 0$.

4.C Verifying Hypothesis For Coupling Potential \mathbb{E} as Defined in Section 4.2.1

We first present some properties of functions W and V individually. We do this in the case where the networks for W and V are time-dependent and connected for all times.

4.C.1 Properties For function W

By definition, W can be written as

$$\begin{aligned} W(t, \theta, r) &= \frac{1}{2} \sum_{\substack{k=1 \\ j>k}}^n a_{k,j}(t) ((r_k \mathbf{p}_k)^2 + (r_j \mathbf{p}_j)^2 - 2r_k r_j \mathbf{p}_k \mathbf{p}_j \cos(\theta_k - \theta_j)) \\ &= \frac{1}{2} \sum_{\substack{k=1 \\ j>k}}^n a_{k,j}(t) \left\langle \begin{pmatrix} r_k \mathbf{p}_k \\ r_j \mathbf{p}_j \end{pmatrix} \middle| \begin{pmatrix} 1 & -\cos(\theta_k - \theta_j) \\ -\cos(\theta_k - \theta_j) & 1 \end{pmatrix} \begin{pmatrix} r_k \mathbf{p}_k \\ r_j \mathbf{p}_j \end{pmatrix} \right\rangle \end{aligned}$$

with here $\mathbf{p}_k = \frac{\mathbf{f}_k}{\mathbf{b}_k}$.

[I] When the network is connected, we have: for $r_k > 0$,

$$\theta_k = \phi_j \quad \text{and} \quad \frac{r_k}{r_j} = \frac{\mathbf{p}_j}{\mathbf{p}_k} \quad \forall k, j \quad \iff \quad W(t, \theta, r, \phi) = 0 \quad \forall t.$$

[\Rightarrow] For $\theta_k = \theta_k$ and $r_k = r_j \frac{\mathbf{p}_j}{\mathbf{p}_k}$ for all k, j , we have $\cos(\theta_k - \theta_j) = 1$ and $\mathbf{B}_{k,j}(\theta_k - \theta_j) = 0$ so

$$W(t, \theta, r, \phi) = \frac{1}{2} \sum_{\substack{k=1 \\ j>k}}^n a_{k,j}(t) \underbrace{((r_j \frac{\mathbf{p}_j}{\mathbf{p}_k} \mathbf{p}_k)^2 + (r_j \mathbf{p}_j)^2 - 2r_j \frac{\mathbf{p}_j}{\mathbf{p}_k} \mathbf{p}_k r_j \mathbf{p}_j)}_{=0} = 0.$$

[\Leftarrow] Since the eigenvalues of $\begin{pmatrix} 1 & -\cos(\theta_k - \theta_j) \\ -\cos(\theta_k - \theta_j) & 1 \end{pmatrix}$ are $1 \pm \cos(\theta_k - \theta_j) \geq 0$ and since $\mathbf{B}_{k,j}(\phi_k - \phi_j) \geq 0$ then

$$W(t, \theta, r, \phi) = 0 \quad \forall t \quad \iff \quad \begin{aligned} &a_{k,j}(t) ((r_k \mathbf{p}_k)^2 + (r_j \mathbf{p}_j)^2 - 2r_k r_j \mathbf{p}_k \mathbf{p}_j \cos(\theta_k - \theta_j)) = 0 \\ &\text{and} \quad a_{k,j}^\phi(t) \mathbf{B}_{k,j}(\phi_k - \phi_j) = 0 \end{aligned} \quad \forall k, j, t.$$

Since the network is connected at all times, then for any t and any vertex k there exists a path in the network to any other vertex j . By definition of a path between two vertices, there exists a non-zero sequence $\{a_{k,j_1}(t), a_{j_1,j_2}(t), \dots, a_{j_{m-1},j_m}(t), a_{j_m,j}(t)\}$. Therefore, for any pair of indices (s, m) corresponding to a term in the non-zero sequence, $a_{s,m}(t) > 0$ and so

$$\begin{aligned} &a_{s,m}(t) ((r_s \mathbf{p}_s)^2 + (r_m \mathbf{p}_m)^2 - 2r_s r_m \mathbf{p}_s \mathbf{p}_m \cos(\theta_s - \theta_m)) \\ \iff &\left\langle \begin{pmatrix} r_s \mathbf{p}_s \\ r_m \mathbf{p}_m \end{pmatrix} \middle| \begin{pmatrix} 1 & -\cos(\theta_s - \theta_m) \\ -\cos(\theta_s - \theta_m) & 1 \end{pmatrix} \begin{pmatrix} r_s \mathbf{p}_s \\ r_m \mathbf{p}_m \end{pmatrix} \right\rangle = 0. \end{aligned}$$

By the analysis done with Equation (4.14), $\theta_s \equiv \theta_m \pmod{2\pi}$ and $r_s \mathbf{p}_s = r_m \mathbf{p}_m$ for any pair of indices (s, m) corresponding to a term in the non-zero sequence of a path between vertex k and vertex j at time t . Hence $\theta_k \equiv \theta_j \pmod{2\pi}$ and $\frac{r_k}{r_j} = \frac{\mathbf{p}_j}{\mathbf{p}_k}$ for all k, j since k, j and t where chosen arbitrarily.

[II] By direct computation, we have $\sum_{k=1}^n \frac{\partial W}{\partial \theta_k}(t, \theta, r) = -\sum_{k=1}^n \left(\sum_{j=1}^n l_{k,j} r_k r_j \mathbf{p}_k \mathbf{p}_j \sin(\theta_k - \theta_j) \right) = 0$ since for any term $l_{s,m} r_s r_m \mathbf{p}_s \mathbf{p}_m \sin(\theta_s - \theta_m)$ there is also the term $l_{m,s} r_m r_s \mathbf{p}_m \mathbf{p}_s \sin(\theta_m - \theta_s) = -l_{s,m} r_s r_m \mathbf{p}_s \mathbf{p}_m \sin(\theta_s - \theta_m)$.

[III] When the network is connected, we have: for $\bar{\lambda} = (\bar{\theta}_1, \dots, \bar{\theta}_n, \frac{1}{\mathbf{p}_1}, \dots, \frac{1}{\mathbf{p}_n})$ with $\bar{\theta}_k = \bar{\theta}_j \forall k, j$,

$$\theta_k = \theta_j \quad \text{and} \quad r_k = \frac{y}{\mathbf{p}_k} \quad \forall k, j \quad \text{and} \quad y \in \mathbb{R} \quad \iff \quad \langle \lambda | \mathfrak{D}^2 W(t, \bar{\lambda}) \lambda \rangle = 0 \quad \forall t.$$

Computing the first derivative with respect to (ϕ, r) gives

$$\mathfrak{D}_{(\bar{\lambda})}^1 \mathbb{W}(t, \theta, r) = \left(- \sum_{j=1}^n l_{1,j}(t) r_1 r_j \mathbf{p}_1 \mathbf{p}_j \sin(\theta_1 - \theta_j), \dots, - \sum_{j=1}^n l_{n,j}(t) r_n r_j \mathbf{p}_n \mathbf{p}_j \sin(\theta_n - \theta_j), \right. \\ \left. \sum_{j=1}^n l_{1,j}(t) r_j \mathbf{p}_1 \mathbf{p}_j \cos(\theta_1 - \theta_j), \dots, \sum_{j=1}^n l_{n,j}(t) r_j \mathbf{p}_n \mathbf{p}_j \cos(\theta_n - \theta_j) \right).$$

Computing the second derivative with respect to (θ, r) gives

$$\left(\begin{array}{cccc} - \sum_{j \neq 1}^n l_{1,j}(t) r_1 r_j \mathbf{p}_1 \mathbf{p}_j c_{1,j} & l_{1,2}(t) r_1 r_2 \mathbf{p}_1 \mathbf{p}_2 c_{1,2} & \dots & l_{1,n}(t) r_1 r_n \mathbf{p}_1 \mathbf{p}_n c_{1,n} \\ l_{2,1}(t) r_2 r_1 \mathbf{p}_2 \mathbf{p}_1 c_{2,1} & - \sum_{j \neq 2}^n l_{2,j}(t) r_2 r_j \mathbf{p}_2 \mathbf{p}_j c_{2,j} & \dots & l_{2,n}(t) r_2 r_n \mathbf{p}_2 \mathbf{p}_n c_{2,n} \\ \vdots & \vdots & \ddots & \vdots \\ l_{n,1}(t) r_n r_1 \mathbf{p}_n \mathbf{p}_1 c_{n,1} & l_{n,2}(t) r_n r_2 \mathbf{p}_n \mathbf{p}_2 c_{n,2} & \dots & - \sum_{j \neq n}^n l_{n,j}(t) r_n r_j \mathbf{p}_n \mathbf{p}_j c_{n,j} \\ - \sum_{j \neq 1}^n l_{1,j}(t) r_j \mathbf{p}_1 \mathbf{p}_j s_{1,j} & l_{1,2}(t) r_2 \mathbf{p}_1 \mathbf{p}_2 s_{1,2} & \dots & l_{1,n}(t) r_n \mathbf{p}_1 \mathbf{p}_n s_{1,n} \\ l_{2,1}(t) r_1 \mathbf{p}_2 \mathbf{p}_1 s_{2,1} & - \sum_{j \neq 2}^n l_{2,j}(t) r_j \mathbf{p}_2 \mathbf{p}_j s_{2,j} & \dots & l_{2,n}(t) r_n \mathbf{p}_2 \mathbf{p}_n s_{2,n} \\ \vdots & \vdots & \ddots & \vdots \\ l_{n,1}(t) r_1 \mathbf{p}_n \mathbf{p}_1 s_{n,1} & l_{n,2}(t) r_2 \mathbf{p}_n \mathbf{p}_2 s_{n,2} & \dots & - \sum_{j \neq n}^n l_{n,j}(t) r_j \mathbf{p}_n \mathbf{p}_j s_{n,j} \\ - \sum_{j \neq 1}^n l_{1,j}(t) r_j \mathbf{p}_1 \mathbf{p}_j s_{1,j} & - l_{1,2}(t) r_1 \mathbf{p}_1 \mathbf{p}_2 s_{1,2} & \dots & - l_{1,n}(t) r_1 \mathbf{p}_1 \mathbf{p}_n s_{1,n} \\ - l_{2,1}(t) r_2 \mathbf{p}_2 \mathbf{p}_1 s_{2,1} & - \sum_{j \neq 2}^n l_{2,j}(t) r_j \mathbf{p}_2 \mathbf{p}_j s_{2,j} & \dots & - l_{2,n}(t) r_2 \mathbf{p}_2 \mathbf{p}_n s_{2,n} \\ \vdots & \vdots & \ddots & \vdots \\ - l_{n,1}(t) r_n \mathbf{p}_n \mathbf{p}_1 s_{n,1} & - l_{n,2}(t) r_n \mathbf{p}_n \mathbf{p}_2 s_{n,2} & \dots & - \sum_{j \neq n}^n l_{n,j}(t) r_j \mathbf{p}_n \mathbf{p}_j s_{n,j} \\ l_{1,1}(t) \mathbf{p}_1 \mathbf{p}_1 & l_{1,2}(t) \mathbf{p}_1 \mathbf{p}_2 c_{1,2} & \dots & l_{1,n}(t) \mathbf{p}_1 \mathbf{p}_n c_{1,n} \\ l_{2,1}(t) \mathbf{p}_2 \mathbf{p}_1 c_{2,1} & l_{2,2}(t) \mathbf{p}_2 \mathbf{p}_2 & \dots & l_{2,n}(t) \mathbf{p}_2 \mathbf{p}_n c_{2,n} \\ \vdots & \vdots & \ddots & \vdots \\ l_{n,1}(t) \mathbf{p}_n \mathbf{p}_1 c_{n,1} & l_{n,2}(t) \mathbf{p}_n \mathbf{p}_2 c_{n,2} & \dots & l_{n,n}(t) \mathbf{p}_n \mathbf{p}_n \end{array} \right)$$

with $c_{k,j} = \cos(\theta_k - \theta_j)$ and $s_{k,j} = \sin(\theta_k - \theta_j)$. Evaluating this Jacobian on $(t, \bar{\lambda})$, we have

$$\mathfrak{D}^2 \mathbb{W}(t, \bar{\lambda}) = \begin{pmatrix} L(t) & \mathbf{0} \\ \mathbf{0} & [\mathbf{p}] L(t) [\mathbf{p}] \end{pmatrix},$$

where $[\mathbf{p}]$ is a diagonal matrix with $(\mathbf{p}_1, \dots, \mathbf{p}_n)$ on its diagonal. Hence

$$\left\langle \begin{pmatrix} \theta \\ r \end{pmatrix} \middle| \begin{pmatrix} L(t) & \mathbf{0} \\ \mathbf{0} & [\mathbf{p}] L(t) [\mathbf{p}] \end{pmatrix} \begin{pmatrix} \phi \\ r \end{pmatrix} \right\rangle = 0 \quad \forall t \iff \langle \phi | L(t) \phi \rangle = 0 \quad \text{and} \\ \langle r | [\mathbf{p}] L(t) [\mathbf{p}] r \rangle = 0 \quad \forall t.$$

The matrix $L(t)$ is positive semi-definite and symmetric for all t , and since the network is connected then $\{x \in \mathbb{R}^n \mid \langle x | L(t) x \rangle = 0 \forall t\} = \{x \in \mathbb{R}^n \mid L(t) x = \mathbf{0} \forall t\} = \{x \in \mathbb{R}^n \mid x_k = x_j \forall k, j\}$. Therefore

$$\langle \theta | L(t) \theta \rangle = 0 \quad \text{and} \quad \langle r | [\mathbf{p}] L(t) [\mathbf{p}] r \rangle = 0 \quad \forall t \iff \theta_k = \theta_j, r_k = \frac{y}{\mathbf{p}_k} \quad \forall k, j.$$

4.C.2 Properties For function \mathbf{V}

[1] When the network is connected, we have: for $r_k > 0$,

$$\phi_k = \phi_j \quad \forall k, j \quad \iff \quad \mathbf{V}(t, \phi) = 0 \quad \forall t .$$

[\Rightarrow] For $\phi_k = \phi_j$, we have, by definition, $\mathbf{B}_{k,j}(\theta_k - \theta_j) = 0$ for all k, j , and so $\mathbf{V}(t, \phi) = 0$ for all t .

[\Leftarrow] Since the network is connected at all times, then, for any t and any vertex k , there exists a path in the network to any other vertex j . By definition of a path between two vertices, there exists a non-zero sequence $\{a_{k,j_1}(t), a_{j_1,j_2}(t), \dots, a_{j_{m-1},j_m}(t), a_{j_m,j}(t)\}$. Therefore, for any pair of indices (s, m) corresponding to a term in the non-zero sequence, $a_{s,m}(t) > 0$ and so

$$a_{s,m}(t)\mathbf{B}_{s,m}(\phi_s - \phi_m) = 0 \quad \iff \quad \mathbf{B}_{s,m}(\phi_s - \phi_m) = 0 .$$

Therefore, $\phi_s = \phi_m$ for any pair of indices (s, m) corresponding to a term in the non-zero sequence of a path between vertex k and vertex j at time t . Hence $\phi_k = \phi_j$ for all k, j since k, j and t where chosen arbitrarily.

[II] By direct computation, we have $\sum_{k=1}^n \frac{\partial \mathbf{V}}{\partial \phi_k}(t, \phi) = \sum_{k=1}^n \left(\sum_{\substack{j=1 \\ j \neq k}}^n a_{k,j} \mathbf{B}'_{k,j}(\phi_k - \phi_j) \right) = 0$ since for any term $a_{k,j} \mathbf{B}_{k,j}'(\phi_k - \phi_j)$, there is also the term $a_{j,k} \mathbf{B}_{j,k}'(\phi_j - \phi_k) = -a_{k,j} \mathbf{B}'_{k,j}(\phi_k - \phi_j)$ since $\mathbf{B}'_{k,j}$ is odd.

[III] When the network is connected, we have: for $\bar{\phi} = (\bar{\phi}_1, \dots, \bar{\phi}_n)$ with $\bar{\phi}_k = \bar{\phi}_j \quad \forall k, j$,

$$\phi_k = \phi_j \quad \iff \quad \langle \phi | \mathfrak{D}^2 \mathbf{V}(t, \bar{\phi}) \phi \rangle = 0 \quad \forall t .$$

The second derivative with respect to ϕ evaluated on $\bar{\phi}$ is

$$\mathfrak{D}^2 \mathbf{V}(t, \bar{\phi}) = L_{\mathbf{B}''}(t)$$

with $L_{\mathbf{B}''}(t)$ an $n \times n$ symmetric matrix with diagonal entries $\sum_{\substack{k=1 \\ j \neq k}}^n a_{k,j}^\phi \mathbf{B}''_{k,j}(0)$ and off-diagonal entries $-a_{k,j}^\phi \mathbf{B}''_{k,j}(0)$, $0 < \mathbf{B}''_{k,j}(0)$ for all k, j . Hence

$$\langle \theta | L_{\mathbf{B}''}(t) \theta \rangle = 0 \quad \forall t \quad \iff \quad \phi_k = \phi_j \quad \forall k, j .$$

4.C.3 Verification of Hypothesis

Let us verify the properties for the coupling potential \mathbf{E} . We here suppose that the network for \mathbf{V} is connected.

Hypothesis I: This directly follows from the properties of \mathbf{Q}_k and Property I from Section 4.C.2.

Hypothesis II: This directly follows from Property III from Section 4.C.2 and Property III from Section 4.C.2.

Hypothesis III: Define $\mathbf{F}(\theta, r, \phi) := \sum_{k=1}^n \mathbf{Q}_k(\theta_k, r_k, \phi_k)$. Since $\mathfrak{D}^2 \mathbf{E}(\bar{\lambda})$ is positive semi-definite (because $\bar{\lambda}$ is a minimum of \mathbf{E}) and symmetric, then $\ker(\mathfrak{D}^2 \mathbf{E}(\bar{\lambda})) = \{\lambda \in (\mathbb{S}^1)^n \times \mathbb{R}_{\geq 0}^n \times (\mathbb{S}^1)^n \mid \langle \lambda | \mathfrak{D}^2 \mathbf{E}(\bar{\lambda}) \lambda \rangle = 0\}$ and so $\langle \lambda | \mathfrak{D}^2 \mathbf{E}(\bar{\lambda}) \lambda \rangle = \langle \lambda | \mathfrak{D}^2 \mathbf{F}(\bar{\lambda}) \lambda \rangle + \langle \lambda | \mathfrak{D}^2 \mathbf{W}(\bar{\lambda}) \lambda \rangle + \langle \lambda | \mathfrak{D}^2 \mathbf{V}(\bar{\lambda}) \lambda \rangle$ with all three terms being positive semi-definite (since $\bar{\lambda}$ is a minimum for all three). Thus

$$\lambda \in \ker(\mathfrak{D}^2 \mathbf{E}(\bar{\lambda})) \quad \iff \quad \langle \lambda | \mathfrak{D}^2 \mathbf{F}(\bar{\lambda}) \lambda \rangle = 0 \quad \text{and} \quad \langle \lambda | \mathfrak{D}^2 \mathbf{W}(\bar{\lambda}) \lambda \rangle = 0 \quad \text{and} \quad \langle \lambda | \mathfrak{D}^2 \mathbf{V}(\bar{\lambda}) \lambda \rangle = 0 .$$

By direct computation, we have $\langle \lambda | \mathfrak{D}^2 \mathbf{F}(\bar{\lambda}) \lambda \rangle = \sum_{k=1}^n \langle \lambda_k | \mathfrak{D}^2 \mathbf{Q}_k(\bar{\lambda}_k) \lambda_k \rangle$ with $\bar{\lambda}_k = (\bar{\theta}_k, \frac{\mathbf{b}_k}{\mathbf{r}_k}, \bar{\phi}_k)$, $\bar{\theta}_k = \bar{\phi}_k$ and $\lambda_k = (\theta_k, r_k, \phi_k)$. Since $\mathfrak{D}^2 \mathbf{Q}_k(\bar{\lambda}_k)$ is positive semi-definite for all k (because $\bar{\lambda}_k$ is a minimum of \mathbf{Q}_k for all k), then $\langle \lambda | \mathfrak{D}^2 \mathbf{F}(\bar{\lambda}) \lambda \rangle = 0 \iff \langle \lambda_k | \mathfrak{D}^2 \mathbf{Q}_k(\bar{\lambda}_k) \lambda_k \rangle = 0$ for all k , and this by

hypothesis is equivalent to $\theta_k = \phi_k$ and $r_k = 0 \quad \forall k$.

By hypothesis,

$$\langle \phi | \mathfrak{D}^2 \mathbf{V}(\bar{\lambda}) \phi \rangle = 0 \iff \phi_k = \phi_j \quad \forall k, j$$

with no constraints on θ nor on r . Hence

$$\langle \lambda | \mathfrak{D}^2 \mathbf{F}(\bar{\lambda}) \lambda \rangle = 0 \quad \text{and} \quad \langle \lambda | \mathfrak{D}^2 \mathbf{V}(\bar{\lambda}) \lambda \rangle = 0 \iff \theta_k = \phi_j \quad \text{and} \quad r_k = 0 \quad \forall k, j,$$

where these points satisfy $\langle \lambda | \mathfrak{D}^2 \mathbf{E}(\bar{\lambda}) \lambda \rangle = 0$.

4.D Determining the $r_{c,k}$

The $r_{c,k}$ are one of the two positive roots of the polynomial

$$\left(\frac{f_k}{b_k}\right)^2 x^4 - x^2 + \left(\frac{q_k - q_c}{a_k}\right)^2 = 0 \quad k = 1, \dots, n.$$

From Equations (4.12), we have $\dot{r}_k(t) = 0 = -f_k r_{c,k} + b_k \cos(\vartheta_k - \varphi_k)$, so $\frac{f_k r_{c,k}}{b_k} = \cos(\vartheta_k - \varphi_k)$. From Equations (4.12), we also have $\dot{\theta}_k(t) = q_c = q_k - a_k \sin(\vartheta_k - \varphi_k)$, so $\frac{q_k - q_c}{a_k r_{c,k}} = \sin(\vartheta_k - \varphi_k)$.

Therefore, $1 = \cos(\vartheta_k - \varphi_k)^2 + \sin(\vartheta_k - \varphi_k)^2 = \left(\frac{f_k r_{c,k}}{b_k}\right)^2 + \left(\frac{q_k - q_c}{a_k r_{c,k}}\right)^2$, which is equivalent to

$$x^2 e - x + g = 0$$

with $x := r_{c,k}^2$, $e := \left(\frac{f_k}{b_k}\right)^2$ and $g := \left(\frac{q_k - q_c}{a_k}\right)^2$. The roots are $x_{\pm} = \frac{1 \pm \sqrt{1 - 4eg}}{2e}$. Both roots x_{\pm} are positive because $0 \leq 1 - 4eg$ and $1 \geq \sqrt{1 - 4eg}$. This is true since $\frac{1}{r_{c,k}} = \frac{f_k}{b_k \cos(\vartheta_k - \varphi_k)}$, so $\left(\frac{q_k - q_c}{a_k}\right) \frac{f_k}{b_k \cos(\vartheta_k - \varphi_k)} = \sin(\vartheta_k - \varphi_k)$, and so $2\left(\frac{q_k - q_c}{a_k b_k}\right) f_k = \sin(2(\vartheta_k - \varphi_k))$. Hence, for consistency, $|2\frac{q_k - q_c}{a_k b_k} f_k| \leq 1$ and therefore $4\left(\frac{f_k}{b_k}\right)^2 \left(\frac{q_k - q_c}{a_k}\right)^2 \leq 1$, and so $0 \leq 1 - 4\left(\frac{f_k}{b_k}\right)^2 \left(\frac{q_k - q_c}{a_k}\right)^2 = 1 - 4eg$. Since $0 \leq e, g$, then $1 \geq 1 - 4eg$, and therefore $1 \geq \sqrt{1 - 4eg}$. Thus, the polynomial $y^4 e - y^2 + g = 0$, has four roots, two positive and two negative.

Stochastic Parametric Resonance in Time-Dependent Networks of Adaptive Frequency Oscillators

Поймите, [...], это механизм наших человеческих душ - это механизм качелей, где от наисильнейшего взлета в сторону Благородства Духа и бозникает наисильнейший отлет в сторону Ярости Скота.

Михаил АГЕЕВ

Abstract

We consider a network of interacting phase oscillators endowed with adaptive mechanisms, leading the collective motion to a consensual dynamical state. Specifically, for a given network topology (i.e. an adjacency matrix) governing the mutual interactions, the adaptive mechanisms enable all oscillators to ultimately adopt a consensual frequency. Once reached, the consensual frequency subsists even if interactions between the oscillators are switched off. For the class of models we consider, the consensual frequency is independent of the network topology. Even though this independence might suggest that extension to time-dependent networks is straightforward, this is not true here. For time-dependent networks and spectra of the underlying Laplacian matrices, one may observe the emergence of more complex dynamics. Due to their high degree of complexity, these dynamics generally offer little hope for analytical tractability. In this paper, we focus on connected time-dependent networks with circulant adjacency matrices. The simple spectral structures and commutativity properties enjoyed by circulant matrices enable an analytical instability analysis of the consensus state. We are able to reduce the instability analysis to a dissipative harmonic oscillator with parametric pumping.

5.1 Introduction

The concepts of synchronization, adaptation and learning capabilities cross disciplinary boundaries and there is ongoing demand for tractable dynamical models unveiling their numerous facets. One fruitful approach is given by studying the emerging collective behavior observed in networks of mutually interacting dynamical systems, for example oscillators. These complex systems can be approximately discussed via analytical tools, an approach which offers insights into the underlying mechanisms enabling self-organization and adaptation.

Adaptation can be seen as the modification of local agents' characteristics through the interactions with their environment, in order to make them less dependent on their surroundings. To illustrate this idea, consider the basic example of coupled phase oscillators which is given by

$$\dot{\phi}_k = \underbrace{w_k}_{\text{local dynamics}} - \underbrace{c_k \frac{\partial \mathcal{V}}{\partial \phi_k}(\phi)}_{\text{coupling dynamics}} \quad k = 1, \dots, n, \quad (5.1)$$

where w_k are local individual frequencies, coupling strengths $c_k > 0$ and where \mathcal{V} is a coupling potential. If the complex system synchronizes, then, by definition,

$$\lim_{t \rightarrow \infty} \phi_k(t) = w_c t + \varphi_k \quad \forall k$$

with phase shift φ_k . For coupling potentials satisfying the orthogonal relation $\langle \mathbf{1} | \nabla \mathcal{V}(\phi) \rangle = 0$, the synchronized frequency is given by

$$w_c = \frac{\sum_{j=1}^n \frac{w_j}{c_j}}{\sum_{k=1}^n \frac{1}{c_k}}$$

and the phase shift φ_k can be explicitly determined in certain cases (see Appendix 5.A for details). Although w_c does not depend on the topology, the synchronized state is attained and maintained by the interactions and thus dependent on its environment. Furthermore, if a phase oscillator is isolated, it will converge back to oscillate at its eigenfrequency w_k . Hence, and following what has been done in [44, 42], local systems may adapt their frequencies by letting w_k acquire the status of variables of the global dynamical system and have their own dynamics (i.e. $w_k \rightsquigarrow \omega_k(t)$). These dynamics are to be interpreted as adaptive mechanisms and lead to an extension of Equations (5.1) in the form

$$\begin{aligned} \dot{\phi}_k &= \underbrace{\omega_k}_{\text{local dynamics}} - \underbrace{c_k \frac{\partial \mathcal{V}}{\partial \phi_k}(\phi)}_{\text{coupling dynamics}} \\ \dot{\omega}_k &= \underbrace{-s_k \frac{\partial \mathcal{V}}{\partial \phi_k}(\phi)}_{\text{adaptive mechanisms}} \end{aligned} \quad k = 1, \dots, n \quad (5.2)$$

with susceptibility constants $s_k > 0$ (technically playing the role of coupling strengths). For coupling potentials satisfying $\langle \mathbf{1} | \nabla \mathcal{V}(\phi) \rangle \leq 0$, the complex system will be driven towards a consensual oscillatory state, that is

$$\lim_{t \rightarrow \infty} |\phi_j(t) - \phi_k(t)| = 0 \quad \text{and} \quad \lim_{t \rightarrow \infty} \omega_k(t) = \omega_c \quad \forall k, j$$

for a certain value ω_c (see Appendix 5.B). Once this state is reached, the coupling dynamics are zero (by definition), and thus the local systems no longer depend on the environment in order to keep oscillating with ω_c . This is due to the permanent change in their local frequencies. Further imposing the orthogonality hypothesis $\langle \mathbf{1} | \nabla \mathcal{V}(\phi) \rangle = 0$, ω_c is determined as (see Appendix 5.B)

$$\omega_c = \frac{\sum_{j=1}^n \frac{\omega_j(0)}{s_j}}{\sum_{k=1}^n \frac{1}{s_k}} .$$

Again, the value ω_c is a weighted average (weighted with respect to s_k instead of c_k for the synchronized orbit of Equations (5.1)), and independent of the network topology. However, the convergence rate is strongly affected by the network connectivity [44]. Therefore, and as mentioned in [42], adaptation can alternatively be interpreted as an optimal control problem where the aim is to find potential functions \mathcal{V} from an admissible set \mathbb{V} (see Appendix 5.B) in order to minimize the payoff functional

$$E(\mathcal{V}) = \int_0^{\infty} |\langle \mathbf{1} | \nabla \mathcal{V}(\phi(t)) \rangle| dt .$$

Frequency adaptation, whether in a coupled oscillator framework [20, 56, 4, 45] or in an individual forced oscillator context [41], is a well studied and ongoing field of research. Recently, frequency adaptation has been studied in a noisy environment [57], with time delayed interactions [47], and in deterministic time-dependent networks [42].

Except for a rather small portion ([9, 11, 55, 38, 59]), the vast literature devoted to complex systems focuses on time-independent connections between the dynamical subsystems forming the network. Often, however, connections ruling the interactions are themselves subject to varying with time. Connections can be oscillating in strength, prone to deterministic or random intermittence. Though the effects of such time-dependent connectivity states between the members of an interacting assembly are obviously difficult to determine in general, they may potentially generate new types of dynamics.

In this contribution, we discuss the dynamical behavior of coupled phase oscillators when the network for the adaptive mechanisms randomly switches from one topology to an other. The presence of time-dependent network connections introduces extra time-dependent control parameters into the dynamics. This ultimately enhances the complexity of the dynamical analysis. Among the simplest possible examples of time-dependent parameter systems, there is the parametric harmonic oscillator subject to parametric pumping instability. One might remember having sat on a set of swings as a child, where oscillating energy can be scavenged from suitably tuned time oscillations of an eigenfrequency.

As far as networks are concerned, we may legitimately raise the following question: “What happens when switches between different network configurations are implemented over time and in particular, does the common consensual state remains stable?”. We shall show that the answer is closely related to the parametric pumping paradigm. Indeed, two time scales compete: i) the time scale characterizing the oscillations between the different network connection states and ii) the characteristic rate convergence towards the consensus. If both time scales are appropriately tuned - and the present paper will analytically state the conditions - a parametric instability is created and the consensual state becomes unstable (i.e. the local oscillators actually scavenge energy from the time-dependent connection). Finally, we show how the phenomenon of parametric resonance depends on coupling strengths, susceptibility constants, topologies of the underlying networks, and the randomness of the switching.

This paper is organized as follows: We present the network’s dynamical system in Section 5.2, which we then discuss analytically in Section 5.3. We report a selection of numerical experiments which corroborate our analytical findings in Section 5.4. We finally conclude and present perspective works in Section 5.5.

5.2 Network of Phase Oscillators with Time-dependent Adaptive Mechanisms

The dynamical system of interest is

$$\begin{aligned} \dot{\phi}_k &= \underbrace{\omega_k}_{\text{local dynamics}} - \underbrace{c \sum_{j=1}^n a_{k,j}^{\phi} \sin(\phi_k - \phi_j)}_{\text{coupling dynamics}} & k = 1, \dots, n. \\ \dot{\omega}_k &= -s \underbrace{\sum_{j=1}^n a_{k,j}^{\omega}(t) \sin(\phi_k - \phi_j)}_{\text{adaptive mechanisms}} \end{aligned} \quad (5.3)$$

Local Dynamics Local systems are phase oscillators with frequencies ω_k . Here ω_k are variables of the global system with their dynamics governed by the adaptive mechanisms that we discuss below.

Coupling Dynamics Interactions among the local systems are characterized by the gradient of the coupling potential

$$V(\phi) = \frac{1}{2} \sum_{k=1}^n \sum_{j=1}^n a_{k,j}^\phi (1 - \cos(\phi_k - \phi_j)) \geq 0$$

with $0 \leq a_{k,j}^\phi = a_{j,k}^\phi$ being the entries of the adjacency matrix of a connected and undirected network. The gradient of this potential produces KURAMOTO-type interactions. The coupling strength $0 < c$ is vertex independent.

Adaptive Mechanisms KURAMOTO-type interactions modify the local frequencies ω_k . In the general case, these interactions occur via a different network than for the phase interactions. This network is time-dependent, connected, and undirected at all times. The entries $0 \leq a_{k,j}^\omega(t) = a_{j,k}^\omega(t) < +\infty$ of its adjacency matrix are positive and bounded for all time. The vertex-independent susceptibility constant $0 < s$ is technically the same as c but has another interpretation here. A “small” s describes a community of oscillators unwilling to change their frequencies. Conversely, a “large” s indicates that oscillators are prone to modify their individual behaviors according to their neighbors.

Edge Dynamics As mentioned above, we consider two networks: a time-independent one for the interactions of the state variables ϕ_k , and another, time-dependent one, governing the adaptive mechanisms. Let L^ϕ and $L^\omega(t)$ be, respectively, the associated Laplacian¹ matrices. We here focus only on networks that possess the two following commutation rules

auto-commutation rule $L^\omega(s)L^\omega(t) = L^\omega(t)L^\omega(s)$ for all t, s ,

hetero-commutation rule $L^\phi L^\omega(t) = L^\omega(t)L^\phi$ for all t .

Such commutation rules are fulfilled in particular by the class of circulant matrices defined as (c.f. [17] for details)

$$\text{circ}(a_1, \dots, a_n) := \begin{pmatrix} a_1 & a_2 & \cdots & a_n \\ a_n & a_1 & \cdots & a_{n-1} \\ \vdots & & \ddots & \vdots \\ a_2 & a_3 & \cdots & a_1 \end{pmatrix}.$$

In what follows, the adaptive mechanisms’ network will switch from one topology to another at given times. Let us define these switching times and topologies for System (5.3).

Switching Times

The time line $\mathbb{R}_{\geq 0}$ is partitioned into disjoint intervals $\mathbb{I}_j^{\mathbb{B}_j}$ (i.e. $\mathbb{R}_{\geq 0} = \bigcup_{j=0}^{\infty} \mathbb{I}_j^{\mathbb{B}_j}$), where $\{\mathbb{B}_j\}_{j=0}^{\infty}$ is a sequence of independent BERNOULLI random variables with states \mathbf{u} and \mathbf{d} , that is

$$\mathbb{B}_j = \begin{cases} \mathbf{u} & \text{with probability } p \\ \mathbf{d} & \text{with probability } 1 - p \end{cases} \quad j = 0, 1, 2, \dots$$

The intervals $\mathbb{I}_j^{\mathbf{u}}$ and $\mathbb{I}_j^{\mathbf{d}}$ are defined as

$$\mathbb{I}_j^{\mathbf{u}} := [t_j, t_j + t_{\mathbf{u}}] \cup [t_j + t_{\mathbf{u}}, t_{j+1}] \quad \mathbb{I}_j^{\mathbf{d}} := [t_j, t_j + t_{\mathbf{d}}] \cup [t_j + t_{\mathbf{d}}, t_{j+1}]$$

with $t_j := j(t_{\mathbf{u}} + t_{\mathbf{d}})$, where $t_{\mathbf{u}}, t_{\mathbf{d}} > 0$ are two positive real numbers. This partitioning is sketched in Figure 5.1.

¹ The Laplacian matrix associated to a given network is defined as $L(t) := A(t) - D(t)$, where $A(t)$ is the adjacency matrix $D(t)$ is the diagonal matrix with $d_{k,k}(t) := \sum_{j=1}^n a_{k,j}(t)$.

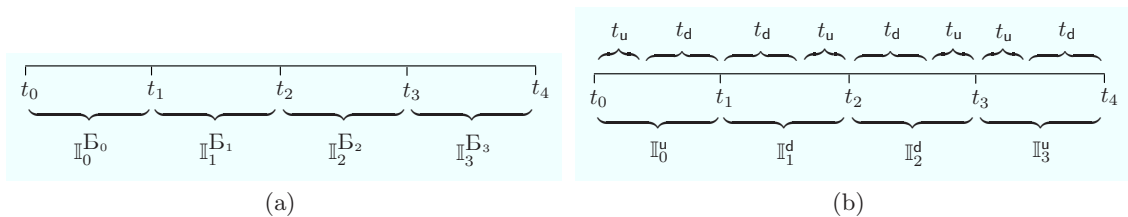


Fig. 5.1: $\mathbb{R}_{\geq 0}$ is partitioned into disjoint intervals $\mathbb{I}_j^{\mathbb{B}_j}$, here $j = 0, 1, 2, 3$ (Figure 5.1(a)). Depending on the random realization (here, for example, $\mathbb{B}_0 = \mathbf{u}$, $\mathbb{B}_1 = \mathbf{d}$, $\mathbb{B}_2 = \mathbf{d}$ and $\mathbb{B}_3 = \mathbf{u}$), the intervals $\mathbb{I}_j^{\mathbb{B}_j}$ are partitioned with $t_{\mathbf{u}}$ and $t_{\mathbf{d}}$ respectively (Figure 5.1(b)).

Switching Topologies

Consider two different networks for the adaptive mechanisms and denote the adjacency matrices by $A_{\mathbf{u}}^{\omega}$ and $A_{\mathbf{d}}^{\omega}$ respectively. On interval $\mathbb{I}_j^{\mathbf{u}}$, System (5.3) evolves with $A_{\mathbf{u}}^{\omega}$ between t_j and $t_j + t_{\mathbf{u}}$ with initial condition taking the values of the state of the system at t_j . Between $t_j + t_{\mathbf{u}}$ and t_{j+1} , System (5.3) evolves with $A_{\mathbf{d}}^{\omega}$, with initial condition being the values of the system's state at $t_j + t_{\mathbf{u}}$. Similarly, on interval $\mathbb{I}_j^{\mathbf{d}}$, System (5.3) evolves with $A_{\mathbf{d}}^{\omega}$ between t_j and $t_j + t_{\mathbf{d}}$, with initial condition taking the values of the state of the system at t_j . Between $t_j + t_{\mathbf{d}}$ and t_{j+1} , System (5.3) evolves with $L_{\mathbf{u}}^{\omega}$ with initial condition being the values of the system's state $t_j + t_{\mathbf{d}}$.

5.3 Network's Dynamical System with Random Switching Topologies

For sufficiently continuously differentiable functions $\omega_{k,j}^{\omega}(t)$, and under appropriate conditions (c.f. [42] for details), the adaptive mechanisms tune the ω_k so that the global dynamical system given by Equations (5.3) reaches a consensual oscillatory state:

$$\lim_{t \rightarrow \infty} \|(\phi_k(t), \omega_k(t)) - (\omega_c t, \omega_c)\| = 0 \quad \forall k \quad (5.4)$$

with constant ω_c determined as

$$\omega_c = \frac{1}{n} \sum_{j=1}^n \omega_j^{(0)}.$$

Once reached, the consensual state remains unchanged even if interactions are switched off. That is, if the coupling dynamics and adaptive mechanism are both zero after convergence, all local systems keep oscillating in phase with identical ω_c .

We here want to study the resulting dynamics when $A^{\omega}(t)$ randomly alternates between two different adjacency matrices $A_{\mathbf{u}}^{\omega}$ and $A_{\mathbf{d}}^{\omega}$ as defined at the end of Section 5.2. For both $A_{\mathbf{u}}^{\omega}$ and $A_{\mathbf{d}}^{\omega}$ taken individually, the system is encompassed in Equations (5.2), therefore Limit (5.4) holds. The core of this paper can be summarized with the following question:

“Can these time-dependent alternating topologies affect the convergence in Limit (5.4)?”

We answer this question within the framework of a linear stability analysis around a consensual state. We therefore compute the first order approximation of the vector field given by Equations (5.3), and we diagonalize the resulting Jacobian.

First Order Approximation

Rearranging the variables (i.e. the first n are the ϕ_k and the n others are ω_k), the first order approximation of Equations (5.3) is

$$\begin{pmatrix} \dot{\epsilon}_\phi \\ \dot{\epsilon}_\omega \end{pmatrix} = \begin{pmatrix} -cL^\phi & Id \\ -sL^\omega(t) & \mathbf{0} \end{pmatrix} \begin{pmatrix} \epsilon_\phi \\ \epsilon_\omega \end{pmatrix} \quad (5.5)$$

with the $n \times n$ identity matrix Id , Laplacian matrices L^ϕ and $L^\omega(t)$ associated with their respective network and $\epsilon_\phi := (\epsilon_{\phi_1}, \dots, \epsilon_{\phi_n})$ and $\epsilon_\omega := (\epsilon_{\omega_1}, \dots, \epsilon_{\omega_n})$.

Diagonalization

Both L^ϕ and $L^\omega(t)$ are symmetric for all t , and thanks to their commutation rules there exists an orthogonal matrix O with real time-independent entries that simultaneously diagonalizes L^ϕ and $L^\omega(t)$ for all t (see Appendix 5.C). That is, there exists an orthogonal matrix O such that $O^\top L^\phi O = D(\zeta^\phi)$ and $O^\top L^\omega(t) O = D(\zeta^\omega(t))$ for all t , with diagonal matrices $D(\zeta^\phi)$ and $D(\zeta^\omega(t))$ having, respectively, on their diagonals, the spectrum ζ_k^ϕ and $\zeta_k^\omega(t)$ ($k = 1, \dots, n$) of L^ϕ and $L^\omega(t)$. As O is time-independent, for a change of variable $(\varepsilon_\phi, \varepsilon_\omega) = (O^\top \epsilon_\phi, O^\top \epsilon_\omega)$ we have $(\dot{\epsilon}_\phi, \dot{\epsilon}_\omega) = (O^\top \dot{\epsilon}_\phi, O^\top \dot{\epsilon}_\omega)$. Therefore, changing the basis of System (5.5) with a 2×2 bloc matrix (each bloc of size $n \times n$) with O^\top on its diagonal, we obtain n 2-dimensional systems of the form

$$\begin{pmatrix} \dot{\varepsilon}_{\phi_k} \\ \dot{\varepsilon}_{\omega_k} \end{pmatrix} = \begin{pmatrix} -c\zeta_k^\phi & 1 \\ -s\zeta_k^\omega(t) & 0 \end{pmatrix} \begin{pmatrix} \varepsilon_{\phi_k} \\ \varepsilon_{\omega_k} \end{pmatrix} \quad (5.6)$$

or equivalently

$$\ddot{\varepsilon}_{\phi_k} + c\zeta_k^\phi \dot{\varepsilon}_{\phi_k} + s\zeta_k^\omega(t) \varepsilon_{\phi_k} = 0. \quad (5.7)$$

In order to study the linear stability of System (5.3), we focus on the general form of Equation (5.7) which is

$$\ddot{x} + f\dot{x} + F(t)x = 0. \quad (5.8)$$

Despite the apparent simplicity of Equation (5.8), stability conditions and related dynamics are an ongoing research topic (c.f. [19, 6, 24]). In this contribution, we focus on parametric resonance instabilities that may occur in Equation (5.8) (c.f. [6, 24]).

Let $F(t)$ from Equation (5.8) switch between two different values, that is, on interval \mathbb{I}_j^u

$$F(t) = \mathbf{u} \quad \text{for } t \in [t_j, t_j + t_u] \quad \text{and} \quad F(t) = \mathbf{d} \quad \text{for } t \in [t_j + t_u, t_{j+1}]$$

and on \mathbb{I}_j^d

$$F(t) = \mathbf{d} \quad \text{for } t \in [t_j, t_j + t_d] \quad \text{and} \quad F(t) = \mathbf{u} \quad \text{for } t \in [t_j + t_d, t_{j+1}].$$

Let us now study the asymptotic behavior of Equation (5.8) for the particular choice $\mathbf{u} := 1 + \mathbf{h}$, $\mathbf{d} := 1 - \mathbf{h}$ with $0 < \mathbf{h} \ll 1$, $\bar{u} := 4\mathbf{u} - f^2$, $\bar{d} := 4\mathbf{d} - f^2$, and finally $t_u = \frac{\pi}{\sqrt{\bar{u}}}$ and $t_d = \frac{\pi}{\sqrt{\bar{d}}}$. For $F(t)$, taking a constant value \mathbf{v} , Equation (5.8) is

$$\begin{aligned} \dot{x} &= y \\ \dot{y} &= -\mathbf{v}x - fy \end{aligned}$$

and the solution is

$$\begin{pmatrix} x(t) \\ y(t) \end{pmatrix} = \frac{\exp(-\frac{ft}{2})}{\sqrt{\bar{v}}} \begin{pmatrix} f \sin(\frac{t}{2}\sqrt{\bar{v}}) + \sqrt{\bar{v}} \cos(\frac{t}{2}\sqrt{\bar{v}}) & 2 \sin(\frac{t}{2}\sqrt{\bar{v}}) \\ -2\mathbf{v} \sin(\frac{t}{2}\sqrt{\bar{v}}) & -f \sin(\frac{t}{2}\sqrt{\bar{v}}) + \sqrt{\bar{v}} \cos(\frac{t}{2}\sqrt{\bar{v}}) \end{pmatrix} \begin{pmatrix} x_0 \\ y_0 \end{pmatrix} \quad (5.9)$$

with $\bar{v} := 4\mathbf{v} - f^2$ and initial condition (x_0, y_0) . Denote by (x_j, y_j) the state of the system at time t_j . On interval \mathbb{I}_j^u , the system first evolves with $\mathbf{v} = \mathbf{u}$ (i.e. $\bar{v} := \bar{u}$) on $[t_j, t_j + t_u]$. Hence, the state of the system at time $t_j + t_u$ is

$$\frac{\exp(-\frac{\pi f}{2\sqrt{\bar{u}}})}{\sqrt{\bar{u}}} \begin{pmatrix} f & 2 \\ -2u & -f \end{pmatrix} \begin{pmatrix} x_j \\ y_j \end{pmatrix}. \quad (5.10)$$

On the interval $[t_j + \frac{\pi}{\sqrt{\bar{u}}}, t_{j+1}]$, the system evolves according to Equation (5.9), with $v = d$ (i.e. $\bar{v} := \bar{d}$) and with initial condition given by Equation (5.10). Hence, at time t_{j+1} , the system is at state

$$\begin{aligned} & \frac{\exp(-\frac{\pi f}{2\sqrt{\bar{d}}})}{\sqrt{\bar{d}}} \frac{\exp(-\frac{\pi f}{2\sqrt{\bar{u}}})}{\sqrt{\bar{u}}} \begin{pmatrix} f & 2 \\ -2d & -f \end{pmatrix} \begin{pmatrix} f & 2 \\ -2u & -f \end{pmatrix} \begin{pmatrix} x_j \\ y_j \end{pmatrix} \\ &= \frac{\exp(-\frac{\pi f}{2}(\frac{1}{\sqrt{\bar{d}}} + \frac{1}{\sqrt{\bar{u}}}))}{\sqrt{\bar{d}}\sqrt{\bar{u}}} \begin{pmatrix} -\bar{u} & 0 \\ 2f(u-d) & -\bar{d} \end{pmatrix} \begin{pmatrix} x_j \\ y_j \end{pmatrix}. \end{aligned} \quad (5.11)$$

Similarly, on interval \mathbb{I}_j^d , the system first evolves with $v = d$ (i.e. $\bar{v} := \bar{d}$) on $[t_j, t_j + t_d]$, and then with $v = u$ (i.e. $\bar{v} := \bar{u}$) on $[t_j + \frac{\pi}{\sqrt{\bar{u}}}, t_{j+1}]$. Hence, at time t_{j+1} , the system is at state

$$\frac{\exp(-\frac{\pi f}{2}(\frac{1}{\sqrt{\bar{u}}} + \frac{1}{\sqrt{\bar{d}}}))}{\sqrt{\bar{u}}\sqrt{\bar{d}}} \begin{pmatrix} -\bar{d} & 0 \\ 2f(d-u) & -\bar{u} \end{pmatrix} \begin{pmatrix} x_j \\ y_j \end{pmatrix}. \quad (5.12)$$

Observe that in both cases the resulting matrices are lower triangular matrices.

5.3.1 Stability Analysis

We separately consider different regimes. The first two are deterministic and without friction [$p = 1$ and $p = 0, f = 0$]. The next two are deterministic with small friction [$p = 1$ and $p = 0, 0 < f \ll 1$]. Finally, we look at case with random switching and with small friction [$0 < p < 1, 0 < f \ll 1$].

$[p = 1, f = 0]$ In this case, we have to study the eigenvalues of the matrix in Equation (5.11), which are

$$\xi_1 = -\frac{\sqrt{\bar{u}}}{\sqrt{\bar{d}}} = -\frac{\sqrt{1+h}}{\sqrt{1-h}} \quad \xi_2 = -\frac{\sqrt{\bar{d}}}{\sqrt{\bar{u}}} = -\frac{\sqrt{1-h}}{\sqrt{1+h}}$$

with eigenspaces $\mathbb{E}_{\xi_1} = \langle (1, 0)^\top \rangle$ and $\mathbb{E}_{\xi_2} = \langle (0, 1)^\top \rangle$. Hence, $|\xi_1| > 1$ and $|\xi_2| < 1$, and so for any initial condition belonging to \mathbb{E}_{ξ_2} the system is stable, and for any initial condition not belonging to \mathbb{E}_{ξ_2} the system is unstable.

$[p = 0, f = 0]$ In this case, we have to study the eigenvalues of the matrix in Equation (5.12). This case is symmetric to the case above, where here $\xi_1 = -\frac{\sqrt{1-h}}{\sqrt{1+h}}$ and $\xi_2 = -\frac{\sqrt{1+h}}{\sqrt{1-h}}$ and so $|\xi_1| < 1$ and $|\xi_2| > 1$. Therefore, for any initial condition belonging to \mathbb{E}_{ξ_1} the system is stable, and for any initial condition not belonging to \mathbb{E}_{ξ_1} the system is unstable.

$[p = 1, 0 < f \ll 1]$ The eigenvalues of the matrix in Equation (5.11) are

$$\xi_1 = -\exp\left(-\frac{\pi f}{2}\left(\frac{1}{\sqrt{\bar{u}}} + \frac{1}{\sqrt{\bar{d}}}\right)\right)\left(\frac{\sqrt{\bar{u}}}{\sqrt{\bar{d}}}\right) \quad \text{and} \quad \xi_2 = -\exp\left(-\frac{\pi f}{2}\left(\frac{1}{\sqrt{\bar{u}}} + \frac{1}{\sqrt{\bar{d}}}\right)\right)\left(\frac{\sqrt{\bar{d}}}{\sqrt{\bar{u}}}\right).$$

It is immediate that $|\xi_2| < 1$, hence for any initial condition belonging to the eigenspace $\mathbb{E}_{\xi_2} = \langle (0, 1)^\top \rangle$, the system is stable. For the system to be stable for all initial conditions, f and h must satisfy

$$|\xi_1| < 1 \iff \exp\left(-\frac{\pi f}{2}\left(\frac{1}{\sqrt{\bar{u}}} + \frac{1}{\sqrt{\bar{d}}}\right)\right)\left(\frac{\sqrt{\bar{u}}}{\sqrt{\bar{d}}}\right) < 1 \iff \frac{1}{f} \frac{\ln\left(\frac{\sqrt{4(1+h)-f^2}}{\sqrt{4(1-h)-f^2}}\right)}{\left(\frac{1}{\sqrt{4(1+h)-f^2}} + \frac{1}{\sqrt{4(1-h)-f^2}}\right)} < \frac{\pi}{2}.$$

Since $\frac{1}{\sqrt{(4-f^2)(1 \pm \frac{4h}{4-f^2})}} = \frac{1}{\sqrt{(4-f^2)}} \frac{1}{\sqrt{1 \pm \frac{4h}{4-f^2}}} = \frac{1}{\sqrt{(4-f^2)}} \left(1 \pm \frac{1}{2} \frac{4h}{4-f^2} + \mathcal{O}\left(\left(\frac{4h}{4-f^2}\right)^2\right)\right)$, then

$$\frac{1}{\sqrt{4(1+h)-f^2}} + \frac{1}{\sqrt{4(1-h)-f^2}} \simeq \frac{2}{\sqrt{4-f^2}}.$$

Since $\ln\left(\frac{1+x}{1-x}\right) = 2 \sum_{j=1}^{\infty} \frac{x^{2j-1}}{2j-1}$ for $x^2 < 1$, then $\frac{1}{2} \ln\left(\frac{1+\frac{4h}{4-f^2}}{1-\frac{4h}{4-f^2}}\right) = \frac{4h}{4-f^2} + \mathcal{O}\left(\left(\frac{4h}{4-f^2}\right)^2\right)$, then

$$\frac{\pi}{2} > \frac{1}{f} \frac{\ln\left(\frac{\sqrt{4(1+h)-f^2}}{\sqrt{4(1-h)-f^2}}\right)}{\left(\frac{1}{\sqrt{4(1+h)-f^2}} + \frac{1}{\sqrt{4(1-h)-f^2}}\right)} \simeq \frac{1}{f} \frac{2h}{\sqrt{4-f^2}}.$$

Neglecting f^2 gives a further approximation, which is

$$\frac{\pi}{2} > \frac{h}{f}.$$

[$p = 0, 0 < f \ll 1$] This case is symmetric to the case directly above, where here any initial condition belonging to the eigenspace $\mathbb{E}_{\xi_1} = \langle (1, \frac{2f(u-d)}{\sqrt{d}-\sqrt{u}})^\top \rangle$ (with eigenvalue $\xi_1 = -\exp\left(-\frac{\pi f}{2}\left(\frac{1}{\sqrt{u}} + \frac{1}{\sqrt{d}}\right)\right)\left(\frac{\sqrt{d}}{\sqrt{u}}\right)$) will converge to zero (asymptotic stability). The conditions on f and h for asymptotic stability for any general initial condition are similar to the above case.

[$0 < p < 1, 0 < f \ll 1$] We first analyze how the perturbations evolve on a finite time interval. At time t_m , the state of the system is given by the matrix

$$\frac{\exp\left(-\frac{m\pi f}{2}\left(\frac{1}{\sqrt{u}} + \frac{1}{\sqrt{d}}\right)\right)}{(\sqrt{u}\sqrt{d})^m} \begin{pmatrix} (-\bar{u})^q (-\bar{d})^{m-q} & 0 \\ z & (-\bar{d})^q (-\bar{u})^{m-q} \end{pmatrix} \quad (5.13)$$

with $z \in \mathbb{R}$, and where q is the number of times the dynamical system evolved with $\mathbf{v} := \mathbf{u}$. Hence $m - q$ is the number of times the dynamical system evolved with $\mathbf{v} := \mathbf{d}$. In other words, q is the realization of the the random variable $\mathfrak{R}_m := \sum_{j=1}^m \mathbf{l}_u(\mathbb{B}_j)$.² The eigenvalues of Matrix (5.13) are

$$\begin{aligned} \xi_{1,m} &= (-1)^m \exp\left(-\frac{m\pi f}{2}\left(\frac{1}{\sqrt{u}} + \frac{1}{\sqrt{d}}\right)\right) \left(\frac{\sqrt{u}}{\sqrt{d}}\right)^{2q-m} \\ \xi_{2,m} &= (-1)^m \exp\left(-\frac{m\pi f}{2}\left(\frac{1}{\sqrt{u}} + \frac{1}{\sqrt{d}}\right)\right) \left(\frac{\sqrt{u}}{\sqrt{d}}\right)^{-(2q-m)}. \end{aligned}$$

The initial perturbation (x_0, y_0) decreases in magnitude at time t_m if

$$|\xi_{1,m}| < 1 \quad \text{and} \quad |\xi_{2,m}| < 1.$$

This implies

$$\begin{aligned} |\xi_{1,m}| < 1 &\iff \exp\left(-\frac{m\pi f}{2}\left(\frac{1}{\sqrt{u}} + \frac{1}{\sqrt{d}}\right)\right) \left(\frac{\sqrt{u}}{\sqrt{d}}\right)^{2q-m} < 1 \\ &\iff (2q - m) \ln\left(\frac{\sqrt{u}}{\sqrt{d}}\right) < m \frac{\pi f}{2} \left(\frac{1}{\sqrt{u}} + \frac{1}{\sqrt{d}}\right) \\ &\iff \frac{q}{m} < \frac{\frac{\pi f}{4} \left(\frac{1}{\sqrt{u}} + \frac{1}{\sqrt{d}}\right)}{\ln\left(\frac{\sqrt{u}}{\sqrt{d}}\right)} + \frac{1}{2} =: \bar{o} \end{aligned}$$

and

² We define the function $\mathbf{l}_{\mathbf{v}(x)}$ as

$$\mathbf{l}_{\mathbf{v}(x)} = \begin{cases} 1 & \text{if } x = \mathbf{v} \\ 0 & \text{if } x \neq \mathbf{v} \end{cases}.$$

$$\begin{aligned}
|\xi_{2,m}| < 1 &\iff \exp\left(-\frac{m\pi f}{2}\left(\frac{1}{\sqrt{u}} + \frac{1}{\sqrt{d}}\right)\right)\left(\frac{\sqrt{u}}{\sqrt{d}}\right)^{-(2q-m)} < 1 \\
&\iff \frac{q}{m} > \frac{1}{2} - \frac{\frac{\pi f}{4}\left(\frac{1}{\sqrt{u}} + \frac{1}{\sqrt{d}}\right)}{\ln\left(\frac{\sqrt{u}}{\sqrt{d}}\right)} =: \underline{p}.
\end{aligned}$$

For large m , the random variable $\Pi_m := \frac{1}{m}\mathfrak{H}_m \in [0, 1]$ (for which $\frac{q}{m}$ is a realization) approximately behaves as $\mathcal{N}(p, \frac{p(1-p)}{m})$ (normally distributed with mean p and variance $\frac{p(1-p)}{m}$). Therefore, as m approaches infinity, then $\Pi_\infty \sim \mathcal{D}(p)$, a DIRAC distribution with parameter p in the sense that $\mathbb{P}(\Pi_\infty = p) = 1$. Hence, the necessary and sufficient condition for the system to be asymptotically stable is

$$\lim_{m \rightarrow \infty} |\xi_{1,m}| < 1 \quad \text{and} \quad \lim_{m \rightarrow \infty} |\xi_{2,m}| < 1 \quad \iff \quad \underline{p} < p < \bar{p}.$$

A sufficient condition for the system to be unstable for all initial conditions is that at time t_m ,

$$|\xi_{1,m}| > 1 \quad \text{and} \quad |\xi_{2,m}| > 1$$

and so proceeding with similar calculations, we have

$$\lim_{m \rightarrow \infty} |\xi_{1,m}| > 1 \quad \text{and} \quad \lim_{m \rightarrow \infty} |\xi_{2,m}| > 1 \quad \iff \quad p \in [0, 1] \setminus [\underline{p}, \bar{p}].$$

Figure (5.2) shows the resulting stability diagram. The black domain represents the stable region, and its boundaries are given by \bar{p} and \underline{p} for a given $h = 0.05$. The unstable regions are given in gray. Therefore, for this specific second order linear differential equation with time-dependent coefficients, we analytically calculated the bifurcation values between three parameters: the friction of the system (i.e. f), the change in shape of the trajectories (i.e. h), and the randomness from the environment affecting the system (i.e. p). This analysis enables us to discuss the stability of the first order approximation of a network of coupled phase oscillators with frequency adaptation. Numerical simulations show that this linear stability analysis is indeed precise, even when the nonlinear contributions are considered.

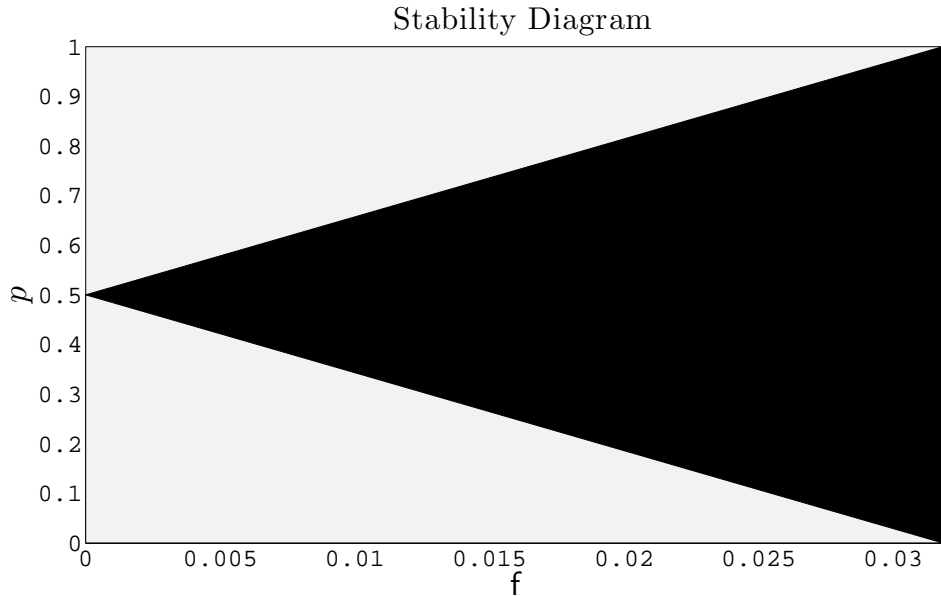


Fig. 5.2: Stability diagram for parameters f and p for the System (5.8) with discrete stochastic switching $F(t)$. The stable region is given in black, the unstable regions in gray.

Conditions for Parametric Resonance in Switching Networks

To summarize, linear analysis shows that parametric resonance occurs in Equations (5.3) when

the associated Laplacian matrices of the switching networks A_u and A_d have at least one eigenvector (i.e. there exists a k in Equation (5.7)) for which the corresponding eigenvalues are such that $0 < |\zeta_{u,k}^\omega - \zeta_{d,k}^\omega| \ll 1$,

the susceptibility constant is defined as $s := \frac{2}{\zeta_{u,k}^\omega + \zeta_{d,k}^\omega}$,

the coupling strength c is sufficiently small,

the switching times are defined as $t_u := \frac{\pi}{\sqrt{4s\zeta_{u,k}^\omega - (c\zeta_k^\phi)^2}}$ and $t_d := \frac{\pi}{\sqrt{4s\zeta_{d,k}^\omega - (c\zeta_k^\phi)^2}}$.

With these hypotheses, $s\zeta_k^\omega(t)$ is switching between $1 + h$ and $1 - h$ (as $F(t)$ in Equation (5.8)) and $c\zeta_k^\phi$ plays the role of f . Hence, one can find values of c and p in order to be in the gray zone of Figure 5.2, for which parametric resonance destabilizes the dynamical system.

Geometric Interpretation of Parametric Resonance Phenomena

Equation (5.8) describes a damped oscillator with alternating frequencies. For each realization of the frequency taken individually (i.e. not switching between two values), the fixed point zero is an attractor (c.f. Figure 5.3). However, due to parametric resonance, instabilities occur for an appropriate switching of the frequencies. A similar phenomenon occurs for the alternating networks we are here discussing. Following [37], this can be heuristically understood as explained in Figure 5.4.

Note that in Figure 5.4(a), at end point (i.e. black point), the trajectory will either switch to a gray spiral with probability p or continue on the same black spiral with probability $1 - p$. If this is the case (i.e. case with probability $1 - p$), after one revolution, the system will be at a state closer to the origin (i.e. converging towards it). Therefore, one immediately sees the interplay between the friction of the system and its stochasticity. For a fixed friction value (in the appropriate parameter range), the system will perform parametric resonance as long as p is close enough to one. If there is too much randomness, parametric pumping may not occur.

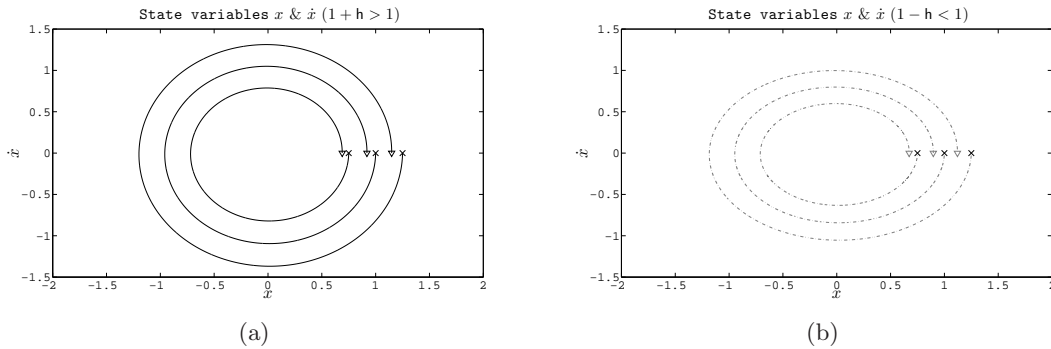


Fig. 5.3: Qualitative sketches of orbits of System 5.8 when $F(t) = 1 + h$ for all t (Figure 5.3(a)), and when $F(t) = 1 - h$ for all t (Figure 5.3(b)) with here, $0 < h \ll 1$. Therefore, one has, a priori, the illusion that the system is always asymptotically stable no matter when the switchings occur - and this because of the dissipative nature of the system. However, by adequately switching from one type of spiral to another at specific times, the perturbation may increase, and this even when the system is damped (Figure 5.4). Crosses represent the initial conditions (starting points) and arrows the direction of the dynamics.

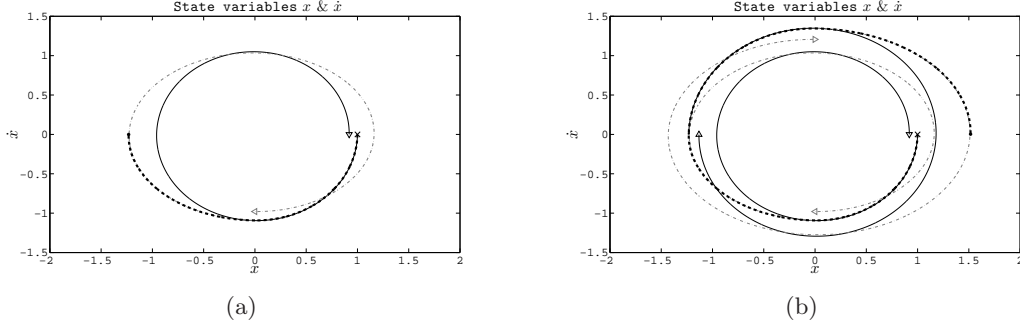


Fig. 5.4: Qualitative sketches of the parametric resonance phenomenon. The systems starts at $(1, 0)$, follows a black spiral orbit, automatically switches to a gray orbit once crossing the y -axis, and circulates along it until it reaches the x -axis (Figure 5.4(a)). With probability p , it switches to a black spiral orbit and evolves on it until, again, it automatically switches to a gray orbit once crossing the y -axis. It follows this gray spiral until it reaches the x -axis (once more) (Figure 5.4(a)). Hence, after one revolution, the system is further away from the origin compared with its initial state (i.e. an increase in amplitude). The cross represents the initial condition (starting point), the thick black line is the evolution of the system with the black point its end point, and the arrows show the direction of the dynamics.

5.4 Numerical Simulations

We numerically exhibit the parametric resonance phenomenon produced by the time-dependent adaptive mechanism. For this, four phase oscillators are coupled through a “All-to-All” network $A^\phi = \text{circ}(0, 1, 1, 1)$. The networks for the adaptive mechanisms are $A_u^\phi = \text{circ}(0, 1, 1, 1)$ and $A_d^\phi = \text{circ}(0, 1, \frac{17}{21}, 1)$ (i.e. a switching between an “All-to-All” network and a “Second Neighbor” topology with second neighbor weights being smaller than one). The respective spectra of the Laplacian matrices are $(\zeta_1^\phi, \dots, \zeta_4^\phi) = (\zeta_{u,1}^\omega, \dots, \zeta_{u,4}^\omega) = (0, 4, 4, 4)$ and $(\zeta_{d,1}^\omega, \dots, \zeta_{d,4}^\omega) = (0, \frac{76}{21}, 4, \frac{76}{21})$. The coupling strength is chosen as $c = 0.005$ and the susceptibility constant as $s = \frac{21}{80}$. The initial conditions $(\phi_k(0), \omega_k(0))$ are randomly uniformly drawn from $]-0.1, 0.1[\times]0.9, 1.1[$.

With this set up, we analytically obtain $s\zeta_{u,k}^\omega = \frac{21}{80} 4 = 1.05$, $s\zeta_{d,k}^\omega = \frac{21}{80} \frac{76}{21} = 0.95$ for $k = 2, 4$ and $c\zeta_k^\phi = 0.02$ for $k = 2, 3, 4$. Hence, depending on the value of p , the network will either converge towards a consensual oscillatory state (for $p < 0.81417\dots$) or be destabilized by a parametric resonance effect (for $p > 0.81417\dots$). This is clearly observed in Figure 5.5. Note that for both simulations, the parameter p is chosen close to the theoretical bifurcation value. The simulations, which take into consideration the none linearities of the system, corroborate the theory.

5.5 Conclusions and Perspectives

Sustaining permanent communications between subparts of complex systems may often be impossible for structural or technical reasons, and/or prohibitively costly. Also, the ubiquitous presence of environmental noise can contribute to communication failures and hence fluctuating interactions between the various subsystems. Despite their direct relevance for applications, switching networks remain scarcely investigated. One practical reason for this is that any time-dependence affecting the networks introduces additional complications into the analytical discussion of the dynamics. Difficulties remain even for linear stability analysis which are essentially based on sets of FLOQUET exponents. Highly stylized, our class of models nevertheless enables to analytically unveil how parametric resonance occurs for local systems wired via stochastically flashing networks. An appropriate tuning between the local relaxation time and the flashing rate of the networks produces parametric resonance. In other words, part of the energy which sustains the network switchings

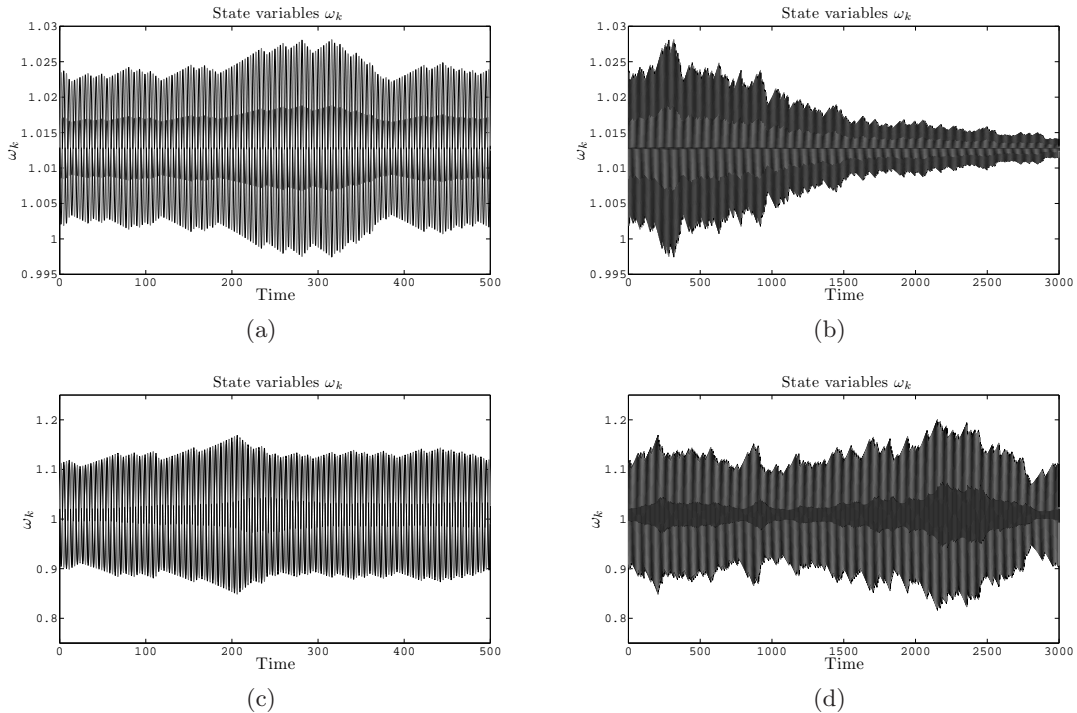


Fig. 5.5: Time evolution of the ω_k of four coupled phase oscillators, interacting through a “All-to-All” network. The networks for the adaptive mechanisms switch from an “All-to-All” to a “Second Neighbor” network. For the converging case (Figures 5.5(a) & 5.5(b)), the probability parameter is $p = 0.8$, and for the parametric resonance case (Figures 5.5(c) & 5.5(d)), $p = 0.82$. The coupling strength is $c = 0.005$ and the susceptibility constant is $s = \frac{21}{80}$. The numerical integration is for the interval $[0, 500]$ (Figures 5.5(a) & 5.5(c)) and for the interval $[0, 3000]$ (Figures 5.5(b) & 5.5(d)).

is scavenged by the local systems which are parametrically pumped. This is fully reminiscent of a child’s swing subject to alternating changes of its barycenter. Since our work is situated in the context of resonance phenomena, it opens a door for applications concerning signal detection and spectral analysis.

Among perspective works, one could consider other stochastic processes in the adjacency matrices. The challenge here is to find stochastic processes on the $a_{k,j}^\omega(t)$, such that the networks remain connected at all times and where we have information on the resulting stochastic eigenvalues $\zeta_k^\omega(t)$ of the associated Laplacian matrix. Also, further developments enabling to relax the two commutation rules of the respective Laplacian matrices would be welcome.

Appendix

5.A Synchronized Solution

Consider a network of coupled phase oscillators

$$\dot{\phi}_k = \omega_k - c_k \frac{\partial \mathcal{V}}{\partial \phi_k}(\phi) \quad k = 1, \dots, n \quad (5.14)$$

with a coupling potential satisfying $\langle \mathbf{1} | \nabla \mathcal{V}(\phi) \rangle = 0$ for all ϕ . If the complex system synchronizes, then, by definition, we have, for $k = 1, \dots, n$,

$$\lim_{t \rightarrow \infty} \phi_k(t) = \omega_c t + \varphi_k$$

with phase shift φ_k . Lets determine the value w_c . Observe that

$$\sum_{k=1}^n \frac{\dot{\phi}_k(t)}{c_k} = \sum_{k=1}^n \left(\frac{w_k}{c_k} - \frac{\partial V}{\partial \phi_k}(\phi) \right) = \sum_{k=1}^n \frac{w_k}{c_k}$$

and therefore, integrating with respect to time, gives

$$\sum_{k=1}^n \frac{\phi_k(t)}{c_k} = \left(\sum_{k=1}^n \frac{w_k}{c_k} \right) t + \mathbf{K} \quad \forall t$$

with a constant of integration that is determined as $\sum_{k=1}^n \frac{\phi_k(0)}{c_k} = \mathbf{K}$. Therefore, for a synchronized state $(w_c t + \varphi_1, \dots, w_c t + \varphi_n)$, we have

$$\sum_{k=1}^n \frac{w_c t + \varphi_k}{c_k} = \left(w_c \sum_{k=1}^n \frac{1}{c_k} \right) t + \sum_{k=1}^n \frac{\varphi_k}{c_k} = \left(\sum_{k=1}^n \frac{w_k}{c_k} \right) t + \mathbf{K} \quad \forall t$$

and hence

$$w_c = \frac{\sum_{k=1}^n \frac{w_k}{c_k}}{\sum_{k=1}^n \frac{1}{c_k}} \quad \text{and} \quad \sum_{k=1}^n \frac{\varphi_k}{c_k} = \sum_{k=1}^n \frac{\phi_k(0)}{c_k} .$$

We want to determine the φ_k . For this we consider the following coupling potential

$$V(\phi) := \frac{1}{2} \sum_{k=1}^n \sum_{j=1}^n a_{k,j} (1 - \cos(\phi_k - \phi_j)) \geq 0$$

with $0 \leq a_{k,j} = a_{j,k}$ the entries of the adjacency matrix of a connected and undirected network. The components of the gradient of this potential give the famous KURAMOTO-type interactions

$$c_k \frac{\partial V}{\partial \phi_k}(\phi) = c_k \sum_{j=1}^n a_{k,j} \sin(\phi_k - \phi_j) .$$

Evaluating Equations (5.14) with KURAMOTO-type interactions at a synchronized state gives

$$w_c = w_k + c_k \sum_{j=1}^n l_{k,j} \sin(\varphi_k - \varphi_j) \quad k = 1, \dots, n .$$

This leaves us with the $n + 1$ equations for the φ_k

$$\frac{w_k - w_c}{c_k} = \sum_{j=1}^n a_{k,j} \sin(\varphi_k - \varphi_j) \quad k = 1, \dots, n \quad \text{and} \quad \sum_{k=1}^n \frac{\varphi_k}{c_k} = \sum_{k=1}^n \frac{\phi_k(0)}{c_k} .$$

This nonlinear system is, in general, not explicitly solvable. However, in the particular case for a ‘‘All-to-One’’ network (i.e. all vertices are connected to the n^{th} vertex), one can explicitly calculate the φ_k . In this case we have

$$\frac{w_k - w_c}{c_k} = a_{k,n} \sin(\varphi_k - \varphi_n) \quad k = 1, \dots, n - 1$$

and therefore $\varphi_k = \varphi_n + \sin^{-1}\left(\frac{w_k - w_c}{c_k a_{k,n}}\right)$. We then have

$$\begin{aligned} \mathbf{K} &= \sum_{k=1}^n \frac{\varphi_k}{c_k} = \frac{\varphi_n}{c_n} + \sum_{k=1}^{n-1} \frac{\varphi_n + \sin^{-1}\left(\frac{w_k - w_c}{c_k a_{k,n}}\right)}{c_k} \\ &= \varphi_n \sum_{k=1}^n \frac{1}{c_k} + \sum_{k=1}^{n-1} \frac{\sin^{-1}\left(\frac{w_k - w_c}{c_k a_{k,n}}\right)}{c_k} \end{aligned}$$

and so

$$\varphi_n = \frac{\mathbf{K} - \sum_{k=1}^{n-1} \frac{\sin^{-1}\left(\frac{w_k - w_c}{c_k a_{k,n}}\right)}{c_k}}{\sum_{k=1}^n \frac{1}{c_k}}.$$

The case $n = 2$, we have (we here drop the index of the edge, that is $a_{1,2} = a_{2,1} = a > 0$)

$$\varphi_1 = \left(\frac{1}{c_1} + \frac{1}{c_2}\right)^{-1} \left(\mathbf{K} + \frac{\sin^{-1}\left(\frac{w_1 - w_c}{c_1 a}\right)}{c_2}\right) \quad \text{and} \quad \varphi_2 = \left(\frac{1}{c_1} + \frac{1}{c_2}\right)^{-1} \left(\mathbf{K} + \frac{\sin^{-1}\left(\frac{w_2 - w_c}{c_2 a}\right)}{c_1}\right)$$

since

$$\frac{w_1 - w_c}{c_1 a} = \frac{\frac{w_1}{c_1} + \frac{w_1}{c_2} - \frac{w_1}{c_1} - \frac{w_2}{c_2}}{\frac{1}{c_1} + \frac{1}{c_2}} = \frac{\left(\frac{c_2}{c_1}\right) \frac{w_1 - w_2}{c_1} - \frac{w_2}{c_2}}{\left(\frac{c_2}{c_1}\right) \frac{1}{c_1} + \frac{1}{c_2}} = \frac{\frac{w_1 + w_2}{c_1} - \frac{w_2}{c_1} - \frac{w_2}{c_2}}{\frac{1}{c_1} + \frac{1}{c_2}} = \frac{w_c - w_2}{c_2 a} = -\frac{w_2 - w_c}{c_2 a}.$$

5.B Proof of Convergence

Let V be a coupling potential (see Section 2.3 in [45] for precise definition) with basic hypothesis

$$V(\phi) = 0 \iff \phi_k = \phi_j \quad \forall k, j \quad (5.15a)$$

$$\forall \bar{\phi} \in \mathbb{M}, \quad \langle \phi | \mathfrak{D}^2 V(\bar{\phi}) \phi \rangle = 0 \iff \phi_k = \phi_j \quad \forall k, j, \quad (5.15b)$$

where $\mathfrak{D}^2 V(\bar{\phi})$ is the second total derivative (i.e. the Hessian) of V evaluated at $\bar{\phi}$, and \mathbb{M} is the consensual compact submanifold defined as

$$\mathbb{M} := \{\phi \in (\mathbb{S}^1)^n \mid \hat{L}\phi = \mathbf{0}\}$$

where \hat{L} is an $(n-1) \times n$ matrix with $\hat{l}_{k,k} = n-1$ for $k = 1, \dots, n-1$, and all other entries are -1 .

Define the set of potential as

$$\mathbb{V} := \{V : (\mathbb{S}^1)^n \rightarrow \mathbb{R}_{\geq 0} \mid 5.15a \text{ and } 5.15b \text{ are satisfied and } \langle \mathbf{1} | \nabla V(\phi) \rangle \leq 0 \quad \forall \phi\}.$$

Define the none empty and compact set $\mathbb{K} := \{(\phi, \omega) \in (\mathbb{S}^1)^n \times \mathbb{R}^n \mid \phi \in \mathbb{M} \text{ and } \omega = \omega_c \mathbf{1}\}$. We have to prove that there exists a neighborhood \mathbb{U} of \mathbb{K} such that for all orbits $(\phi(t), \omega(t))$ of Equations (5.2) with initial conditions in \mathbb{U} converge towards \mathbb{K} . The convergence towards \mathbb{K} follows from ЛЯПУНОВ's second method with ЛЯПУНОВ function

$$L(\phi, \omega) = V(\phi) + \frac{1}{2} \sum_{k=1}^n \frac{(\omega_c - \omega_k)^2}{s_k} \geq 0.$$

We then have that $\mathbb{K} = \{(\phi, \omega) \in (\mathbb{S}^1)^n \times \mathbb{R}^n \mid L(\phi, \omega) = 0\}$. The time derivation of $\frac{d[L(\phi(t), \omega(t))]}{dt}$ is (omitting the dependence on time)

$$\begin{aligned} \langle \nabla L(\phi, \omega) | (\dot{\phi}, \dot{\omega})^\top \rangle &= \sum_{k=1}^n \left(\frac{\partial V}{\partial \phi_k}(\phi) (\omega_k - c_k \frac{\partial V}{\partial \phi_k}(\phi)) - \frac{(\omega_c - \omega_k)}{s_k} (-s_k \frac{\partial V}{\partial \phi_k}(\phi)) \right) \\ &= - \sum_{k=1}^n c_k \frac{\partial V}{\partial \phi_k}(\phi)^2 + \omega_c \sum_{k=1}^n \frac{\partial V}{\partial \phi_k}(\phi) \leq 0. \end{aligned}$$

Observe that $\sum_{k=1}^n c_k \frac{\partial V}{\partial \phi_k}(\phi)^2 = 0$ if and only if $\nabla V(\phi) = \mathbf{0}$. We therefore need to prove the existence of a neighborhood \mathbb{U}_ϕ of \mathbb{M} such that $\nabla V(\phi) \neq \mathbf{0}$ for all $\phi \in \mathbb{U}_\phi \setminus \mathbb{M}$. Such a neighborhood exists

since for all $\bar{\phi} \in \mathbb{M}$, the kernel $\ker(\mathfrak{D}^2\mathbf{V}(\bar{\phi}))$ is equal to the kernel of the submanifold \mathbb{M} which is $\ker(\hat{L})$. Then, invoking Corollary E.2 in [45] guarantees the existence of \mathbb{U}_ϕ . We then define a neighborhood \mathbb{U} of \mathbb{K} as $\mathbb{U} := \mathbb{U}_\phi \times \mathbb{U}_{\omega_c}$, where \mathbb{U}_{ω_c} is a neighborhood of $\omega_c \mathbf{1}$. Therefore, there exists a neighborhood \mathcal{U} of \mathbb{K} such that for all orbits $(\phi(t), \omega(t))$ of Equations (5.2) with initial conditions in \mathbb{U} , strict negativity $\langle \nabla \mathbf{L}(\phi, \omega) | (\dot{\phi}, \dot{\omega})^\top \rangle < 0$ holds for all $(\phi, \omega) \in \mathcal{U} \setminus \mathbb{M}$.

In the case where $\langle \mathbf{1} | \nabla \mathbf{V}(\phi) \rangle = 0$ for all ϕ , the above arguments for the convergence still hold, but one must define \mathbb{U}_{ω_c} as a neighborhood of $\omega_c \mathbf{1}$ included in the hyperplane

$$\{\omega \in \mathbb{R}^n \mid \sum_{k=1}^n \frac{\omega_k}{s_k} = \sum_{k=1}^n \frac{\omega_k(0)}{s_k}\}. \quad (5.16)$$

This is due to the system's constant of motion

$$J(\omega_1, \dots, \omega_n) = \sum_{k=1}^n \frac{\omega_k}{s_k}.$$

Indeed, for $\omega_k(t)$ orbits of Equations (5.2), we have

$$\frac{d[J(\omega_1(t), \dots, \omega_n(t))]}{dt} = \sum_{k=1}^n \frac{\dot{\omega}_k(t)}{s_k} = \sum_{k=1}^n \frac{-s_k}{s_k} \frac{\partial \mathbf{V}}{\partial \phi_k}(\phi) = 0.$$

Thus orbits with initial conditions in Hyperplane (5.16) will, for all time, belong to this set. Therefore, $\sum_{k=1}^n \frac{\omega_k(0)}{s_k} = \sum_{k=1}^n \frac{\omega_k(t)}{s_k}$ for all t , and due to the convergence, $\sum_{k=1}^n \frac{\omega_k(0)}{s_k} = \omega_c \sum_{k=1}^n \frac{1}{s_k}$ and therefore

$$\omega_c = \frac{\sum_{k=1}^n \frac{\omega_k(0)}{s_k}}{\sum_{k=1}^n \frac{1}{s_k}}.$$

5.C Commuting Matrices

Lemma 2. *Let $\{A(t)\}_{t \in \mathbb{I}}$ be a collection of symmetric matrices. We have*

$$A(t)A(s) = A(s)A(t) \quad \forall t, s \in \mathbb{I} \iff \begin{cases} \text{there exists an orthonormal matrix } O \text{ with real entries} \\ \text{such that} \\ O^\top A(t)O = \begin{pmatrix} \xi_1(t) & \dots & 0 \\ & \dots & \\ 0 & \dots & \xi_n(t) \end{pmatrix} \quad \forall t \in \mathbb{I}. \end{cases}$$

Proof.

[\implies] Let $\{A(t)\}_{t \in \mathbb{I}}$ be a family of symmetric and commutative matrices. Denote by \mathbb{H} the vector subspace generated by the family (i.e. $\mathbb{H} = \langle A(t) \mid t \in \mathbb{I} \rangle$). We have that

$$AB = BA \quad \forall A, B \in \mathbb{H}.$$

This is because any A and B in V are expressed as $A = \sum_{i=1}^l a_i A(t_i)$ and $B = \sum_{j=1}^k b_j A(s_j)$. Hence

$$AB = \sum_{i=1}^l \sum_{j=1}^k a_i b_j A(t_i) A(s_j) = \sum_{i=1}^l \sum_{j=1}^k a_i b_j A(s_j) A(t_i) = BA.$$

Since \mathbb{H} is finite dimensional (because it is a subspace of the space of symmetric matrices), there exists $A_1, \dots, A_m \in \mathbb{H}$ such that $\mathbb{H} = \langle A_1, \dots, A_m \rangle$. Therefore any matrix $A(t)$ in \mathbb{H} is expressed as $A(t) = \sum_{j=1}^m a_j(t)A_j$. By Lemma 3, there exists an orthogonal matrix O such that $O^\top A_j O$ is diagonal for every j and so

$$O^\top A(t)O = O^\top \left(\sum_{j=1}^m a_j(t)A_j \right) O = \sum_{j=1}^m a_j(t)O^\top A_j O$$

is diagonal.

[\Leftarrow] Let $t, s \in \mathbb{I}$. Denote by $[\xi(t)]$ (respectively $[\xi(s)]$) the diagonal matrix with $\xi_1(t), \dots, \xi_n(t)$ (respectively $\xi_1(s), \dots, \xi_n(s)$) on its diagonal. Since $[\xi(t)]$ and $[\xi(s)]$ commute, then

$$A(t)A(s) = O[\xi(t)]O^\top O[\xi(s)]O^\top = O[\xi(t)][\xi(s)]O^\top = O[\xi(s)][\xi(t)]O^\top = A(s)A(t) .$$

□

Lemma 3. *Let A_1, \dots, A_m be symmetric matrices such that $A_i A_j = A_j A_i$ for every $1 \leq i, j \leq m$, then there exists an orthonormal matrices O such that $O^\top A_j O$ is diagonal for every $1 \leq j \leq m$.*

Proof.

We proceed by induction. We first consider the case $m = 2$. Let A and B be symmetric and commutative matrices. The eigenspaces of A form an orthogonal decomposition

$$\mathbb{R}^n = \mathbb{E}_{\xi_1} \oplus \dots \oplus \mathbb{E}_{\xi_k} .$$

If $x \in \mathbb{E}_{\xi_j}$, then $A(Bx) = BAx = \xi_j(Bx)$ and thus $Bx \in \mathbb{E}_{\xi_j}$. Therefore $B(\mathbb{E}_{\xi_j}) \subseteq \mathbb{E}_{\xi_j}$ for every j . Since, for each j , $B|_{\mathbb{E}_{\xi_j}}$ (i.e. B restricted to \mathbb{E}_{ξ_j}) is a symmetric operator, there exists an orthonormal basis ${}_j x_1, \dots, {}_j x_{s_j}$ of \mathbb{E}_{ξ_j} . The reunion of these forms simultaneously an orthonormal basis of eigenvectors of A and B .

We now consider the case $m \Rightarrow m + 1$. Let A_1, \dots, A_m, B be a family of commutative symmetric matrices. By induction hypothesis, there exists an orthonormal matrix O whose columns, denoted by o_1, \dots, o_n , are eigenvectors for every A_j ($j = 1, \dots, m$). For every j , the eigenspaces form an orthogonal decomposition

$$\mathbb{R}^n = \mathbb{E}_1^j \oplus \dots \oplus \mathbb{E}_{v_j}^j .$$

Each of the subspace \mathbb{E}_k^j are generated by a choice of o_1, \dots, o_n . The indices of the vectors o_1, \dots, o_n that belong to \mathbb{E}_k^j are denoted as \mathbb{I}_k^j (i.e. $\mathbb{I}_k^j := \{s \in \{1, \dots, n\} \mid o_s \in \mathbb{E}_k^j\}$). For each j , we have a decomposition

$$\{1, \dots, n\} = \mathbb{I}_1^j \sqcup \dots \sqcup \mathbb{I}_{v_j}^j .$$

We can take the minimal decomposition generated by these decompositions (i.e. the decomposition that is included in all others), and we denoted it as

$$\{1, \dots, n\} = \mathbb{J}_1 \sqcup \dots \sqcup \mathbb{J}_k .$$

Define $\mathbb{F}_p = \langle o_s \mid s \in \mathbb{J}_j \rangle$ for $j = 1, \dots, p$. The corresponding orthogonal decomposition

$$\mathbb{R}^n = \mathbb{F}_1 \oplus \dots \oplus \mathbb{F}_p$$

is such that each vector of \mathbb{F}_j is an eigenvector for each A_j and that $B(\mathbb{F}_j) \subseteq \mathbb{F}_j$ (as in the case $m = 2$). Since B preserves all orthogonal decomposition, there exists an orthonormal basis of \mathbb{R}^n which consists of eigenvectors of B and which are in the spaces \mathbb{F}_i (same argument as in the case $m = 2$). So o_1, \dots, o_n forms a basis of orthonormal eigenvectors of A_j for all j and B .

□

Noise Induced Temporal Patterns in Populations of Globally Coupled Oscillators

El tiempo se bifurca perfectamente hacia innumerables futuros.

Jorge Luis BORGES

Abstract

The population dynamics of an assembly of globally coupled homogeneous phase oscillators is studied in presence of non-Gaussian fluctuations. The variance of the underlying stochastic process grows as $t + \mathbf{b}^2 t^2$ (\mathbf{b} being a constant) and therefore exhibits a super-diffusive behavior. The cooperative evolution of the oscillators is represented by an order parameter which, due to the ballistic $\mathbf{b}^2 t^2$ contribution, obeys to a surprisingly complex bifurcation diagram. The specific class of super-diffusive noise sources can be represented as a random superposition of two Brownian motions with opposite drift and this allows to derive exact analytic results. We observe that besides the existence of the well known incoherent to coherent phase transition already present for Gaussian noise, entirely new and purely noise induced temporal patterns of the order parameter are realized. Hence, the ballistic contributions of the fluctuating environment does structurally modify the bifurcation diagram obtained for Gaussian noise. To illustrate potential implications of the developed class of models, we explore the dynamic behavior of a swarm formed by a planar society of particles with coupled oscillator dynamics. For this collective dynamics, we discuss how noise induced periodic orbits of the swarm's barycenter may emerge.

6.1 Introduction

In the vast research domain in relation with cooperative dynamics, a wealth of applications are successfully stylized by the dynamics of interacting phase oscillators evolving in a random environment. In this context, one of the most successful models is doubtlessly the KURAMOTO-SAKAGUCHI (KS) model [34], [51]. It consists of a population of n coupled phase oscillators where the phase of the k^{th} oscillator, denoted by ϕ_k , evolves in time according to

$$\dot{\phi}_k = \omega_k + \frac{c}{n} \sum_{j=1}^n \sin(\phi_j - \phi_k) + \sqrt{2e} \mathcal{X}_k(t) \quad k = 1, \dots, n. \quad (6.1)$$

Here, c is an ‘‘All-to-All’’ coupling constant and ω_k is the natural frequency of oscillator k which is drawn at random from some probability distribution $\mathcal{G}(\omega)$. The random environment is additive Gaussian white noise (GWN), $\sqrt{2e} \mathcal{X}_k(t)$, with noise strength $e > 0$. The model can be studied in terms of a complex order parameter $\rho \exp(i\alpha)$ given by

$$\rho \exp(i\alpha) := \frac{1}{n} \sum_{j=1}^n \exp(i\phi_j) \quad (6.2)$$

with notation $\iota^2 = -1$. The amplitude $\rho \in [0, 1]$ measures the phase coherence of the oscillators and α represents an average phase of the system. Thanks to ρ , we can identify the cooperative state of the oscillators assembly, namely $\rho = 1$ indicates a fully synchronized motion (see Appendix 6.A for details), $\rho = 0$ characterizes a fully incoherent behavior and when $0 < \rho < 1$, the assembly possesses a partially synchronized state.

After the pioneering works [34, 51], the behavior of Equations (6.1) has been further analyzed in presence of Gaussian noise sources $\mathfrak{X}_k(t)$ having white or colored spectral densities [1, 50]. In the limit $n \rightarrow \infty$, it can be shown that, tuned by the coupling strength c , a second order type phase transition occurs between the fully incoherent and a partially synchronized state at a critical bifurcation value \check{c} . The explicit dependence of \check{c} on the underlying control parameters, (noise amplitude e , noise coloration, . . .), has been derived analytically for several Gaussian noise sources and a rather large class of frequency distributions $\mathcal{G}(w)$. These analytical and numerical studies underline the following intuitive picture: an increase of the noise correlations decreases the value of \check{c} .

The injection of non-Gaussian noise into the dynamics given by Equations (6.1) will generally preclude analytical discussion and hence do enforce numerical studies to be performed. This numerical approach has recently been adopted in [7] for a class of stationary processes for which the invariant measure exhibits a symmetric non-Gaussian, uni-modal probability density. The authors report that the global qualitative picture of the phase transition is preserved. However, the bifurcation value \check{c} explicitly depends on the non-Gaussian character of the noise. Adopting a similar research direction, the present work aims to analyze the behavior of Equations (6.1) in presence of a super-diffusive, non-Gaussian noise having a variance growing as $t + b^2 t^2$, b being a constant. The b -controlled non-Gaussian character, produces a surprisingly enriched phase transition diagram which includes regimes with time oscillations of the order parameter ρ . This stable temporal modulation is entirely due to the non-Gaussian character of the driving noise tuned by b . For the limiting case $b = 0$, the noise model coincides with the standard WGN case. Note that contrary to [7], our noise process is non-stationary and exhibits a bi-modal transition probability density.

6.2 KURAMOTO-SAKAGUCHI Model Driven by Super-Diffusive Noise

In the following, we consider the KS like-dynamics given in Equations (6.1) where the $\mathfrak{X}_k(t)$ are replaced with non-Gaussian noise sources and where all the natural frequencies w_k are equal. By going into a rotating frame we can assume $w_k = 0$ and the homogeneous frequency model reads as

$$\dot{\phi}_k = \frac{c}{n} \sum_{j=1}^n \sin(\phi_j - \phi_k) + \sqrt{2e}\mathfrak{V}_k(t) \quad k = 1, \dots, n. \quad (6.3)$$

The non-Gaussian noise sources $\mathfrak{V}_k(t)$ we will consider in Equations (6.3) are formal derivatives $\frac{d\mathfrak{Z}_k(t)}{dt}$ of none linear diffusion processes $\mathfrak{Z}_k(t)$ with LANGEVIN equation

$$\mathfrak{V}_k(t) = \frac{d\mathfrak{Z}_k(t)}{dt} = b \tanh(b\mathfrak{Z}_k(t)) + \mathfrak{X}_k(t), \quad \mathfrak{Z}_k(0) = 0 \quad (6.4)$$

and where the $\mathfrak{X}_k(t)$ are independent WGN processes verifying for $k = 1, \dots, n$,

$$\langle \mathfrak{X}_k(t) \rangle = 0 \quad \text{and} \quad \langle \mathfrak{X}_k(t) \mathfrak{X}_j(s) \rangle = \bar{\mathcal{D}}_{k,j} \mathcal{D}(t-s). \quad (6.5)$$

To study the dynamics given by Equations (6.3), we briefly review some relevant features of the noise source delivered by Equations (6.4).

6.2.1 A None Gaussian, Super-Diffusive Noise

Due to the absence of correlations between the noise components in Equations (6.5), we focus on a single noise component and will omit the subscript. Observe that the transition probability density (TPD) $\mathcal{P}(z, t|0, 0)$ associated with the non-linear diffusion process Equations (6.4) reads as [27, 28]

$$\begin{aligned}\mathcal{P}(z, t|0, 0) &= \cosh(bz) \frac{1}{\sqrt{2\pi t}} \exp\left(-\frac{b^2 t^2 - z^2}{2t}\right) \\ &= \frac{1}{2} \mathcal{N}^+(z, t) + \frac{1}{2} \mathcal{N}^-(z, t),\end{aligned}\tag{6.6}$$

where

$$\mathcal{N}^\pm(z, t) = \frac{1}{\sqrt{2\pi t}} \exp\left(-\frac{(z \pm bt)^2}{2t}\right).\tag{6.7}$$

The TPD Equation (6.6) is the sum of two Gaussian densities and therefore the non-Gaussian character of $\mathcal{V}(t)$ is obvious. Elementary quadratures using the density given by Equation (6.6) yield the moments

$$\langle 3^{2m+1}(t) \rangle = 0, \quad \langle 3^{2m}(t) \rangle = \left(\frac{-t}{2}\right)^n \text{H}_{2m}\left(i\sqrt{\frac{bt}{2}}\right)\tag{6.8}$$

for $m = 1, 2, \dots$ and where H_{2m} are the HERMITE polynomials. In particular we have

$$\langle 3(t)3(s) \rangle = \min(t, s) + b^2 ts\tag{6.9}$$

for the covariance and for the second moment we find

$$\langle 3^2(t) \rangle = t + b^2 t^2.\tag{6.10}$$

The b parameter multiplies the ballistic contribution of order t^2 and hence controls in a simple way the super-diffusive character of the noise source. For $b \rightarrow 0$, $\mathcal{V}(t)$ converges to the standard WGN. The process $3(t)$ defined by Equations (6.4), possesses several interesting mathematical properties which renders $3(t)$ particularly useful for stochastic modeling. We cite the two mayor ones.

I L. ROGERS and J. PITMAN remarked in [48] (See example 2, on page 581) that $3(t)$ can be represented as the random Gaussian mixture (see also Equation (6.6)):

$$3(t) = \mathbb{B}bt + \text{III}(t), \quad 3(0) = 0,\tag{6.11}$$

where $\text{III}(t)$ is the standard WIENER process and $\mathbb{B} \in \{-1, +1\}$ is a symmetric Bernoulli variable independent of $\text{III}(t)$.

II I. BENJAMINI and S. LEE remarked in [10] that conditioning the $3(t)$ process so that $3(0) = 3(t) = 0$, with $t > 0$ a fixed time instant, the resulting conditioned new process, say $\tilde{3}(t)$, is a Brownian bridge. Moreover, it is the unique Brownian bridge with none linear drift term. Note that the time-discrete version of the $3(t)$ process is discussed in [31].

6.2.2 The Effect of The Non-Gaussian Noise

By using the representation given by Equation (6.11), it is straightforward to see that Equations (6.3) can be effectively rewritten as

$$\dot{\phi}_k = w_k + \frac{c}{n} \sum_{j=1}^n \sin(\phi_j - \phi_k) + \sqrt{2e} \mathcal{V}_k(t) \quad k = 1, \dots, n\tag{6.12}$$

where the frequencies w_k are now drawn randomly from a probability distribution $\mathcal{G}(w)$

$$\mathcal{G}(w) = \frac{1}{2} \mathcal{D}(w - b\sqrt{2e}) + \frac{1}{2} \mathcal{D}(w + b\sqrt{2e})\tag{6.13}$$

Hence we can summarize this observation by saying

“The effective action of the non-Gaussian noise sources on the homogeneous frequency model of Equations (6.3) is equivalent to drive an heterogenous bi-frequency KS model with Gaussian noise sources”.

The stronger the non-Gaussian character (i.e the stronger b), the larger the variance of the distribution $\mathcal{G}(w)$ in Equation (6.13). The resulting dynamics defined by Equations (6.12) and (6.13) is thoroughly discussed in [3, 15]. It exhibits the following salient features

- a) **Close to Gaussian noise regime.** When $0 \leq \mathbf{b} < \sqrt{\frac{\mathbf{e}}{2}}$, a phase transition between a fully incoherent state to a partially synchronized state occurs at a bifurcation value $\check{c}(\mathbf{b}, \mathbf{e}) = 2\mathbf{e} + 4\mathbf{b}^2$. While the bifurcation value $\check{c}(\mathbf{b}, \mathbf{e})$ is \mathbf{b} -dependent, the resulting bifurcation diagram topologically coincides with the Gaussian $\mathbf{b} = 0$ case (cf. Figure 1, in [12]).
- b) **Far from Gaussian noise regime.** When $\mathbf{b} > \sqrt{\frac{\mathbf{e}}{2}}$ entirely new dynamic features emerge and a sketch of the (conjectured) global bifurcation diagram is given in Figure 5, Ref. [12]. In summary, one finds \mathbf{b} and \mathbf{e} dependent critical values $c_1(\mathbf{b}, \mathbf{e}) > 4\mathbf{e}$ and $c_2(\mathbf{b}, \mathbf{e}) < c_1(\mathbf{b}, \mathbf{e})$ such that

For $4\mathbf{e} \leq c < c_1(\mathbf{b}, \mathbf{e})$, temporal oscillations of the OP occur and the zero value $\rho(t) = 0$ is repeatedly attained. Both the oscillations amplitude and their period increase with c . Due to the symmetry of $\mathcal{G}(\mathbf{w})$ in Equation (6.13), the global average phase α in Equation (6.2) is time-independent during partial synchronization with $\rho > 0$. Its value depends on the initial angle distributions [2, 12]. Hence, the value of the average global phase can be modified at times when full incoherence, $\rho(t) = 0$, is reached.

For $c_1(\mathbf{b}, \mathbf{e}) \leq c < c_2(\mathbf{b}, \mathbf{e})$ and depending on the initial conditions, one observes either a temporal oscillating behavior of $\rho(t)$ or a purely stationary partially synchronized regime with $\rho(t) = \bar{\rho} \in]0, 1[$ ($\bar{\rho}$ a constant).

For $c_2(\mathbf{b}, \mathbf{e}) \leq c$, only stationary synchronized regimes exist and the fully synchronized case $\rho = 1$ is asymptotically reached for $c \rightarrow \infty$.

6.2.3 Extensions to More Complex Noise Sources

Several generalizations of the basic KS model Equations (6.3) have recently being discussed, for example with frequency distributions given by

- a) $\mathcal{G}(\mathbf{w}) = a\mathcal{D}(\mathbf{w} - \mathbf{w}_0) + (1 - a)\mathcal{D}(\mathbf{w} + \mathbf{w}_0)$, this case is studied in [2],
- b) $\mathcal{G}(\mathbf{w}) = a\mathcal{D}(\mathbf{w}) + (1 - a)(\frac{1}{2}\mathcal{D}(\mathbf{w} - \mathbf{w}_0) + \frac{1}{2}\mathcal{D}(\mathbf{w} + \mathbf{w}_0))$, this case is studied in [3],

with $a \in [0, 1]$. The results obtained for both cases a) and b) can be reinterpreted as resulting from KS dynamics with specific non-Gaussian noise sources.

In case a) the corresponding dynamics will be

$$\dot{\phi}_k = \frac{c}{n} \sum_{j=1}^n \sin(\phi_j - \phi_k) + \sqrt{2\mathbf{e}}\hat{\Psi}_k(t), \quad (6.14)$$

where $\hat{\Psi}_k(t)$ is a biased super-diffusive process which can be represented as the solution to the stochastic differential equation

$$\hat{\Psi}_k(t)dt = d\mathfrak{Z}_k(t) = (\hat{\mathfrak{B}}_k \mathbf{b})dt + d\mathfrak{III}_k(t), \quad \mathfrak{Z}_k(0) = z. \quad (6.15)$$

Here $\hat{\mathfrak{B}}_k$ is a biased BERNOULLI random variable taking, independently of the WIENER processes $\mathfrak{III}_k(t)$, the values $+1$ and -1 with respective probabilities $\frac{1+\tanh(\mathbf{b}z)}{2}$ and $1 - \frac{1+\tanh(\mathbf{b}z)}{2}$.

The global bifurcation diagram corresponding to this case is given in [2]. The asymmetry of $\mathcal{G}(\mathbf{w})$ reduces the parameter range for which the incoherent behavior is stable and precludes the existence of purely stationary synchronized states (i.e. states having simultaneously constant ρ and α). The synchronized phases branch off from incoherence as traveling waves thereby implying a time increasing phase $\alpha(t)$ and either a constant amplitude (for coupling strength c close to the bifurcation point) or time oscillating amplitudes (for larger c).

In the case b), the corresponding dynamics is

$$\dot{\phi}_k = \frac{c}{n} \sum_{j=1}^n \sin(\phi_j - \phi_k) + a\sqrt{2\mathbf{e}}\mathfrak{K}_k(t) + (1 - a)\sqrt{2\mathbf{e}}\Psi_k(t), \quad (6.16)$$

where the parameter $a \in [0, 1]$ is a mixing constant to balance between a non-Gaussian contribution due to $\mathcal{U}_k(t)$ as defined by Equations (6.4) and a Gaussian white noise part $\mathcal{X}_k(t)$. Again, for small deviations from Gaussian noise, characterized by $b < \sqrt{\frac{e}{2}}$, a transition from de-synchronized to a synchronized regime, similar to the pure Gaussian case, arises. For strongly non-Gaussian regimes $b > \sqrt{\frac{e}{2}}$ the following picture emerge [3]

$4e < c_1 < c \leq c_2$. Bifurcation to a stationary partially synchronized regime.

$c_2 < c < c_3$. Strictly positive time-oscillations of $\rho(t) > 0$.

$c_3 < c < c_4$. Bi-stable region with possibility, depending on initial conditions, of either time-oscillations of $\rho(t)$ or pure stationary states with partial synchronization.

$c_4 < c$. Stationary and partially synchronized states with $\rho = \bar{\rho}$ ($\bar{\rho}$ a constant).

The above results clearly exhibit the possibility to generate synchronized stable time-oscillating patterns by a non-Gaussian noise injection and this even in presence of symmetric noise (i.e. vanishing odd moments to any order).

6.3 Noise Induced “Zig-Zagging” - a Case Study

The complex dynamic pattern observed in the previous section opens new potentialities for applications. As an illustration, let us study how super-diffusive noise environments may potentially produce spectacular effects in the collective motion of large assemblies of agents such as bacteria, flies, quadrupeds, fish, etc In this context, recently published self-driven particle models have been shown to capture the collective mechanisms for the formation of compact swarms evolving as quasi-solid bodies [16, 32, 58]. In [16], the authors are able to quantify the agents interactions strength leading to the swarms formations. In particular, observations of the barycenter of a swarm’s collective often reveals “zig-zag” type motions with alternations between traveling in definite direction, almost stopping and restart in a new direction. To unveil one possible mechanism behind this collective dynamics, one now considers simple situations involving n agents, with fixed unit amplitudes velocities, traveling on a plane. In these models, the agents individual direction angles ϕ_k , $k = 1, \dots, n$ will be autonomously updated according to interaction rules dependent on the behavior of observed neighbors. Due to the ubiquitous presence of random fluctuations, noise sources are injected into the dynamics and this obviously produces a tendency to weaken the mechanisms generating collective patterns. This type of modeling is exposed in [40]. Therein particles with coupled oscillators dynamics describe the collective behavior of a planar assembly of n agents with positions $r_k(t) \in \mathbb{C}$ (the plane is identified with the complex \mathbb{C} -plane) and the orientations $\phi_k(t) \in [0, 2\pi[$. The velocity norm being fixed to unity, the assembly dynamics follows:

$$\begin{aligned} \dot{\phi}_k &= P_k(\phi, r, \mathcal{X}_k(t)) \\ \dot{r}_k &= \exp(i\phi_k) \end{aligned} \quad k = 1, \dots, n \quad (6.17)$$

with $\phi = (\phi_1, \dots, \phi_n)$ and $r = (r_1, \dots, r_n)$, and where the agents’ phases interact via functions P_k and where $\mathcal{X}_k(t)$ are independent stochastic processes. Restricting, similar to [23] and [5], the P_k functions to pure angle dependence of the additive form

$$P_k(\phi, \mathcal{X}_k(t)) = \arg\left(\frac{1}{n} \sum_{j=1}^n \exp(i\phi_j)\right) + \sqrt{e}\mathcal{X}_k(t)$$

with $e \in \mathbb{R}_{\geq 0}$ a constant, the swarm’s barycentric position $G(t) = \frac{1}{n} \sum_{k=1}^n r_k(t)$ moves with velocity

$$\dot{G}(t) = \frac{1}{n} \sum_{k=1}^n \dot{r}_k(t) = \frac{1}{n} \sum_{k=1}^n \exp(i\phi_k(t)) =: \rho(t) \exp(i\alpha(t)). \quad (6.18)$$

The variable $\rho(t) \in [0, 1]$, in Equations (6.18) coincides with the OP introduced in Equation (6.2). Hence, for $\rho = 0$ which characterizes the fully incoherent motion (named the balanced-phase motion

in [40]), the swarm's barycenter stays fixed in time. When $\rho > 0$ the swarm's barycenter performs a net motion in direction $\alpha(t)$. The complex behavior of the OP, due to non-Gaussian noise sources, affects the swarm's motion. In particular, from the previous sections, we can conclude that for symmetric $\mathcal{G}(\mathbf{w})$ distributions and appropriate \mathbf{b} and \mathbf{c} parameters, noise induced temporal modulation of the barycentric swarm's velocity occur. An increase of \mathbf{b} reduces the oscillation frequency and increases its amplitude, [12]. Remember that for symmetric $\mathcal{G}(\mathbf{w})$ distributions, oscillations may force the OP to periodically vanish. In such instances of full incoherence a re-actualization of the global phase follows. This changes the velocity direction of the swarm's barycenter and ultimately produces a zig-zag motion. This is shown in the two graphs Figure (6.1) and Figure (6.2) where Equations (6.12) is numerically integrated (EULER's method, step size $h = 0.005$) with $\mathbf{w}_k = 0$ (i.e. $\mathcal{G}(\mathbf{w}) = 0$), $N = 7500$, $\mathbf{c} = 6$, $\mathbf{e} = 1$ and $\mathbf{b} = \frac{2}{\sqrt{2}}$. Figure 6.1 shows the oscillating modulus of the OP.

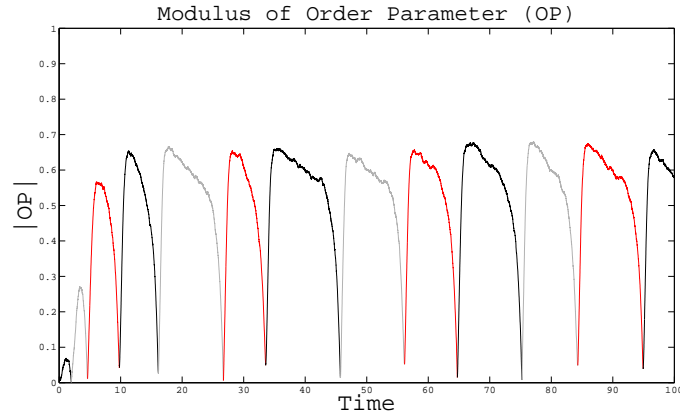


Fig. 6.1: Time evolution of the OP.

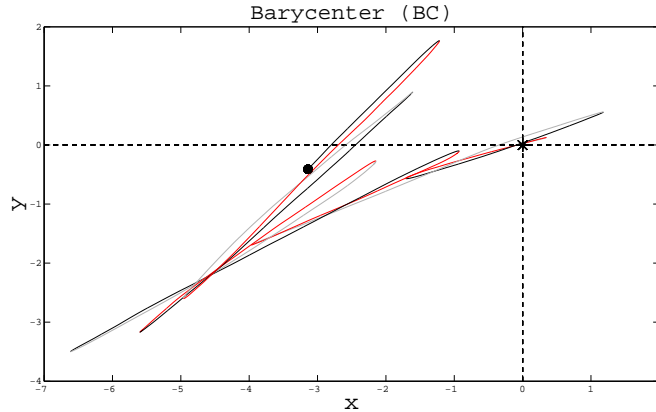


Fig. 6.2: Time evolution of the swarm's BC. The BC starts at the origin. At instances of almost full incoherence (OP small) a re-actualization of the global phase changes the velocity direction of the swarm's BC and produces a zig-zag motion.

Due to finite size effects, the balanced-phase motion is not completely reached and accordingly the various local minima of ρ do not completely vanish. The time evolution of the swarm's BC is captured in Figure 6.2. The evolution of both, the OP and the swarm's BC are displayed in a sequence of black, grey and red curves, starting at the origin $(0, 0)$ and finishing at the black spot.

Color changes synchronously for the BC and the OP every time the OP passes through a local minimum.

6.4 Conclusion

It is truly remarkable that the dynamics of the KURAMOTO-SAKAGUCHI model can be analytically explored for a class of non-Gaussian noise sources characterized by the presence of a ballistic type term $b^2 t^2$ in the variance growth of the process. This ballistic contribution does fundamentally alter the bifurcation scenario previously calculated for dynamics driven by purely Gaussian fluctuations. Even in presence of noise sources with vanishing odd moments of any order, surprisingly complex and entirely noise-induced temporal patterns of the underlying order parameter emerge.

Appendix

6.A Characterization of Full Synchronization via the Oder Parameter

For the oder parameter $\rho \exp(i\alpha) := \frac{1}{n} \sum_{k=1}^n \exp(i\phi_k)$ we have

$$\rho = 1 \iff \phi_k \equiv \phi_j \pmod{2\pi} \quad \forall k, j .$$

Proof. [\Rightarrow] By definition

$$\rho = \left| \frac{1}{n} \sum_{k=1}^n \exp(i\phi_k) \right| = \left| \frac{1}{n} \sum_{k=1}^n \cos(\phi_k) + i \sin(\phi_k) \right| = \sqrt{\left(\frac{1}{n} \sum_{k=1}^n \cos(\phi_k) \right)^2 + \left(\frac{1}{n} \sum_{k=1}^n \sin(\phi_k) \right)^2}$$

and therefore

$$1 = \rho = \frac{1}{n} \sqrt{\left(\sum_{k=1}^n \cos(\phi_k) \right)^2 + \left(\sum_{k=1}^n \sin(\phi_k) \right)^2} \iff n^2 = \left(\sum_{k=1}^n \cos(\phi_k) \right)^2 + \left(\sum_{k=1}^n \sin(\phi_k) \right)^2 .$$

By direct computation, we have

$$\begin{aligned} n^2 &= \sum_{k=1}^n \cos(\phi_k)^2 + \sum_{k>j} 2 \cos(\phi_j) \cos(\phi_k) + \sum_{k=1}^n \sin(\phi_k)^2 + \sum_{k>j} 2 \sin(\phi_j) \sin(\phi_k) \\ &= \sum_{k=1}^n (\cos(\phi_k)^2 + \sin(\phi_k)^2) + \sum_{k>j} \left(\underbrace{2 \cos(\phi_k) \cos(\phi_j)}_{\cos(\phi_k + \phi_j) + \cos(\phi_k - \phi_j)} + \underbrace{2 \sin(\phi_k) \sin(\phi_j)}_{\cos(\phi_k - \phi_j) - \cos(\phi_k + \phi_j)} \right) \\ &= n + 2 \sum_{k>j} \cos(\phi_k - \phi_j) . \end{aligned}$$

We hence have

$$\frac{n(n-1)}{2} = \sum_{k>j} \cos(\phi_k - \phi_j)$$

and the right hand side of the above equality has $\frac{n(n-1)}{2}$ terms, each being between -1 and 1 . Since they must sum up to $\frac{n(n-1)}{2}$, then all terms must equal one and so

$$\cos(\phi_k - \phi_j) = 1 \iff \phi_k \equiv \phi_j \pmod{2\pi} \quad \forall k, j .$$

[\Leftarrow] By direct computation, we have

$$\frac{1}{n} \sum_{k=1}^n \exp(i\phi_k) = \frac{1}{n} \left(\sum_{k=1}^n \cos(\phi_k) + i \sum_{k=1}^n \sin(\phi_k) \right) = \frac{1}{n} (cn + i sn) = (c + is)$$

with $c := \cos(\phi_k) = \cos(\phi_j + m_{k,j}2\pi)$ and $s := \sin(\phi_k) = \sin(\phi_j + m_{k,j}2\pi)$. Hence $\rho = |c + is| = \sqrt{c^2 + s^2} = 1$.

□

Conclusions and Perspectives

Que ferai-je à l'avenir? Si tous les projets ne se mesuraient à longueur de la vie, je voudrais reprendre des études mathématiques et physiques délaissées depuis un quart de siècle, rapprendre cette belle langue. J'aurais alors l'ambition de faire de la « Poétique » un chapitre des mathématiques. Projet démesuré certes, mais dont la réussite ne porterait préjudice ni à l'inspiration, ni à l'intuition, ni à la sensualité. La Poésie n'est-elle pas aussi science des nombres?

Robert DESNOS

7.1 Conclusions

Adaptation to time-dependent environments and efficient coordination and synchronization of actions can be found in nature and are often central to sustaining life forms or economic activity. Adopting an holistic point of view as synthesized by Nicholas GEORGESCU-ROEGEN in his contribution "The Entropy Law and the Economic Process", our human activity is pursued away from thermodynamical equilibrium - thus implying a permanent and coordinated supply of matter, energy and information. The following short list of keywords should serve to outline a possible context of such a philosophical perception translated into mathematical terms: dynamical systems complex networks, steady and time-dependent network connectivity, feedback mechanisms, emerging dissipative dynamical patterns, synchronization, learning and adaptation rules, consensual states for multi-agents systems, centralized and decentralized optimal control theory, leaders and soft control, fluctuating environments. Based on these theoretical cornerstones, our work tries to offer an explicit mathematical playground to better understand and quantify some aspects of dynamic adaptation for different configurations and environments, including those with randomness. We are fully aware of basic limitations inherent to our approach - and analytical results can often be obtained only at the price of renouncing generality. Nevertheless, we think that our models contribute to the necessary corpus of analytical illustrations in this field.

Through out the main part of this thesis, we investigated adaptive mechanisms in coupled oscillatory systems with delayed and time-dependent interactions. Here, adaptation always occurred through additional coupling functions. If these functions were systematically zero (or, if their corresponding susceptibility constants were zero), the systems that we studied no longer belong to the problematic of adaptation, but rather to one of synchronization.

Therefore, to close on this work, we compare the two phenomena, synchronization and adaptation, in a network of adaptive frequency oscillators. For this, consider the two following systems

$$\dot{\phi}_k(t) = \mathbf{w}_k + \mathbf{c} \sum_{j=1}^n l_{k,j}(t) \sin(\phi_k(t-t) - \phi_j(t-t)) \quad k = 1, \dots, n \quad (7.1)$$

and

$$\begin{aligned} \dot{\phi}_k(t) &= \omega_k(t) + \mathbf{c} \sum_{j=1}^n l_{k,j}(t) \sin(\phi_k(t-t) - \phi_j(t-t)) \\ \dot{\omega}_k(t) &= \mathbf{s} \sum_{j=1}^n l_{k,j}(t) \sin(\phi_k(t-t) - \phi_j(t-t)) \end{aligned} \quad k = 1, \dots, n, \quad (7.2)$$

where we suppose that the entries of the adjacency matrix are bounded positive smooth functions of time, and the auto- and hetero-commutation rules from Chapter 5 apply for $L(t)$. We list three important characteristics for the two phenomena below (see Appendix 7.A for details).

Existence of a Common Oscillatory State

The two systems possess a common oscillatory state. System (7.1) possesses a synchronized oscillatory state

$$\phi_k(t) = \mathbf{w}_c t + \varphi_k \quad k = 1, \dots, n$$

with $\mathbf{w}_c = \frac{1}{n} \sum_{j=1}^n \mathbf{w}_k$ existing with certain constrains on \mathbf{c} and L . System (7.2) possesses a consensual oscillatory state

$$\phi_k(t) = \omega_c t \quad k = 1, \dots, n$$

with $\omega_c = \frac{1}{n} \sum_{j=1}^n \omega_k(0)$ existing without any constrains. Note that both systems have the same frequency for their common oscillatory state if $\mathbf{w}_k = \omega_k(0)$, but that oscillators are out of phase for System (7.1).

Convergence Towards a Common Oscillatory State for Non-Delayed Interactions

For non-delayed interactions, both systems converge towards their respective common oscillatory state. There are no conditions on $L(t)$ for converging towards a synchronized oscillatory state. However, conditions on $L(t)$ are required to guarantee convergence towards a consensual oscillator state.

Convergence Towards a Common Oscillatory State for Time-Independent Networks

For time-independent networks, both systems converge towards their respective common oscillatory state but, in both cases, only for a time delay t not exceeding a critical value - $\mathbf{t}_{s,n}$ for System (7.4) and $\mathbf{t}_{a,n}$ for System (7.5). Here, we have $\mathbf{t}_{a,n} \leq \mathbf{t}_{s,n}$, and so System (7.4) allows for a larger time delay.

7.2 Perspectives

The following list contains new ideas for further research based on this work.

Further Investigations on Adaptation vs. Synchronization

As presented in Section 7.1, one can list the advantages and disadvantages between adaptive and synchronization phenomena, and this for different types of local dynamics. Among the different issues to investigate, comparing the basin of attractions would be of great interest.

Frequency Adaptation for Phase Oscillators in Noisy Environment

Having studied coupled phase oscillators in noisy environments without adaptation, we would like to investigate the resulting dynamics when adaptive frequency mechanisms are introduced. More precisely, the explicit system to analyze is

$$\begin{aligned}
d\phi_k &= \left(\omega_k - \frac{c}{n} \sum_{j=1}^n \sin(\phi_k - \phi_j) \right) dt + \sqrt{2e} d\mathcal{Z}_k \\
d\mathcal{Z}_k &= b \tanh(b\mathcal{Z}_k) dt + d\mathcal{Z}_k & k = 1, \dots, n \\
d\omega_k &= -\frac{s}{n} \sum_{j=1}^n \sin(\phi_k - \phi_j) dt
\end{aligned} \tag{7.3}$$

with $r_k(0) = 0$, $\phi(0) \in [0, 2\pi[$ (uniformly distributed), $\omega_k(0) = 0$ and $\mathcal{Z}_k(0) = 0$. To gain some insight, we performed a numerical experiment, considering $n = 10000$, and with parameter values $c = 4$, $s = 1$, $e = 1$ and $b = \frac{2}{\sqrt{2}}$. We used EULER's method with a set size of $h = 0.005$. The dynamics of the modulus of the order parameter (OP) is displayed in Figure 7.1. Observe the oscillatory behavior of the OP before converging towards a steady value.

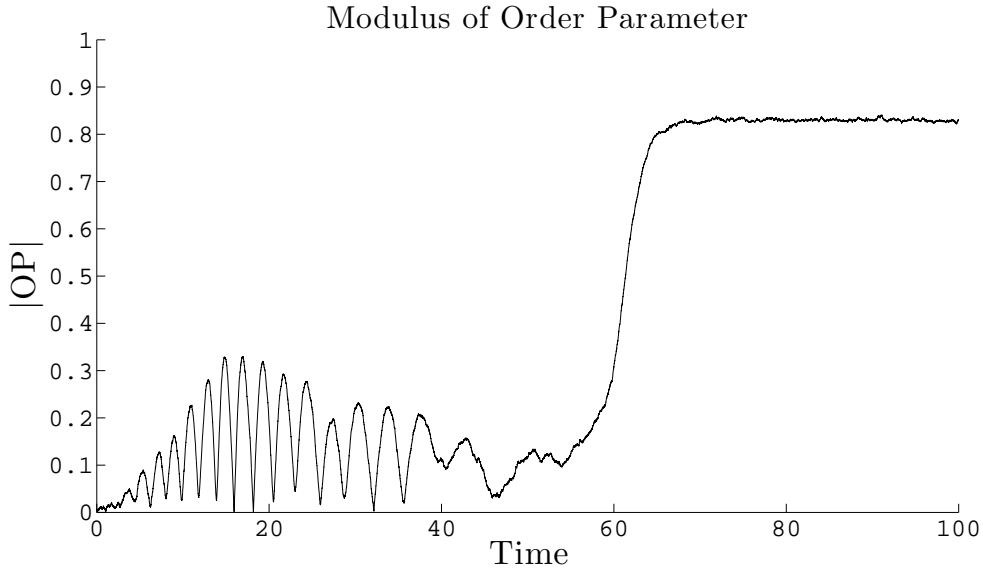


Fig. 7.1: Evolution of the modulus of the oder parameter (OP) for System (7.3).

Analyzing Time-dependent Delayed Differential Equations

To determine conditions (based on linear stability analysis) for convergence towards a consensual oscillatory state for Equations (7.2), we need to find the conditions for asymptotic stability for the zero solution of the linear second order delay differential equation with time-dependent coefficients taking the general form as

$$\ddot{x}(t) + F_1(t)\dot{x}(t-t) + F_2(t)x(t-t) = 0 .$$

Adaptation in the Context of Optimal Control

Although we barely touch upon optimal control theory in this work, our synthetic dynamical models can offer an appropriate framework to derive relevant dynamic programming equations when supplemented by objective functions. While this remains a mere perspective at this stage, let us emphasize that objective functions to be minimized (or maximized) via optimal control can be formulated in terms of ЛЯПУНОВ functions. It goes without saying, and as we mentioned at the beginning of our conclusions, that optimal control issues are of the utmost relevance for example in the context of a steadily increasing world population, where we struggle with the problem of sustaining limited resources.

Appendix

7.A Comparison Between Synchronization and Adaptation

The first variational equations (after digonalization) of Systems (7.1) and (7.2) for their respective common oscillatory states are, respectively,

$$\dot{\varepsilon}_{\phi_k}(t) = -\mathbf{c}\zeta_{\cos_k}(t)\varepsilon_{\phi_k}(t-t) \quad k = 1, \dots, n \quad (7.4)$$

with $\zeta_{\cos_k}(t)$ eigenvalues of matrix $L_{\cos}(t)$ with entries $l_{k,j}(t)\cos(\varphi_k - \varphi_j)$, and

$$\begin{aligned} \dot{\varepsilon}_{\phi_k}(t) &= \varepsilon_{\omega_k}(t) - \mathbf{c}\zeta_k(t)\varepsilon_{\phi_k}(t-t) \\ \dot{\varepsilon}_{\omega_k}(t) &= -\mathbf{s}\zeta_k(t)\varepsilon_{\phi_k}(t-t) \end{aligned} \quad k = 1, \dots, n. \quad (7.5)$$

with $\zeta_k(t)$ eigenvalues of matrix $L(t)$. For the synchronization case, we suppose that $|\varphi_k - \varphi_j|$ is sufficiently small so that $\cos(\varphi_k - \varphi_j) \simeq 1$.

Comparing Stability of Common Oscillatory State for Non-Delayed Interactions

When $t = 0$, the stability of the zero solution of Equations (7.4) is easily discussed since

$$\varepsilon_{\phi_k}(t) = \varepsilon_{\phi_k}(0) \exp\left(-\mathbf{c} \int_0^t \zeta_{\cos_k}(s) ds\right).$$

Hence $\lim_{t \rightarrow \infty} \varepsilon_{\phi_k}(t) = 0$ for $k = 1, \dots, n$ and for $k = 1$, $\varepsilon_{\phi_1}(t) = \varepsilon_{\phi_1}(0)$, which accounts for the phase shift. The stability of the zero solution of Equations (7.4) is delicate since it is the dynamics of a pendulum with time-dependent friction and frequency

$$\ddot{\varepsilon}_{\phi_k}(t) + \mathbf{c}\zeta_k(t)\dot{\varepsilon}_{\phi_k}(t) + (\mathbf{c}\dot{\zeta}_k(t) + \mathbf{s}\zeta_k(t))\varepsilon_{\phi_k}(t) = 0.$$

Conditions for asymptotic stability are given in [42].

Comparing Stability of Common Oscillatory State for Time-Independent Networks

When the edges of the network are time-independent (i.e. constant), the stability of the zero solution of Equations (7.4) is discussed as follows. For each k ($k = 2, \dots, n$), the zero solution is asymptotically stable provided (c.f. [33] for details) $t < t_{s,k}$ with $t_{s,k} = \frac{\frac{\pi}{2}}{\mathbf{c}\zeta_{\cos_k}}$. Since $0 < \zeta_{\cos_2} \leq \dots \leq \zeta_{\cos_n}$, then

$$t_{s,n} = \frac{\frac{\pi}{2}}{\mathbf{c}\zeta_{\cos_n}} \geq \frac{\frac{\pi}{2}}{\mathbf{c}\zeta_{\cos_k}} = t_{s,k} \quad k = 2, \dots, n.$$

Hence, if $t < \check{t}_{s,n}$, the zero solution is asymptotically stable for $k = 2, \dots, n$. The case $k = 1$ accounts for the phase shift.

Among the conditions for the zero solution to be asymptotically stable for Equations 7.5, there is (c.f. Theorem 3.3 in [14]) $t < \check{t}_{a,k}$ with $t_{a,k} = \frac{\frac{\pi}{2}}{\mathbf{c}\zeta_k}$. Therefore, t must at least verify $t < t_{a,n}$. Since L_{\cos} is a subnetwork of L , then by Lemma 4 $\zeta_{\cos_n} \leq \zeta_n$, and so $t_{a,n} \leq t_{s,n}$. Thus, System (7.4) allows for a larger time delay.

Lemma 4. *Let \hat{L} and \check{L} be, respectively, $n \times n$ Laplacian matrices associated to connected and undirected networks with positive adjacency entries (i.e. a Laplacian matrix is defined as $L := D - A$ where D is the diagonal matrix with $d_{k,k} := \sum_{j=1}^n a_{k,j}$ and here, we further suppose, $0 \geq a_{k,j} = a_{j,k} \geq 0$ for all k, j). Suppose that the network associated to \check{L} is a subnetwork of the one associated with \hat{L} (i.e. there exist a $n \times n$ Laplacian matrix L (associated to a connected and undirected network with positive adjacency entries) such that $\hat{L} = L + \check{L}$). We then have*

$$\hat{\zeta}_2 \geq \check{\zeta}_2 \quad \text{and} \quad \hat{\zeta}_n \geq \check{\zeta}_n,$$

where $\hat{\zeta}_j$ and $\check{\zeta}_j$ denote the respective eigenvalues of \hat{L} and \check{L} .

Proof. By Lemma (5), we have $\hat{\zeta}_2 = \min_{x \in \mathbb{E}} \{\langle x | \hat{L}x \rangle\}$, with $\mathbb{E} := \{x \in \mathbb{R}^n \mid \|x\| = 1, \langle x | \mathbf{1} \rangle = 0\}$. Hence

$$\hat{\zeta}_2 = \min_{x \in \mathbb{E}} \{\langle x | \hat{L}x \rangle\} = \min_{x \in \mathbb{E}} \{\langle x | Lx \rangle + \langle x | \check{L}x \rangle\} \geq \min_{x \in \mathbb{E}} \{\langle x | Lx \rangle\} + \min_{x \in \mathbb{E}} \{\langle x | \check{L}x \rangle\} = \zeta_2 + \check{\zeta}_2 \leq \check{\zeta}_2$$

and so $\hat{\zeta}_2 \geq \check{\zeta}_2$. Again by Lemma (5), we have $\hat{\zeta}_n = \max_{x \in \mathbb{E}} \{\langle x | \hat{L}x \rangle\}$ and $\check{\zeta}_n = \max_{x \in \mathbb{E}} \{\langle x | \check{L}x \rangle\}$. Since $\hat{a}_{k,j} \geq \check{a}_{k,j}$ for all k, j , then

$$\langle x | \hat{L}x \rangle = \sum_{j>k}^n \hat{a}_{k,j} (x_k - x_j)^2 \geq \sum_{j>k}^n \check{a}_{k,j} (x_k - x_j)^2 = \langle x | \check{L}x \rangle \quad \forall x \in \mathbb{R}^n$$

and so

$$\hat{\zeta}_n = \max_{x \in \mathbb{E}} \{\langle x | \hat{L}x \rangle\} \geq \max_{x \in \mathbb{E}} \{\langle x | \check{L}x \rangle\} = \check{\zeta}_n .$$

□

Lemma 5. Let A be a symmetric positive semi-definite matrix such that $A\mathbf{1} = \mathbf{0}$ ($\mathbf{1}$ is a n dimensional vector of 1). Denote its spectrum by $0 = \zeta_1 \leq \zeta_2 \leq \dots \leq \zeta_n$. Then

$$\zeta_2 = \min_{x \in \mathbb{E}} \{\langle x | Ax \rangle\} \quad \text{and} \quad \zeta_n = \max_{x \in \mathbb{E}} \{\langle x | Ax \rangle\}$$

with $\mathbb{E} := \{x \in \mathbb{R}^n \mid \|x\| = 1, \langle x | \mathbf{1} \rangle = 0\}$.

Proof. Let $x \in \mathbb{E}$, and so $x = \sum_{j=2}^n y_j o_j$ with $y_j \in \mathbb{R}$ and o_j orthonormal eigenvectors of A . Since $\langle x | x \rangle = \sum_{j=2}^n y_j^2 = 1$ and $\langle x | Ax \rangle = \sum_{j=2}^n y_j^2 \zeta_j$, then

$$\zeta_2 = \zeta_2 \sum_{j=2}^n y_j^2 \leq \langle x | Ax \rangle = \sum_{j=2}^n y_j^2 \zeta_j \leq \zeta_n \sum_{j=2}^n y_j^2 = \zeta_n .$$

Hence the statement is true since the minimum value is reached by taking $x = o_2$ and the maximum value is reached by tacking $x = o_n$.

□

References

1. ACEBRÓN, J., BONILLA, L. Asymptotic description of transients and synchronized states of globally coupled oscillators. *Physica D*, 114 (1998), 296–314.
2. ACEBRÓN, J., BONILLA, L., LEO, S. D., SPIGLER, R. Breaking the symmetry in bimodal frequency distributions of globally coupled oscillators. *Physical Review E*, 57 (1998), 5287–5290.
3. ACEBRÓN, J., PERALES, A., SPIGLER, R. Bifurcations and global stability of synchronized stationary states in the kuramoto model for oscillator populations. *Physical Review E*, 64 (2001), 016218/1–016218/5.
4. ACEBRÓN, J., SPIGLER, R. Adaptive frequency model for phase-frequency synchronization in large populations of globally coupled nonlinear oscillators. *Physical Review Letters*, 81 (1998), 2229–2232.
5. ALDANA, M., DOSSETTI, V., HUEPE, C., KENKRE, V., LARRALDE, H. Phase transitions in systems of self-propelled agents and related network models. *Physical Review Letters*, 98 (2007), 095702/1–095702/4.
6. ARNOLD, V. *Les Méthodes Mathématiques de la Mécanique Classique*. Editions Mir (Moscou), 1976.
7. BAG, B., PETROSYAN, K., HU, C.-K. Influence of noise on the synchronization of the stochastic kuramoto model. *Physical Review E*, 76 (2007), 056210/1–056210–6.
8. BELLMAN, R., COOKE, K. L. *Delay Differential Equations With Applications in Populations Dynamics*. Academic Press (New York London), 1963.
9. BELYKH, V. N., BELYKH, I. V., HASLER, M. Connection graph stability method for synchronized coupled chaotic systems. *Physica D*, 195 (2004), 159–187.
10. BENJAMINI, I., LEE, S. Conditioned diffusions which are brownian bridges. *Journal of Theoretical Probability*, 10 (1997), 733–736.
11. BOCCALETTI, S., HWANG, D.-U., CHAVEZ, M., AMANN, A., KURTHS, J., PECORA, L. M. Synchronization in dynamical networks: Evolution along commutative graphs. *Physical Review E*, 74 (2006), 016102.
12. BONILLA, L., VICENTE, C., SPIGLER, R. Time-periodic phases in populations of nonlinearly coupled oscillators with bimodal frequency distributions. *Physica D*, 113 (1998), 79–97.
13. BUCHLI, J., IJSPEERT, A. J. A Simple, Adaptive Locomotion Toy-System. In *Proceedings of Eighth International Conference on the Simulation of Adaptive Behavior (SAB'04)* (2004).
14. CAHLON, B., SCHMIDT, D. Stability Criteria for Certain Second-Order Delay Differential Equations. *Dynamics of Continuous, Discrete and Impulsive Systems*, 10 (2003), 593–621.
15. CRAWFORD, J. Amplitude expansions for instabilities in populations of globally-coupled oscillators. *Journal of Statistical Physics*, 74 (1994), 1047–1084.
16. CUCKER, F., SMALE, S. Emergent behavior in flocks. *IEEE Transactions on Automatic Control*, 52 (2007), 852–862.
17. DAVIS, P. J. *Circulant Matrices*. Wiley (New York), 1979.
18. DE LELLIS, P., DI BERNARDO, M., GOROCHOWSKI, T. E., RUSSO, G. Synchronization and control of complex networks via contraction, adaptation and evolution. *IEEE Circuits and Systems Magazine*, 10 (2010), 64–82.
19. DUC, L. H., ILCHMANN, A., SIEGMUND, S., TARABA, P. On stability of linear time-varying second-order differential equations. *Quarterly of Applied Mathematics*, 64 (2006), 137–151.
20. ERMENTROUT, B. An adaptive model for synchrony in the firefly pteroptyx malaccae. *Journal of Mathematical Biology*, 29 (1991), 571–585.
21. FRANCIS, M. R., FERTIG, E. J. Quantifying the Dynamics of Coupled Networks of Switches and Oscillators. *PLoS ONE*, 7 (2012), e29497.
22. GERSCHGORIN, S. A. Über die Abgrenzung der Eigenwerte einer Matrix. *Izvestiya Akademii Nauk USSR, Otdelenie matematicheskikh i estestvennih Nauk*, 7 (1931), 749–754.

23. GRÉGOIRE, G., CHATÉ, H. Onset of collective and cohesive motion. *Physical Review Letters*, 92 (2004), 025702/1–025702/4.
24. GRIMSHAW, R. *Nonlinear Ordinary Differential Equations*. Blackwell Scientific Publications (Oxford), 1990.
25. GUCKENHEIMER, J., HOLMES, P. *Nonlinear oscillations, dynamical systems, and bifurcations of vector fields*. Springer (New York), 1990.
26. HAN, J., LI, M., GUO, L. Soft control on collective behavior of a group of autonomous agents by a shill agent. *Journal of Systems Science and Complexity*, 19 (2006), 54–62.
27. HONGLER, M.-O. Exact solutions of a class of non-linear fokker-planck equations. *Physics Letters A*, 75 (1979), 3–4.
28. HONGLER, M.-O., FILLIGER, R., BLANCHARD, P. Soluble models for dynamics driven by a super-diffusive noise. *Physica A*, 370 (2006), 301–315.
29. HONGLER, M.-O., FILLIGER, R., BLANCHARD, Ph., RODRIGUEZ, J. Noise Induced Temporal Patterns in Populations of Globally Coupled Oscillators. In *INDS'09 - Second International Workshop on Nonlinear Dynamics and Synchronization* (2009).
30. HONGLER, M.-O., FILLIGER, R., BLANCHARD, Ph., RODRIGUEZ, J. On Stochastic Processes Driven by Ballistic Noise Sources. In *Contemporary Topics in Mathematics and Statistics with Applications*, A. ADHIKARI, M. R. ADHIKARI, Y. P. CHAUBEY (Eds.). Asian Books Private (New Delhi), 2013, 1–29.
31. HONGLER, M.-O., PARTHASARATHY, P. On a super-diffusive, nonlinear birth and death process. *Physics Letters A*, 372 (2008), 3360–3362.
32. HUEPE, C., ALDANA, M. Intermittency and clustering in a system of self-driven particles. *Physical Review Letters*, 92 (2004), 168701/1–168701/4.
33. KUANG, Y. *Delay Differential Equations With Applications in Populations Dynamics*. Academic Press (San Diego London), 1993.
34. KURAMOTO, Y., NISHIKAWA, I. Statistical macrodynamics of large dynamical systems. case of a phase transition in oscillator communities. *Journal of Statistical Physics*, 49 (1987), 569–605.
35. LAKSHMANAN, M., RAJASEKAR, S. *Nonlinear dynamics: integrability, chaos, and patterns*. Springer (Berlin Heidelberg New York), 2003.
36. LEHNERT, J., HÖVEL, P., FLUNKERT, V., GUZENKO, P. Y., FRADKOV, A. L., SCHÖLL, E. Adaptive tuning of feedback gain in time-delayed feedback control. *Chaos*, 21 (2011), 043111.
37. LINDENBERG, K., SESHADRI, V., WEST, B. J. Brownian motion of harmonic systems with fluctuating parameters. ii. relation between moment instabilities and parametric resonance. *Physical Review A*, 22 (1980), 2171–2179.
38. LU, W., ATAY, F. M., JOST, J. Synchronization of discrete-time dynamical networks with time-varying couplings. *SIAM Journal on Mathematical Analysis*, 39 (2007), 1231–1259.
39. MONTBRIÓ, E., PAZÓ, D., SCHMIDT, J. Time delay in the Kuramoto model with bimodal frequency distribution. *Physical Review E*, 74 (2006), 056201.
40. PALEY, D., LEONARD, N., SEPULCHRE, R., GRÜNBAUM, D., PARRISH, J. Oscillator models and collective motion. *IEEE Control Systems Magazine*, 27 (2007), 89–105.
41. RIGHETTI, L., BUCHLI, J., IJSPEERT, A. Dynamic Hebbian Learning in Adaptive Frequency Oscillators. *Physica D*, 216 (2006), 269–281.
42. RODRIGUEZ, J. *Networks of Self-Adaptive Dynamical Systems*. PhD thesis, Ecole Polytechnique Fédérale de Lausanne, 2011.
43. RODRIGUEZ, J., HONGLER, M.-O. Networks of Limit Cycle Oscillators with Parametric Learning Capability. In *Recent Advances in Nonlinear Dynamics and Synchronization: Theory and Applications*, K. KYAMAKYA, W. A. HALANG, H. UNGER, J. C. CHEDJOU, N. F. RULKOV, Z. LI (Eds.). Springer (Berlin Heidelberg), 2009, 17–48.
44. RODRIGUEZ, J., HONGLER, M.-O. Networks of Mixed Canonical-Dissipative Systems and Dynamic Hebbian Learning. *International Journal of Computational Intelligence Systems*, 2 (2009), 140–146.
45. RODRIGUEZ, J., HONGLER, M.-O. Networks of Self-Adaptive Dynamical Systems. *IMA Journal of Applied Mathematics* (2012). doi: 10.1093/imat/hxs057.
46. RODRIGUEZ, J., HONGLER, M.-O., BLANCHARD, Ph. Self-Adaptive Attractor-Shaping for Oscillators Networks. In *The Joint INDS'11 & ISTET'11 - Third International Workshop on Nonlinear Dynamics and Synchronization and Sixteenth International Symposium on Theoretical Electrical Engineering* (2011).
47. RODRIGUEZ, J., HONGLER, M.-O., BLANCHARD, Ph. Time Delayed Interactions in Networks of Self-Adapting Hopf Oscillators. *ISRN Mathematical Analysis* (2012). Article ID 816353.
48. ROGERS, L., PITMAN, J. Markov functions. *The Annals of Probability*, 9 (1981), 573–582.
49. RONSSE, R., VITIELLO, N., LENZI, T., VAN DEN KIEBOOM, J., CARROZZA, M. C., IJSPEERT, A. J. Human-Robot Synchrony: Flexible Assistance Using Adaptive Oscillators. *IEEE Transactions on Biomedical Engineering*, 58 (2011), 1001–1012.

50. ROUGEMONT, J., NAEF, F. Collective synchronization in populations of globally coupled phase oscillators with drifting frequencies. *Physical Review E*, 73 (2006), 011104/1–011104/5.
51. SAKAGUCHI, H. Cooperative phenomena in coupled oscillator systems under external fields. *Progress of theoretical physics*, 79 (1988), 39–46.
52. SELIVANOV, A. A., LEHNERT, J., DAHMS, T., HÖVEL, P., FRADKOV, A. L., SCHÖLL, E. Adaptive synchronization in delay-coupled networks of Stuart-Landau oscillators. *Physical Review E*, 85 (2012), 016201.
53. SHABANA, A. A. *Theory of Vibration: An Introduction*. Springer (New York), 1996.
54. STEINGRUBE, S., TIMME, M., WÖRGÖTTER, F., MANOONPONG, P. Self-organized adaptation of a simple neural circuit enables complex robot behaviour. *Nature Physics*, 6 (2010), 224–230.
55. STILWELL, D. J., BOLLT, E. M., ROBERSON, D. G. Sufficient Conditions for Fast Switching Synchronization in Time-Varying Network Topologies. *SIAM Journal on Applied Dynamical Systems*, 5 (2006), 140–156.
56. TANAKA, H.-A., LICHTENBERG, A. J., OISHI, S. Self-synchronization of coupled oscillators with hysteretic responses. *Physica D*, 100 (1997), 279–300.
57. TAYLOR, D., OTT, E., RESTREPO, J. G. Spontaneous synchronization of coupled oscillator systems with frequency adaptation. *Physical Review E*, 81 (2010), 046214.
58. VICSEK, T., CZIRK, A., BEN-JACOB, E., COHEN, I., SHOCHET, O. Novel type of phase transition in a system of self-driven particles. *Physical Review Letters*, 75 (1995), 1226–1229.
59. WANG, L., WANG, Q. Synchronization in complex networks with switching topology. *Physics Letters A*, 375 (2011), 3070–3074.
60. YEUNG, M. K. S., STROGATZ, S. H. Time Delay in the Kuramoto Model of Coupled Oscillators. *Physical Review Letters*, 82 (1999), 648–651.

Curriculum Vitae

Dr. Julio RODRIGUEZ

Contact: jrodrigu@physik.uni-bielefeld.de

Education

- 2007 - 2011 Docteur ès Science, Ecole Polytechnique Fédérale de Lausanne. PhD thesis: *Networks of Self-Adaptive Dynamical Systems*, supervised by Professor M.-O. HONGLER (Faculté des Sciences et Techniques de l'Ingénieur, EPFL) and Professor Ph. BLANCHARD (Fakultät für Physik, Uni. Bielefeld)
- 2004 - 2007 Maîtrise universitaire en mathématiques, Université de Genève. Master thesis: *A new portfolio optimization based on entropy*, supervised by Professor M. GANDER (Section de mathématiques) and Professor M. GILLI (Département d'économétrie)
- 2001 - 2004 Licencié en Mathématiques, Université de Genève

Recent Professional Experience

- 2007 - 2011 Assistant at the Laboratoire de Production Microtechnique, Ecole Polytechnique Fédérale de Lausanne. Supervised and guided students's semester projects.
- 2006 - 2007 Assistant at the Section de mathématiques, Université de Genève.

Publications

Articles and Book chapters

J. RODRIGUEZ, M.-O. HONGLER, Ph.BLANCHARD. Self-Shaping Attractors for Coupled Limit Cycle Oscillators. To appear in *Selected Topics in Nonlinear Dynamics and Theoretical Electrical Engineering*. Springer, 2013.

M.-O. HONGLER, R. FILLIGER, Ph. BLANCHARD, J. RODRIGUEZ. On Stochastic Processes Driven By Ballistic Noise Sources. In *Contemporary Topics in Mathematics and Statistics with Applications*, A. ADHIKARI, M. R. ADHIKARI, Y. P. CHAUBEY (Editors). Asian Books Private, 2013, 1-29.

J. RODRIGUEZ, M.-O. HONGLER, Ph. BLANCHARD. Time Delayed Interactions in Networks of Self-Adapting HOPF Oscillators. *ISRN Mathematical Analysis*, (2012). Article ID 816353.

J. RODRIGUEZ, M.-O. HONGLER. Networks of Self-Adaptive Dynamical Systems. *IMA Journal of Applied Mathematics*, (2012), doi: 10.1093/imamat/hxs057.

J. RODRIGUEZ, M.-O. HONGLER. Networks of Limit Cycle Oscillators with Parametric Learning Capability. In *Recent Advances in Nonlinear Dynamics and Synchronization: Theory and Applications*, K. KYAMAKYA, W. A. HALANG, H. UNGER, J. C. CHEDJOU, N. F. RULKOV, Z. LI (Editors). Springer (Berlin Heidelberg), 2009, 17-48.

J. RODRIGUEZ, M.-O. HONGLER. Networks of Mixed Canonical-Dissipative Systems and Dynamic Hebbian Learning. *International Journal of Computational Intelligence Systems*, 2 (2009), 140-146.

International Conference and Workshop Proceedings

M.-O. HONGLER, R. FILLIGER, Ph. BLANCHARD, J. RODRIGUEZ. On stochastic processes driven by ballistic noise sources. In Proceedings of *MSAST 2011 - Mathematical Sciences for Advancement of Science and Technology*, 2011.

J. RODRIGUEZ, M.-O. HONGLER, Ph. BLANCHARD. Self-Adaptive Attractor-Shaping for Oscillators Networks. In Proceedings of *The Joint INDS'11 & ISTET'11 - Third International Workshop on nonlinear Dynamics and Synchronization and Sixteenth International Symposium on Theoretical Electrical Engineering*, 2011.

J. RODRIGUEZ, M.-O. HONGLER. Parametric Resonance in Time-Dependent Networks of Hopf Oscillators. In Proceedings of *ECCS'10 - European Conference on Complex Systems*, 2010. Received a "Special Mention - paper with remarkable overall quality".

M.-O. HONGLER, R. FILLIGER, Ph. BLANCHARD, J. RODRIGUEZ. Noise Induced Temporal Patterns in Populations of Globally Coupled Oscillators. In Proceedings of *INDS'09 - Second International Workshop on Nonlinear Dynamics and Synchronization*, 2009.

J. RODRIGUEZ, M.-O. HONGLER. Networks of Mixed Canonic-Dissipative Systems and Dynamic Hebbian Learning. In Proceedings of *INDS'08 - First International Workshop on Nonlinear Dynamics and Synchronization*, 2008.

Theses

J. RODRIGUEZ. Networks of Self-Adaptive Dynamical Systems. PhD thesis presented at the Ecole Polytechnique Fédérale de Lausanne, supervised by Professor M.-O. HONGLER (Faculté des Sciences et Techniques de l'Ingénieur, EPFL) and Professor Ph. BLANCHARD (Fakultät für Physik, Uni. Bielefeld), 2011.

J. RODRIGUEZ. A new portfolio optimization based on entropy. Master thesis in Mathematics presented at the Université de Genève, supervised by Professor M. GANDER (Section de mathématiques) and Professor M. GILLI (Département d'économétrie), 2007.

Selected Talks

15-18.10.2012 Networks of Adaptive Frequency Oscillators and Stochastic Parametric Resonance. *Stochastics and Real World Models: Recent Progress and New Frontiers*. School of Mathematical Science, Jiangsu Normal University, Xuzhou, People's Republic of China.

- 02.10.2012 Stochastic Switching Networks of Adaptive Frequency Oscillators. Departamento de Ciencias Matemáticas, Universidad de Puerto Rico - Recinto de Mayagüez, Mayagüez, Puerto Rico.
- 26-09.07.2012 Networks of Adaptive Frequency Oscillators with Time-Dependent and Delayed Interactions. *Sonderforschungsbereich 910 - Control of self-organizing nonlinear systems: Theoretical methods and concepts of application*. Institut für Theoretische Physik, Technische Universität, Berlin, Deutschland.
- 25.09.2012 Time Delayed Interactions in Networks of Self-Adapting Hopf Oscillators. *Seminar Netzwerke und Komplexe Systeme*. Max-Planck-Institut für Mathematik in den Naturwissenschaften, Leipzig, Deutschland.
- 02-06.07.2012 Stochastic Parametric Resonance in Networks of Adaptive Frequency Oscillators. *Random Models in Neuroscience*. Université Pierre et Marie Curie, Paris, France.
- 08.06.2012 Networks of Vibrating-Oscillatory Systems with Parametric Resonance Type Perturbation. INRIA - NeuroMathComp, Sophia Antipolis, France.
- 20-27.05.2012 Noise Induced Dynamical Patterns for a Swarm's Barycenter. *Emergent Dynamics of Oscillatory Networks*. Санаторий "Меллас", поселок Санаторий, Ялта, Крым, Україна.
- 04-06.04.2012 Frequency Adaptation and Attractor Shaping in Oscillatory Networks. *Nonlinear Analysis and Applications*. Національний технічний університет України "Київський політехнічний інститут", Київ, Україна.
- 25-27.07.2011 Self-Adaptive Attractor-Shaping for Oscillators Networks. *INDS'11 & ISTET'11 - Third International Workshop on nonlinear Dynamics and Synchronization and Sixteenth International Symposium on Theoretical Electrical Engineering*. Alpen-Adria-Universität Klagenfurt, Klagenfurt, Österreich.
- 18-22.07.2011 Globally Coupled Phase Oscillators driven by Ballistic Noise Source. *Stochastics and Real World Models 2011*. Universität Bielefeld, Bielefeld, Deutschland.
- 13-17.09.2010 Parametric Resonance in Time-Dependent Networks of Phase Oscillators. *ECCS'10 - European Conference on Complex Systems*. ISCTE - Instituto Universitário de Lisboa (Instituto Superior de Ciências do Trabalho e da Empresa), Lisboa, Portugal.
- 05-09.07.2010 Networks of Adaptive Frequency Oscillators and Parametric Resonance. *Nonlinear Dynamics on Networks*. Національна академія наук України, Київ, Україна.
- 12.05.2010 Parametric Resonance in Networks of Adaptive Frequency Oscillators. *Sfb 555 - Complex Nonlinear Processes*. Institut für Physik, Humboldt-Universität, Berlin, Deutschland.
- 03-07.05.2010 Networks of Limit Cycle Oscillators with Parametric Dynamics. *Chinese-German Meeting on Stochastic Analysis and Related Fields*. Academy of Mathematics and Systems Science, Chinese Academy of Science, Beijing, People's Republic of China.
- 14-18.02.2010 Frequency Adaptation in Networks of Coupled Limit Cycle Oscillators. *SOCONT - Stochastic Optimal Control*. Quinta Bela São Tiago Hotel, Funchal, Madeira, Portugal.
- 26-31.07.2009 Globally Coupled Phase Oscillators with Super-diffusive Noise. *Madeira Math Encounters XXXVII*. Centro de Ciências Matemáticas, Universidad da Madeira, Funchal, Madeira, Portugal.
- 20-21.07.2009 Noise Induced Temporal Patterns in Populations of Globally Coupled Oscillators. *INDS'09 - Second International Workshop on Nonlinear Dynamics and Synchronization*. Alpen-Adria-Universität Klagenfurt, Klagenfurt, Österreich.

- 10.06.2009 Networks of Limit Cycle Oscillators with Plastic Dynamics. *Rencontre franco-suisse sur le bruit et les non linéarités*. Laboratoire de Psychologie et NeuroCognition, Université Pierre-Mendès France, Grenoble, France.
- 25-29.05.2009 Networks of Mixed Canonical-Dissipative Systems with Plastic Dynamics. *Stochastics and Real World Models 2009*. Universität Bielefeld, Bielefeld, Deutschland.
- 24.10.2008 Network of Limit Cycle Oscillators with Parametric Learning Capability. *Seminar Analysis und Numerik*. Mathematisches Institut, Universität Basel, Basel, Schweiz.
- 18-19.07.2008 Networks of Mixed Canonic-Dissipative Systems and Dynamic Hebbian Learning. *INDS'08 - First International Workshop on Nonlinear Dynamics and Synchronization*. Alpen-Adria-Universität Klagenfurt, Klagenfurt, Österreich.
- 14.05.2008 Networks of Mixed Canonic-Dissipative Systems and Dynamic Hebbian Learning. *Séminaire d'analyse numérique*. Section de mathématiques, Université de Genève, Genève, Suisse.
- 07.03.2007 A portfolio optimization based on entropy. Swissquote Bank SA, Gland, Suisse.

Research Visits and Exchange Stays

- 20.07-20.08.2010 Collaboration with the Beijing-Bielefeld Internationales Graduiertenkolleg (IGK) - Stochastics and Real World - team at the Academy of Mathematics and Systems Science, Chinese Academy of Science, Beijing, People's Republic of China.
- 15.07-15.08.2010 Collaboration with the Beijing-Bielefeld Internationales Graduiertenkolleg (IGK) - Stochastics and Real World - team at the Academy of Mathematics and Systems Science, Chinese Academy of Science, Beijing, People's Republic of China.
- 12.01-11.12.2009 Continuation of my thesis with Professor Ph. BLANCHARD at the Fakultät für Physik, Universität Bielefeld, Bielefeld, Deutschland.